Development of New Liquid Chromatographic Techniques for the Characterization of Poly(Bisphenol A Carbonate)

Entwicklung neuer flüssigchromatographischer Techniken zur Charakterisierung von Poly(bisphenol A carbonat)

TECHNISCHE UNIVERSITÄT DARMSTADT

vom Fachbereich Chemie
der Technischen Universität Darmstadt

zur Erlangung des Grades

Doctor rerum naturalium
(Dr. rer. nat.)

Dissertation
von Nico Apel

Erstgutachter:	Prof. Dr. Matthias Rehahn
Zweitgutachter:	Prof. Dr. Markus Busch

Darmstadt 2018

Tag der Einreichung: 28. März 2018

Tag der mündlichen Prüfung: 28. Mai 2018

Apel, Nico: Development of New Liquid Chromatographic Techniques for the Characterization of Poly(Bisphenol A Carbonate)
Darmstadt, Technische Universität Darmstadt,
Jahr der Veröffentlichung der Dissertation auf TUprints: 2018

URN: urn:nbn:de:tuda-tuprints-74631
Tag der mündlichen Prüfung: 28.05.2018

This study is a result of the work carried out at Fraunhofer LBF under the supervision of Prof. Dr. Matthias Rehahn from March 2015 to February 2018.

Acknowledgments

Ich möchte mich als erstes bei Herrn Prof. Dr. Matthias Rehahn für die Möglichkeit bedanken, am Fraunhofer LBF meine Promotion zu dem vorliegenden Thema durchzuführen.

Des Weiteren danke ich Herrn Dr. Robert Brüll für die hervorragende Betreuung und das mir entgegengebrachte Vertrauen sowie seine Unterstützung.

Very special thanks to SABIC, the collaboration partner and funder of the research project, which this thesis emerges from. Thus, I would like to thank Dr. Elena Uliyanchenko, Dr. Christian Wold, Dr. Stephan Moyses, Dr. Vaidyanath Ramakrishnan and Mr. Stijn Rommens for their trust, countless discussions, plenty advices and assistance, as well as the extremely pleasant and highly professional working atmosphere.

Herrn Dr. Tibor Macko danke ich für die fortwährende Hilfsbereitschaft bei technischen und wissenschaftlichen Problemstellungen.

Bei meinen Freunden und ehemaligen Kollegen Dr. Tobias Schuster, Dr. Marcel Meub, Dr. Katja Utaloff, Dr. Benjamin Groos, Christian Schmidt und Max Pfeiffer möchte ich mich für die unzähligen fachlichen Gespräche, aber auch die äußerst unterhaltsamen Mittagspausen und die vielen privaten Unternehmungen bedanken. Max Pfeiffer möchte ich außerdem für die umfangreichen Korrekturarbeiten dieser Thesis danken.

Den (ehemaligen) Kollegen des Fraunhofer LBF, danke ich für die stets nette Arbeitsatmosphäre und die wissenschaftlichen und privaten Diskussionen.

Herrn Klaus Lorenz möchte ich für die Unterstützung bei der Wartung und Reparatur elektronischer Bauteile der Messinstrumente danken.

Mit meinen Kommilitonen Lucien Beißwenger, Jennifer Doerfer, Christian Rüttiger, Maria Stimeier, Dominik Ohlig, Michael Appold, Sebastian Schöttner, Felix Schäfer, Michael George und Tamara Winter teile ich die Erinnerung an eine unvergessliche Studienzeit.

Ich möchte mich außerdem bei der BASF SE und der Technischen Universität Darmstadt für ihre finanzielle Unterstützung im Rahmen des Deutschlandstipendiums während meines Chemiestudiums bedanken.

Meinen Eltern und meinem Bruder danke ich dafür, dass sie stets für mich da sind.

Meiner Freundin und langjährigen Lebensgefährtin Insa Maria Schreiber gilt ein ganz besonderer Dank für ihre stete Unterstützung, ihre Zuverlässigkeit und ihr großes Einfühlungsvermögen in allen Lebenslagen.

Unser größter Ruhm liegt nicht darin, niemals zu fallen, sondern jedes Mal wieder aufzustehen, wenn wir gescheitert sind.

Konfuzius

Parts of this work have already been published or are about to be published in form of publications.

Publication:

N. Apel[1], E. Uliyanchenko, S. Moyses, S. Rommens, C. Wold, T. Macko, K. Rode, R. Brüll:

"Selective chromatographic separation of polycarbonate according to hydroxyl end-groups using a porous graphitic carbon column"

Journal of Chromatography A, 2017, 1488, 77-84

N. Apel[1], E. Uliyanchenko, S. Moyses, C. Wold, T. Macko, R. Brüll:

"Separation of Branched Poly(bisphenol A carbonate) Structures by Solvent Gradient at Near-Critical Conditions and Two-Dimensional Liquid Chromatography"

Submitted, 2018

N. Apel[1], V. Ramakrishnan, E. Uliyanchenko, S. Moyses, C. Wold, T. Macko, R. Brüll:

"Correlation between comprehensive 2D liquid chromatography and Monte-Carlo simulations for branched polymers"

In Preparation, 2018

Presentation:

Comprehensive Two-Dimensional Liquid Chromatography Coupled to Triple-Detection for Characterization of Branched Polymers

15th International Symposium on Hyphenated Techniques in Chromatography and Separation Technology: January 24th – 26th 2018 in Cardiff, UK

[1] First authorship

Table of content

ABBREVIATIONS ..... **VII**

1 INTRODUCTION **1**

1.1 POLY(BISPHENOL A CARBONATE) 2

1.1.1 History and polymerization *2*

1.1.2 Properties and applications *5*

1.1.3 Characterization techniques *8*

1.2 PURPOSE OF THE WORK 10

2 THEORETICAL PART **14**

2.1 SIZE-EXCLUSION CHROMATOGRAPHY (SEC) 16

2.2 TRIPLE-DETECTION SIZE-EXCLUSION CHROMATOGRAPHY (TD-SEC) 19

2.3 LIQUID ADSORPTION CHROMATOGRAPHY (LAC) 24

2.4 LIQUID CHROMATOGRAPHY UNDER CRITICAL CONDITIONS (LCCC) 26

2.5 TWO-DIMENSIONAL LIQUID CHROMATOGRAPHY (2D-LC) 28

3 RESULTS AND DISCUSSION **30**

3.1 CHROMATOGRAPHIC INVESTIGATIONS OF PC USING A PGC COLUMN 30

3.1.1 Determination of the critical conditions in the eluent system $CHCl_3$/TCB and $CHCl_3$/DCB *30*

3.1.2 End-group separation at the critical conditions *33*

3.1.3 Temperature influence on the end-group separation at critical conditions *39*

3.1.4 Recovery rate determination *41*

3.1.5 Influence of branching on the separation of PC at critical conditions *46*

3.1.6 Summary *48*

3.2 CHROMATOGRAPHIC INVESTIGATIONS OF PC USING A NORMAL-PHASE COLUMN 49

3.2.1 Solvent gradients at near-critical conditions (SG-NCC) *49*

3.2.2 Off-line two-dimensional chromatography with triple detection *58*

3.2.3 On-line two-dimensional chromatography (2D-LC) *64*

3.2.4 Reversed elution order *69*

3.2.5 On-line two-dimensional chromatography with triple-detection (2D-LC with TD) 72
3.2.6 Monte-Carlo simulations 80
3.2.7 Summary 84

4 CONCLUSIONS 85

5 ZUSAMMENFASSUNG UND SCHLUSSFOLGERUNGEN 88

6 EXPERIMENTAL PART 91

6.1 POLYMER SAMPLES 91
6.2 SOLVENTS AND CHEMICAL SUBSTANCES 93
6.3 CHROMATOGRAPHIC EQUIPMENT AND METHODS 94
6.3.1 Liquid chromatography under critical conditions in PGC stationary phase (LCCC) 94
6.3.2 Recovery rate determination 95
6.3.3 Solvent gradients at near-critical conditions (SG-NCC) in a normal-phase stationary phase 96
6.3.4 On-line two-dimensional liquid chromatography (2D-LC) 97
6.3.5 Triple-detection size-exclusion chromatography (TD-SEC) 99
6.3.6 On-line two-dimensional liquid chromatography with triple-detection (2D-LC with TD) 100
6.4 MALDI-TOF-MS 102
6.4.1 Analysis of samples related with section 3.1 102
6.4.2 Analysis of samples related with section 3.2 103
6.5 THPE QUANTIFICATION BY LIQUID CHROMATOGRAPHY 104

7 REFERENCES 105

Abbreviations

Physical quantity	Labeling	Value	Unit
N_A	Avogadro's number	$6.0221 \cdot 10^{23}$	mol^{-1}
R	Universal gas constant	8.3145	$J \cdot mol^{-1} \cdot K^{-1}$

Variable	Labeling	Unit
A_2	Second virial coefficient	$mol \cdot m^3 \cdot kg^{-2}$
c	Concentration	$mol \cdot m^{-3}$
c	Mass concentration	$kg \cdot m^{-3}$
DP	Differential pressure of the VI	Pa
f	Detector constant	m^2
g	Branching ratio of mean-square radii of branched and linear polymers	-
g'	Branching ratio of intrinsic viscosities of branched and linear polymer	-
IP	Inlet pressure of the VI	Pa
I_0	Incident light intensity	cd
I_θ	Scattered light intensity of a polymer solution at angle θ	cd
K	proportionality constant of the Mark-Houwink equation	$m^3 \cdot kg^{-1}$
K^*	Optical constant	$mol \cdot m^2 \cdot kg^{-2}$
K_D	Distribution coefficient	-
M	Molar mass	$kg \cdot mol^{-1}$
$\bar{M}_n$	Number-average molar mass	$kg \cdot mol^{-1}$

M_p	Peak molar mass	kg·mol^{-1}
$\overline{M}_w$	Weight-average molar mass	kg·mol^{-1}
$M_{w,LS}$	Molar mass of an SEC elution slice as determined by LS	kg/mol
N	Number of repeating units	-
n	Refractive index	
dn/dc	Specific refractive index increment	m^3·kg^{-1}
$P(\theta)$	Particle scattering factor	-
r	Distance between scattering volume and the detector	m
R_g	Radius of gyration	m
R_θ	Excess Rayleigh ratio at angle θ	m^{-1}
T	Temperature	K
V	LS Detector volume	m^3
V_0	Dead volume	m^3
V_h	Hydrodynamic volume	m^3
V_P	Pore volume	m^3
V_R	Retention volume	m^3
V_Z	Interstitial volume	m^3
V_{laser}	Photodiode voltage of laser source	V
V_θ	Photodiode voltage of LS at angle θ	V
α	Exponent constant of the Mark-Houwink equation	-
Δ	Standard deviation	%
ΔG	Gibbs' free energy	J·mol^{-1}
ΔH	Enthalpy change	J·mol^{-1}

ΔS	Entropy change	$J \cdot mol^{-1} \cdot K^{-1}$
ϵ	Viscosity shielding ratio	-
η	Viscosity	Pa·s
η_{sp}	Specific viscosity	-
$[\eta]$	Intrinsic viscosity	$m^3 \cdot kg^{-1}$
θ	Angle	° or rad
λ	Wavelength	m
λ	Wavelength	m

Abbreviations

2D	Two-dimensional
2D-LC	Two-dimensional liquid chromatography
a.u.	Arbitrary units
ACN	Acetonitrile
ATR	Attenuated total reflection
BPA	Bisphenol A
CD	Compact disc
D.S.	Detector signal
DAD	Diode array detector
DCB	Dichlorobenzene
DCM	Dichloromethane
DCTB	Trans-2-[3-(4-*tert*-Butylphenyl)-2-methyl-2-propenylidene]malononitrile
DEE	Diethylether

DVD	Digital video disc
ELSD	Evaporative light scattering detector
FA	Formic acid
FT-IR	Fourier-transform infrared
GE	General Electric
HPLC	High performance liquid chromatography
IR	Infrared
LAC	Liquid adsorption chromatography
LC	Liquid chromatography
LCCC	Liquid chromatography under critical conditions
LS	Light scattering
MALDI-TOF-MS	Matrix-assisted laser desorption/ionization time-of-flight mass spectrometry
MALS	Multi-angle light scattering detector
MC	Monte-Carlo
MDS	Multi-detector suite
MMD	Molar mass distribution
MTBE	Methyl *tert*-butyl ether
NCC	Near-critical conditions
NMR	Nuclear magnetic resonance
No.	Number
PC	Poly(bisphenol A carbonate)
PEO	Poly(ethylene oxide)
PET	Polyethylene terephthalate

PGC	Porous graphitic carbon
PLA	Polylactide
PM	Polymethylene
PMMA	Polymethylmethacrylate
PPPBP	3,3-Bis(4-hydroxyphenyl)-2-phenylisoindolin-1-one
PS	Polystyrene
PSS	Polymer standards services
R&D	Research and development
RI	Refractive index
SDV	Styrene-divinylbenzene copolymer
SEC	Size-exclusion chromatography
SGIC	Solvent gradient interaction chromatography
SG-NCC	Solvent gradients at near-critical conditions
TCB	Trichlorobenzene
TD	Triple-detection
TD-SEC	Triple-detection size-exclusion chromatography
TGIC	Temperature gradient interaction chromatography
THF	Tetrahydrofuran
THPE	1,1,1-Tris(*p*-hydroxyphenyl)ethane
UV	Ultraviolet
VI	Viscosity, viscometer

1 Introduction

Polymers are no invention of mankind, but they have been evolved and used by nature for a variety of highly complex processes for millions of years. Polymer substances are involved in almost all biochemical processes and materials such as cellulose as the main component of wood, enzymes and proteins, which catalyze chemical processes in organisms, or polysaccharides as energy storage are widely spread. The first systematic studies on synthetic polymers were conducted in the 19th century: Exemplarily, in 1839 E. SIMON observed that a heated styrene solution had transformed its phase from a transparent liquid towards a solid state [1]. However, only in the 1920s, H. STAUDINGER could experimentally prove the existence of macromolecules. Consequently, the macromolecular chemistry was founded as scientific discipline and, therefore, became independent from organic chemistry [2]. Today polymers are one of the most important materials and they have found application in virtually all areas of daily life. However, the chemical structure of synthetic polymers is as versatile as their field of applications.

Synthetically produced polymers are highly heterogeneous materials, exhibiting distributions in their molar mass (MMD), molecular architecture, functionality or, in case of copolymers, additionally in their chemical composition distribution (block, statistical, alternating copolymers), which influence the properties of a polymeric material.

Branching, which is an important metric of the molecular architecture, influences the macroscopic properties of polymers, such as glass transition temperature, rheology, crystallinity or solubility [3]. As a rule, these properties are not only affected solely by the degree of branching, but in addition by the characteristics of their population, such as the length of individual branches, the functionality of the branching points and their spacing (distances between them) [4]. Since polymers are also distributed in other molecular metrics, these parameters follow a non-trivial distribution function over all polymer chains.

The end-group distribution is particularly important in case of polycondensates, such as polycarbonates, as the remaining terminal functional groups originate from the monomers as well as the end-capping agent. These are used to control the molar mass of the product and result in a plethora of end-group combinations. Remaining functional end-groups, as a result of incomplete end-capping formed during processing or end-use application, lead to post-synthesis reactions, such as further polymerization or degradation, which then affect the polymer's properties [5]. Thus, establishing structure-property relationships requires an in-depth knowledge about the involved molecular distribution functions and their interrelationship [6].

1.1 Poly(bisphenol A carbonate)

1.1.1 History and polymerization

The first investigations on polycarbonates were carried out by EINHORN in 1898 [7]. The reaction of phosgene with hydroquinone in pyridine yielded an amorphous and yellowish powder, which did not melt at temperatures up to 280 °C. Similar experiments with resorcinol instead of hydroquinone resulted in an amorphous powder with a melting of 190 °C. Due to their unusual thermal and mechanical properties, these substances were postulated as polymeric compounds and were already referred to as "Polycarbonate" [7]. However, the potential of the newly created polymer class was not recognized at that time.

It took more than 50 years to realize the commercial potential of polycarbonate, when in the 1950s SCHNELL at Bayer in Uerdingen [8, 9] and FOX at GE in Schenectady, New York [10] realized the commercial potential of polycarbonate. Although both companies had experimented with a variety of polyvalent alcohols, polycarbonate synthesized with bisphenol A (BPA) exhibited the best heat resistance, impact strength, and dimensional stability. An additional impetus for the use of BPA arose from the cumene-phenol process developed by HOCK and LANG in Clausthal in 1944, where acetone and phenol are produced [11]. As both compounds are the starting materials for BPA, poly(bisphenol A carbonate) (PC) became available in large quantities and at affordable costs [11].

During their studies SCHNELL and his coworkers mainly focused on the direct synthesis of PC from phosgene and BPA, whereof the “interfacial process” was developed (Scheme 1) [8, 9]. Within that BPA is dissolved in an aqueous NaOH-alkaline phase, whereas phosgene is dissolved in an organic CH_2Cl_2 phase. Both components react at the interface between the nonmiscible phases, where the process’ name origins from. The “interfacial process” benefits from the well-defined interface and, thus, the reaction product exhibits complete end-capping as well as controlled MMD [12]. A drawback of the interfacial process is the fact that byproducts, like HCl and NaCl are formed in significant quantities. These are a concern from the engineering point of view, as they may cause corrosion of the plant materials and also have to be separated from the polymer in costly process steps [13, 14]. From the safety standpoint direct application of phosgene is critical due to its toxicity and high reactivity [13].

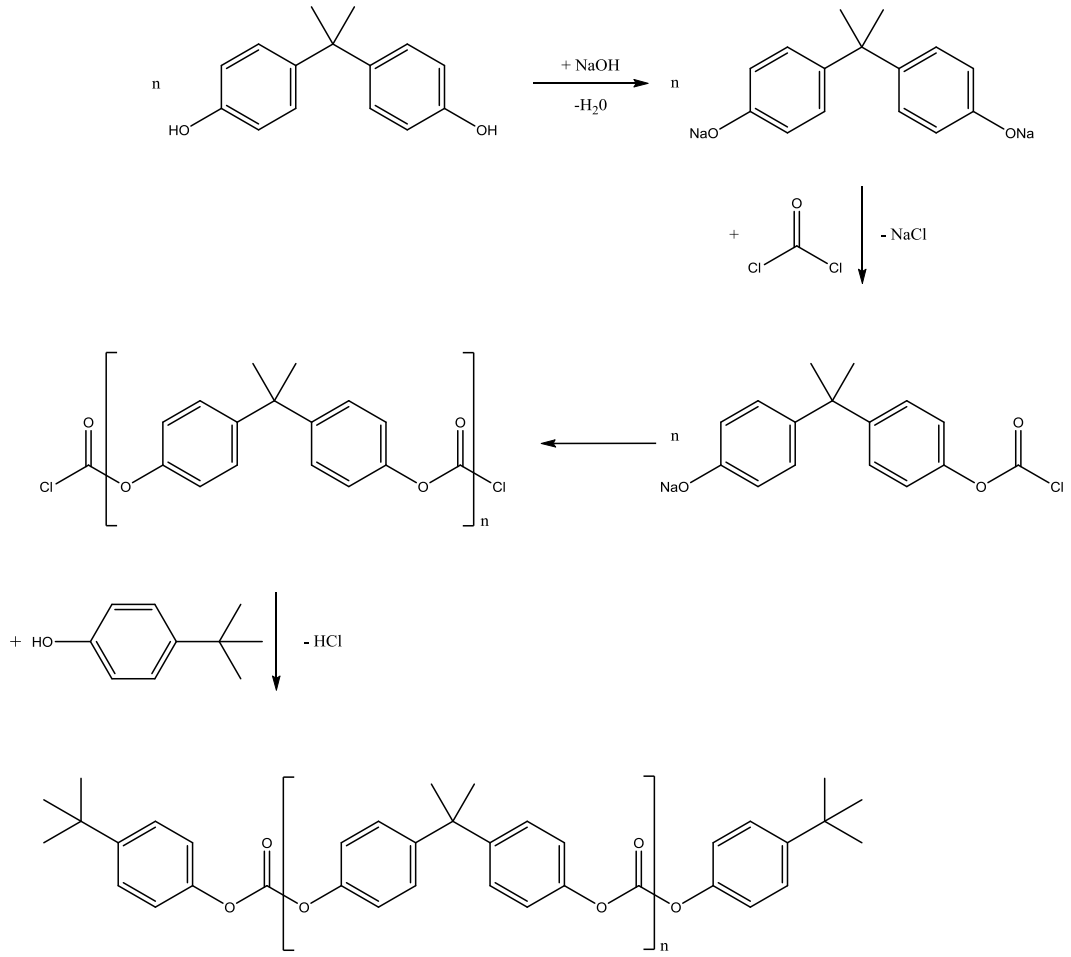

Scheme 1: "Interfacial process" for the synthesis of end-capped poly(bisphenol A carbonate).

An alternative route, the so-called "transesterification" or "melt process", was developed by FOX et al., where diphenyl carbonate is reacted with BPA at temperatures of 150-320 °C. The formed phenol is distilled off in vacuo, which is the driving force of the reaction (Scheme 2) [14]. A significant advantage of the "melt process" is the absence of phosgene and its superior selectivity with regard to by-products, which can easily be isolated. However, due to the incomplete end-capping the resulting PC is more prone towards degradation [5].

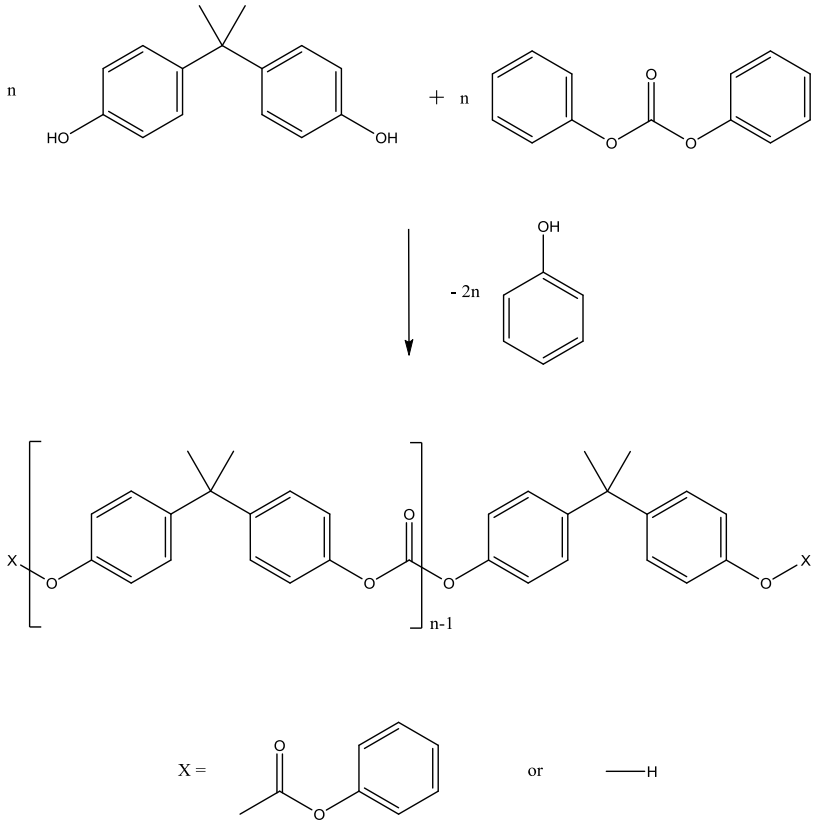

Scheme 2: "Transesterification process" for the synthesis of poly(bisphenol A carbonate).

The simultaneous discovery of PC at Bayer in Germany and at GE in the United States led to a patent dispute, which caused great uncertainties in the respective R&D departments. In order to ensure investment reliability during the ongoing patent litigation, Bayer and GE agreed in that the respective winner of the patent litigation would grant the defeated party access to the corresponding markets by royalty payments [15]. The agreement guaranteed that both companies were becoming the dominant players in the polycarbonate business in the following years.

1.1.2 Properties and applications

PC represents a specialty engineering thermoplastic, which is characterized by relatively low costs, although it cannot compete with commodity polymers such as polyolefins with regard to manufacturing costs. Since its mechanical, optical and thermal properties can be customized over a broad spectrum, a number of PC's applications lie in widely spread niche markets with special material requirements [13]. PC reveals high impact strength, good processability, high electrical insulation, good resistance to thermal deformation and high chemical stability, especially in contact with non-chlorinated solvents [16, 17]. Furthermore, PC is one of few polymers, which shows optical transparency on its own and, hence, the application of clarifiers is dispensable. The controlled depolymerization to dimers, trimers, etc., which are used as feedstock for new syntheses, is of special interest with regard to recyclability and ecological aspects [18, 19].

In 2007 the worldwide production of PC stood at 3500 thousand tons [13]. Based on PC's electrical insulation properties it is used as material for connectors, housings and tools in the electrical and electronic industries [2, 13, 17, 20]. Due to its impact strength and optical transparency PC finds application as windows and coverings for green houses in the construction sector. As an example, the roof top windows of the Olympic Stadium in Athens consist of PC (Figure 1) [21]. Thus, it competes with polymethylmethacrylate (PMMA, Plexiglas®), which reveals better scratch resistance and less yellowing upon long term UV exposure, however [13]. In the automotive sector PC is used for headlamp lenses or as material for helmets and body protections due to its outstanding mechanical resistance [13].

Figure 1: The roof top of the Olympic Stadium in Athens. The roof top windows of the stadium are made of PC. Photographer: Nico Apel, 2009.

The excellent clarity, which is paired with high impact strength, is also the selling point for PC as material for compact and digital versatile discs (CD, DVD) in data storage applications, although the high refractive indices as well as its birefringence cause technological problems for applications in re-writeable devices [22, 23]. In order to solve these technological issues PC is blended with other polymers or copolymers. PC copolymers are also produced to achieve higher heat resistance above the glass transition temperature of PC homopolymer (135 to 155 °C). For example, a copolymer of BPA and 3,3-bis(4-hydroxyphenyl)-2-phenylisoindolin-1-one (PPPBP) has been developed to fulfill these requirements, which, however, reveals lower hydrolytic stability [16].

Moreover, PC finds application as material for the production of water canisters with volumes equal or larger than 5 L. On the one hand, such canisters must have high strength in order to withstand external impacts, on the other hand, they must be as light as possible in order to save transport costs. Besides, strict regulations exist with regard to migrating additives and stabilizer as well as taste of the water. In contrast to other materials such as polyolefins or

polyethylene terephthalate (PET) PC meets these strict requirements, even though residual BPA monomer, which has been suspected to be a potential endocrine disrupter, is a possible migrant as well.

For the production of the water canisters a branched PC is used to control the rheological properties of the melt during the processing: higher degrees of branching reduce the melt viscosity at high shear rates, while low shear rates increase elasticity of the melt [24]. Since the canisters are produced by a blow-molding process, where high shear rates may occur, the branched PC prevents a melt fracture. As a result, lightweight water canisters can be produced exhibiting high mechanical strengths and complying with the strict regulations with regard to potential migrants [17].

All of these examples show the versatility of PC and, on the other hand, demonstrate how sensitive the resulting materials are to small changes in the molecular structure.

1.1.3 Characterization techniques

The branching in case of PC is intentionally generated by adding the triol monomer, for example 1,1,1-tris(*p*-hydroxyphenyl)ethane (THPE) during the polycondensation process with the aim to tune the rheological properties of the PC (Scheme 3). Already minuscule degrees of branching lead to strong changes in the mechanical, thermal and rheological properties [24, 25].

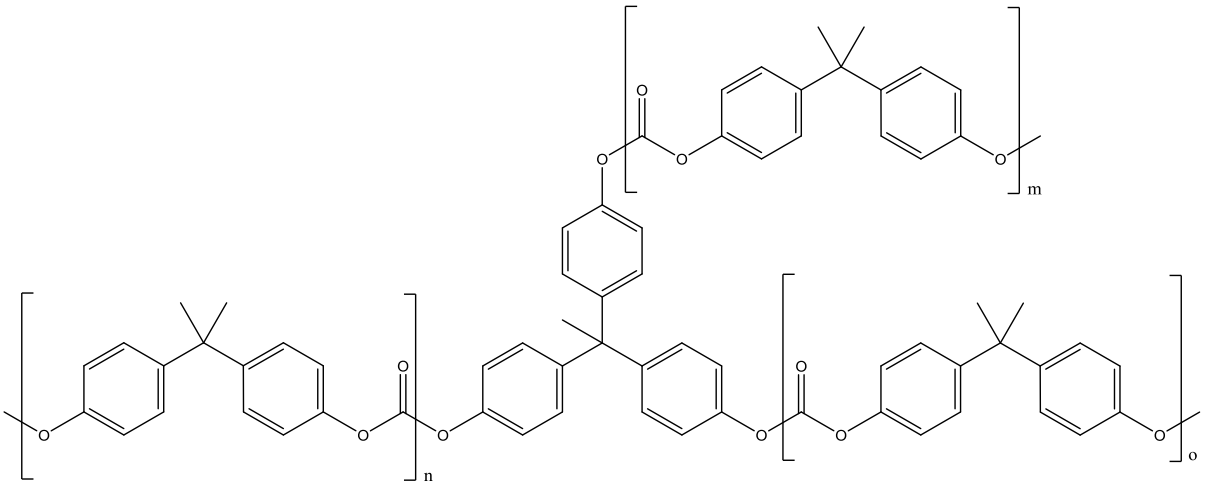

Scheme 3: Intentional branching of poly(bisphenol A carbonate), introduced by the tri-OH functional monomer THPE.

In general, these properties are not only affected by the degree of branching alone but also by the length of the individual branches, the chemical constitution of the branching points and the distance between them [4]. For example, the arm length of a branched polymer chain mainly determines the extent of entanglements with other polymer chains, which has a direct impact on the rheological properties [26-28]. In order to predict the resulting rheological properties depending on the branching, physical models are applied, which require an accurate knowledge of the PC chain structure [29, 30]. However, due to the high structural complexity of the branched chains, this is not a simple task in general. Furthermore, polymers do not only reveal distributions in branching alone but are also distributed with regard to other molecular metrics such as molar mass or end-group [6]. In order to describe the diversity in the PC chain structures, statistic simulations such as Monte-Carlo (MC) models may be used [26]. A number of experimental approaches, such as nuclear magnetic resonance (NMR), liquid chromatography (LC) and matrix-assisted laser desorption/ionization time-of-flight mass spectrometry (MALDI-TOF-MS) have been used with the aim to elucidate the structure of branched PC and link molecular information to rheological properties of the melt.

Exemplarily, NMR, as a typical spectroscopic method, allows the determination of the degree of branching by quantifying the number of branching points (THPE) without prior calibration [31, 32]. However, more detailed information on the arm lengths distribution can only be determined for branches up to 10 carbon atoms with ^{13}C-NMR and no conclusions on the rheological properties can be drawn [33]. Contrary to that, size-exclusion chromatography (SEC) coupled with a viscometer allows analyzing the rheological properties of PC in solution depending on the molar mass. Thus, detailed information on the incorporation of branching along the MMD can be derived and validated with MC models [27, 34]. However, a major drawback arises from the low sensitivity of the method at very low degrees of branching. Furthermore, a transfer from the rheological properties in solution to the ones in the melt is essential, which both are influenced by the underlying polymer chains structure [26, 27]. Up to now no comprehensive analytical approach exists for the structure elucidation of neither branched polymers in general nor PC in particular, due to the high complexity of the scientific issues.

1.2 Purpose of the work

The high structural complexity of the branched polymer chains excludes the suitability of a single analytical method to gain sufficient information on the degree and type of branching [35-37] and only a combination of complementary analytical techniques promises the elucidation of the resulting highly complex distribution functions. In contrast to other techniques such as NMR, LC methods allow a separation according to molecular parameters of interest, such as molar mass or branching. Thus, the influence of the molecular metrics on the macroscopic properties can be investigated independently of each other.

Several LC approaches have already been published enabling a separation according to molecular parameters of PC. GORSHKOV et al. [38] were the first, who could apply LC to separate oligocarbonates according to their functionality, namely end-groups. A similar approach was published by COULIER et al. [39, 40] who could separate PC according to the number of hydroxyl end-groups using an isocratic eluent system consisting of chloroform ($CHCl_3$) and diethylether (DEE) in a normal-phase silica column. Furthermore, COULIER et al. extended this methodology to two-dimensional LC (2D-LC), which allowed correlating the end-group distribution with the MMD. As the hydrolytic degradation of PC is characterized by the formation of hydroxyl end-groups, thus, they could analyze the degradation behavior of the examined PC samples. However, as indicated by the analyses of GORSHKOV et al. [38], some of the analyzed end-group species strongly adsorbed on the stationary phase, which resulted in high elution volumes and very broad peaks and, thus, complicated a quantitative analysis. On the other hand, the strong adsorption on silica stationary phases might be suitable for a characterization of branched PCs since the separation is very sensitive to individual end-group structures. As every branch adds an end-group to the polymer chain, a separation according to number of branches seems possible. Therefore, the aim of this thesis is to develop new LC methods for the characterization of branched PCs, which allow a separation and identification of individual branched PC structures.

In the first part of the thesis, the potential of porous graphitic carbon (PGC), commercially available as Hypercarb™, as a new stationary phase for the analysis of PC will be examined. PGC, which has first been synthesized by KNOX et al. [41], can be considered as a reversed-phase based on polarity, yet shows a unique retention behavior, which differs from that of silica-based reversed stationary phases. The retention mechanism is a combination of dispersive London and charge-induced graphite-analyte interactions [42]. Thus, non-polar analytes are separated due to dispersive London interactions between the graphitic surface and the

analyte, whereas polar analytes can be separated as a result of charge-induced interactions, which manifest as the so-called polar retention effect on graphite [43].

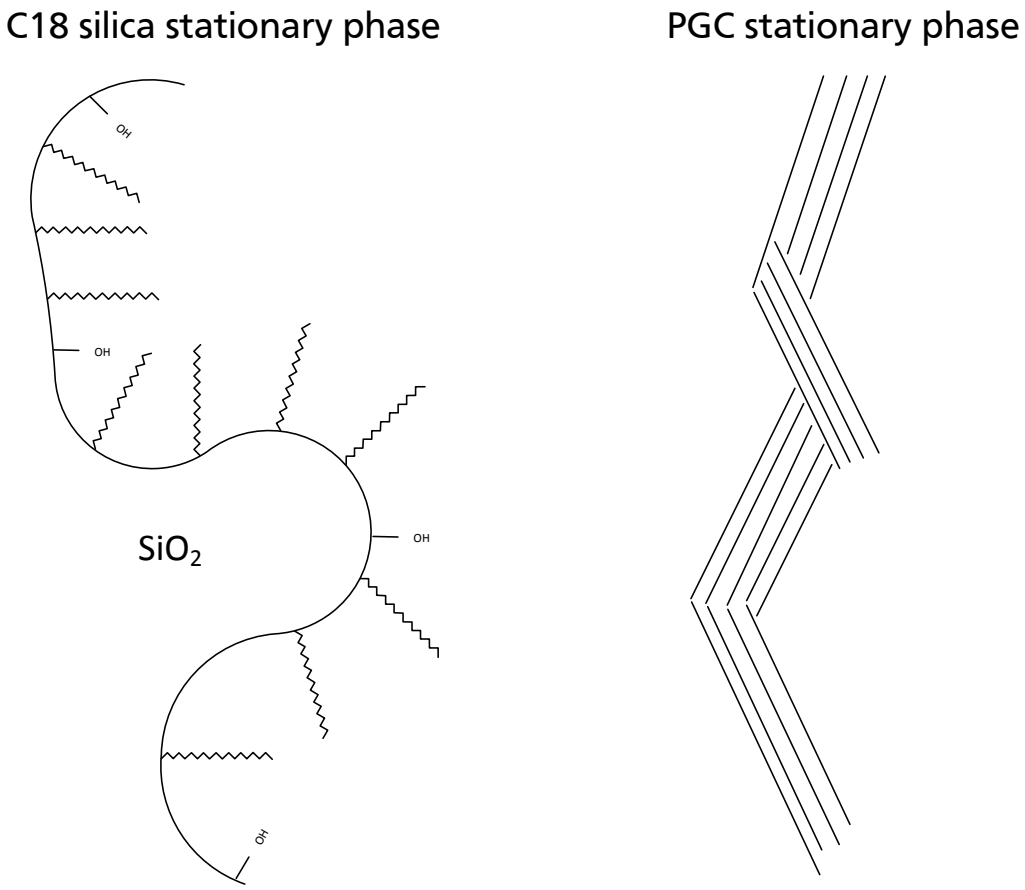

Figure 2: Schematic representation of the surface conditions of a C18 (left) and a PGC stationary phase (right). Inspired by [43, 44].

It is assumed that this effect is based on charge-transfer interactions as well as overlapping between the delocalized π-electron system of the graphite surface and free electron pairs as well as π-electrons of the solutes, respectively [44]. These interactions are highly sensitive towards the electronic density distribution of the analytes. Moreover, the orientation and the positioning of the analyte towards the graphite surface strongly influence the interactions and the retention of the solutes, as the graphene forms a planar layer structure compared with silica stationary phase materials (Figure 2) [45]. Therefore, PGC is able to separate according to the type of polar functional moiety, such as hydroxyl and carboxyl groups as has been shown for substituted benzene [46]. The crystal structure of PGC is depicted in Figure 3.

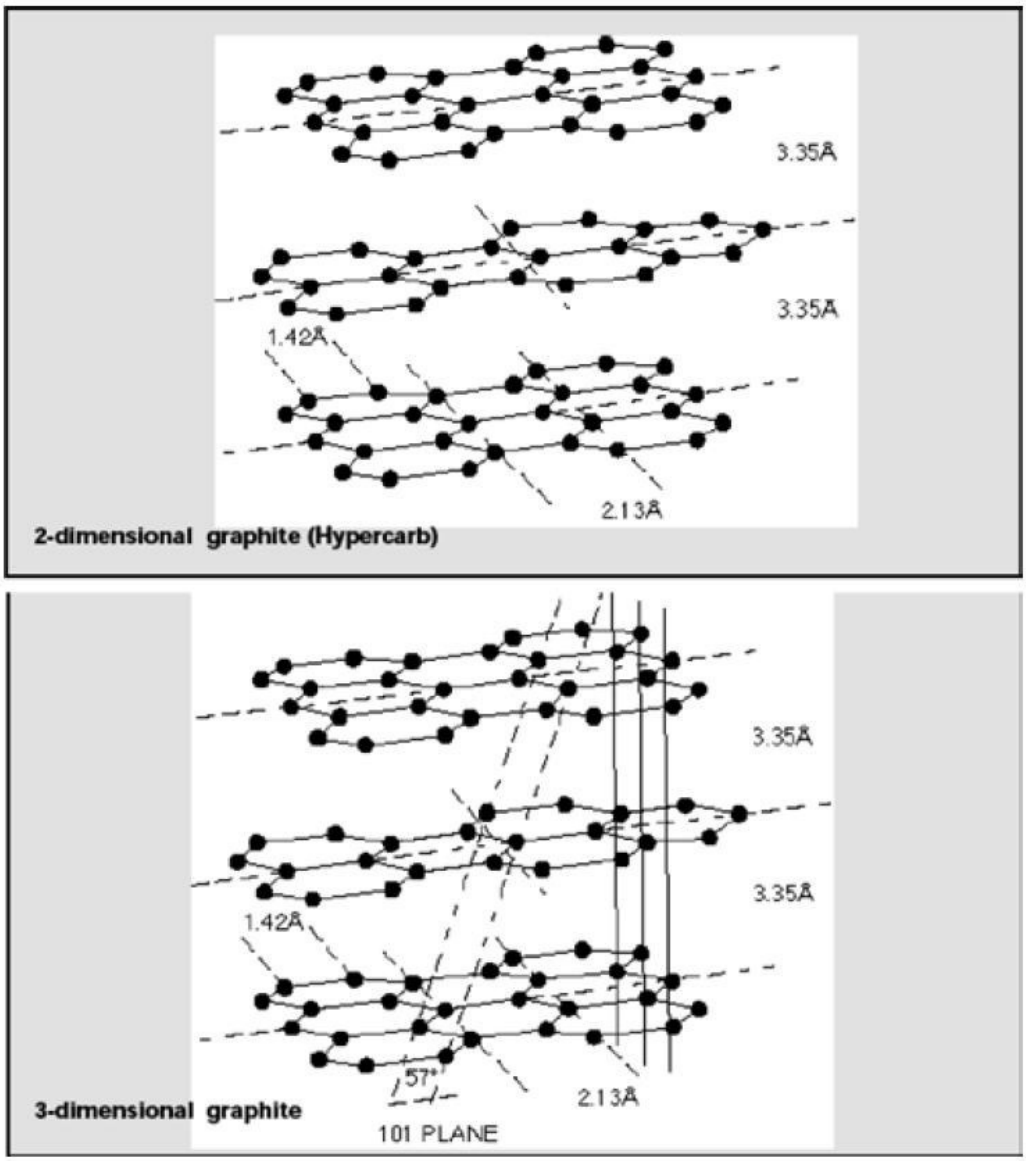

Figure 3: Crystal structures of PGC (top) and graphite (bottom). Figure taken from [42]. Permission granted. © 2008 Taylor & Francis Group, LLC.

The unique separation behavior of PGC has been exploited for small molecules such as drugs or pesticides [44]. The first application of PGC for the separation of synthetic polymers has been reported for polyolefins [47-53]. Since these are as saturated hydrocarbons typical non-polar compounds, the separation is based on dispersive London interactions. MAIKO et al. were able to separate blends of isotactic and syndiotactic PMMA applying solvent gradients in a PGC column at ambient temperature [54]. However, due to its unique retention behavior compared with silica-based column materials, PGC may allow for separation of PC to obtain new structural and functional information. Thus, chromatographic protocols have to be established for PC in a PGC column and the separation principle has to be investigated.

In the second part of the thesis, a chromatographic approach is to be developed based on the results described by COULIER et al. aiming at separating PC according to branching. In order to prove the selectivity of the separation fractions of the eluate are collected and subsequently analyzed. For that purpose, the polymer structures that are present in the single fractions can be identified by MALDI-TOF-MS according to their functionality. In order to determine the degree of branching in the individual fractions they are hydrolyzed and the decomposition products are analyzed by LC, which allows quantifying the amount of THPE present in each fraction. The developed method is then implemented in an on-line 2D-LC approach. Finally, the developed 2D-LC method will be augmented by triple-detection, comprising a concentration, a light scattering (LS) and a viscosity (VI) detector. Hence, in addition to comprehensive separation according to different molecular properties of PC, information on the solution rheology and MMD of the single polymer structures can be retrieved. The results will then be compared with those from MC simulations.

2 Theoretical part

High performance liquid chromatography (HPLC) separates components based on differences in their partition equilibrium between a mobile and a stationary phase. The distribution coefficient (K_D) of the equilibrium is defined as the quotient of the concentrations in the stationary and in the mobile phase as shown in Equation (1) [55, 56].

$$K_D = \frac{c_{stat}}{c_{mob}} = exp\left(-\frac{\Delta G}{R \cdot T}\right) = exp\left(\frac{\Delta S}{R} - \frac{\Delta H}{R \cdot T}\right) \quad (1)$$

The equilibration leads to a change in the Gibbs' free energy (ΔG) of the polymer chains. In a simplified model it is assumed that all interactions of the individual components with the stationary phase occur in the pore volume (V_P) of the separation column, whereas interactions in the interstitial volume (V_Z) are suppressed (outside the pores, cf. Figure 4 and Equation (2)) [6]. Consequently, differences in the partition equilibrium due to thermodynamic changes between stationary and mobile phase also lead to different elution volumes.

$$V_R = V_Z + K_D \cdot V_P \quad (2)$$

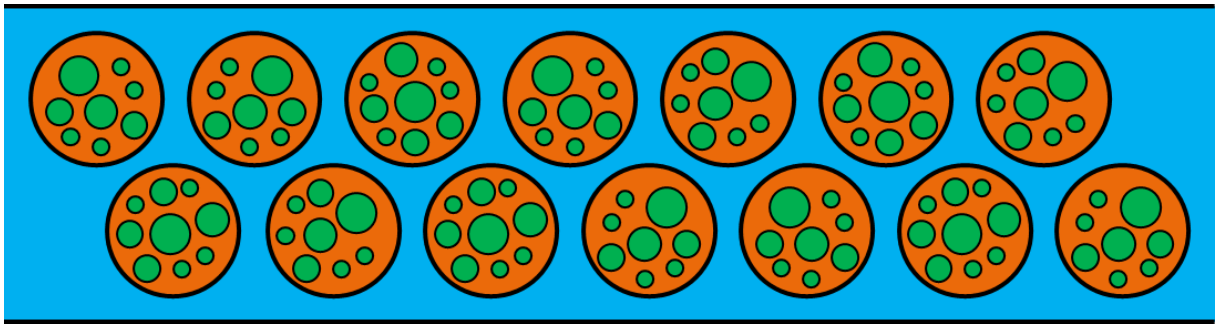

Figure 4: Schematic representation of a LC column. The column is filled with particles (orange), which contain pores of different diameters (green) [57].

The thermodynamic changes can be classified into an enthalpic and an entropic contribution. A change in the entropy (ΔS) of macromolecules is caused by their steric hindrance. Since a polymer chain has to reduce its number of conformational states upon entering a pore ΔS will be negative. At the same time changes in the enthalpy (ΔH) result from interactions of the monomer units with the stationary phase via Coulomb and/or London forces. Yet, not only

the interactions between the analyte and the stationary phase have to be considered but also those between the analyte and the eluent (preferential solvation) and between the stationary phase and the eluent (preferential adsorption) [58]. Thus, eluents can be classified into strong and weak ones, while the first-mentioned prevent adsorption and the later ones promote adsorption between the analyte and the stationary phase.

However, the eluent does not only affect the enthalpy changes, but also has an influence on the hydrodynamic volume of the polymer chains and, thus, the changes in entropy. Three boundary cases can be derived from Equation (1) simplifying the complex chemo-physical processes, which results in three chromatographic modes, being the ideal size-exclusion chromatography (SEC), liquid adsorption chromatography (LAC) and liquid chromatography under critical conditions (LCCC).

2.1 Size-exclusion chromatography (SEC)

SEC is one of the most important methods in polymer analytics to determine the MMD and the separation is based on differences in the hydrodynamic volume of the polymer coils [56, 59]. In case of ideal SEC, the absence of interactions between the analyte and the stationary phase ($\Delta H = 0$) is assumed, which requires the application of sufficiently strong eluents. Thus, Equation (1) is simplified to Equation (3).

$$K_{D,SEC} = exp\left(\frac{\Delta S}{R}\right) \tag{3}$$

Generally, there are two borderline cases for the entering of a polymer coil into a pore, which limit the chromatographic separation. If a polymer coil is sufficiently small it can occupy the same number of conformational states in the pore as outside. Consequently, these small chains do not undergo any entropy change in the pore ($\Delta S = 0$). Thus, according to Equations (2) and (3) they elute within the so called dead volume of the column (V_0) which is referred to as total permeation ($\Delta S = 0 \rightarrow K_{SEC} = 1\,;\; V_R = 1 \cdot V_p + V_z = V_0$). On the other hand, if the steric hindrance of a polymer coil is very high, the number of occupied conformational states is minimized when entering a pore and the entropy change tends to strongly negative values ($\Delta S \rightarrow -\infty$). Hence, based on Equations (2) and (3) it can be deduced that highly sterically-hindered polymer coils elute with V_z ($\Delta S \rightarrow -\infty\,;\; K_{SEC} = 0\,;\; 0 \cdot V_p + V_z = V_R$). Consequently, polymer coils with a high steric hindrance do not enter the pores in order to avoid a loss of entropy and, therefore, are completely excluded. As already described above, the separation range of the SEC is delimited by these borderline cases. Thus, in summa the separation is determined by match between the hydrodynamic volume range of the polymer coils and the characteristic pore size distribution of the chromatographic column (Figure 5) [56, 59, 60].

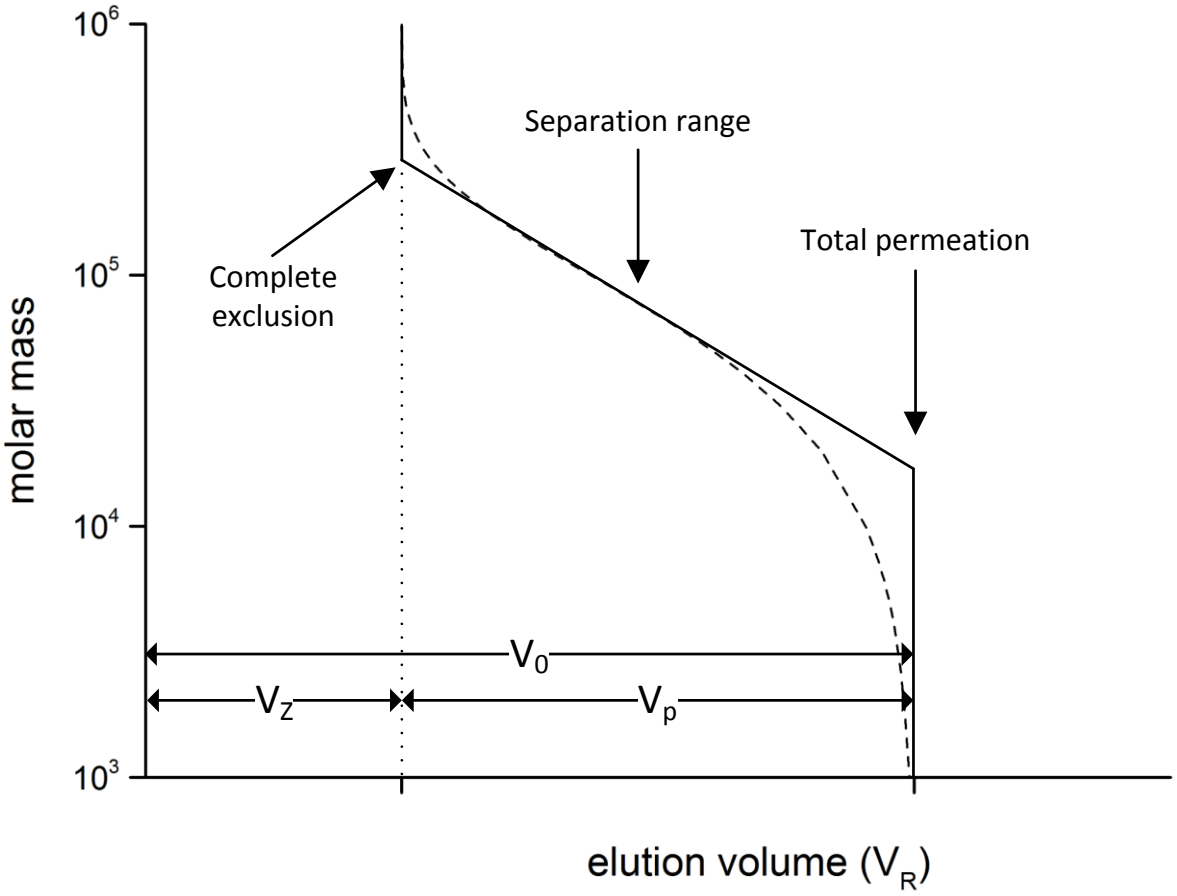

Figure 5: Limitation of the SEC separation principle. The separation range is delimited by the complete exclusion and the total permeation borderlines. Figure inspired by [60].

In order to calculate the MMD from the measured chromatograms the elution volume has to be calibrated, which is usually done by analyzing narrowly distributed standards. In this context SEC is referred to as a relative method. However, SEC can also be used as an absolute method. For that purpose, a combination of a concentration-sensitive detector (usually refractive index detector, RI) and a LS detector is installed in sequence at the outlet of the chromatographic separation column [6]. This approach allows a determination of the absolute molar masses in each elution slice. If a viscometer (VI) is additionally connected, this setup is referred to as triple-detection SEC (TD-SEC), which will be discussed in more detail in the next chapter.

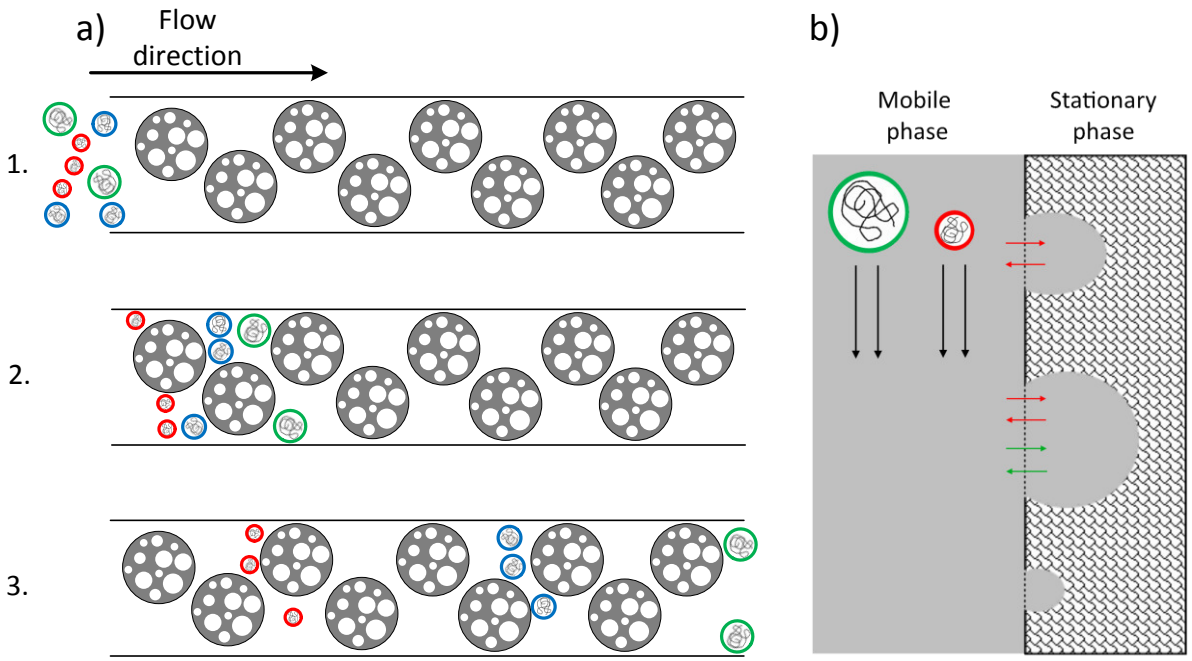

Figure 6: a) Schematic representation of the inverse sieve effect in a SEC column, which allows a separation of polymers according to their hydrodynamic volume and b) schematic representation of the separation principle of SEC. Figure inspired by [60].

2.2 Triple-detection size-exclusion chromatography (TD-SEC)

As already mentioned in section 2.1 in a TD-SEC experiment at the outlet of a SEC column, which separates a polymer according to its hydrodynamic volume, a triple-detection system, consisting of a LS detector, a concentration-sensitive detector (RI) and a VI, is installed [3]. The combination of LS and RI detector allows a determination of the molar masses ($M_{w,LS}$) in each elution slice of the SEC experiment. If a multi-angle light scattering detector (MALS) is applied in addition to the molar mass also the mean-square radius of gyration (${R_g}^2$) can be determined [3, 60].

Light scattering arises from the interaction of matter and light. The oscillating electric field component of the light induces a likewise oscillating dipole in neutral particles. From this oscillating dipole, new radiation is emitted as scattered light. Whether and to which extent a material scatters light depends on its polarizability, which is directly proportional to its specific refractive index increment (dn/dc). In principle, three different types of light scattering can be distinguished: Raman scattering, dynamic light scattering and static light scattering. In contrast to the other ones Raman scattering originates from non-elastic interactions of the radiation with the material. Hence, the wavelength of the scattered light differs from the one of the incident radiation and provides information on the chemical constitution of the analyzed materials. In case of dynamic light scattering the temporal fluctuations of the light scattering that are caused by the Brownian motion of the molecules are investigated. In SEC static scattering is usually applied that represents the temporal average of the dynamic light scattering. Equation (4) relates the intensity of scattered light for particles larger than $\lambda/20$, where λ is the wavelength of the laser light, to the properties of the dissolved polymer [61].

$$\frac{R_\theta}{K^* \cdot c} = M \cdot P(\theta) - 2 \cdot A_2 \cdot c \cdot M^2 \cdot P^2(\theta) + \cdots \tag{4}$$

$$\text{with: } R_\theta = \frac{\left(I_\theta - I_{\theta,solvent}\right) \cdot r^2}{I_0 \cdot V} = f \cdot \frac{V_\theta - V_{\theta,solvent}}{V_{laser}} \tag{5}$$

The excess Rayleigh ratio (R_θ) represents the intensity of light that is angle-dependently scattered by a sample, c is the polymer concentration in solution, M its molar mass, A_2 is the second virial coefficient, K^* is the optical constant and $P(\theta)$ describes the particle scattering fac-

tor. I_θ represents the scattered light intensity of the polymer solution, $I_{\theta,solvent}$ is the intensity of the scattered light of the solvent, I_0 is the incident light intensity, V represents the volume, where light is scattered by the polymer solution and r is the distance between scattering volume and the detector. As r and V are constants they can be summarily treated as an instrumental constant f according to the apparatus geometry comprising the geometry of the scattering cell as well as the refractive indices of the solvent and the scattering cell. The intensity of scattered light (R_θ), is measured by photodiodes and can be expressed using the voltages being V_θ, $V_{\theta,solvent}$ and V_{laser} in accordance with the respective intensities [3]. The optical constant K^* is described in Equation (6) for the case of linearly polarized incident light.

$$K^* = \frac{4\pi^2 \cdot {n_0}^2 \cdot (dn/dc)^2}{{\lambda_0}^4 \cdot N_A} \tag{6}$$

n_0 is the refractive index of the solvent at the wavelength of the incident light (λ_0), dn/dc is the specific refractive index increment of the polymer in solution and N_A is Avogadro's number. The particle scattering factor $P(\theta)$ is defined as the quotient of the intensity of scattered radiation at a specific angle (R_θ) and the intensity of scattered light at zero angle (R_0) (Equation (8)), assuming very low concentrations, which is fulfilled in case of SEC [3].

$$P(\theta) = \left(\frac{R_\theta}{R_0}\right)_{c=0} \tag{7}$$

For $\lim_{\theta \to 0} P(\theta)$ the root-mean square radius, also referred to as radius of gyration (R_g), can be extracted (Equation (8)).

$$\lim_{\theta \to 0} P(\theta) = 1 - \frac{16\pi^2}{3 \cdot (\lambda_0/n_0)^3} \cdot {R_g}^2 \cdot \sin^2(\theta/2) \tag{8}$$

An appropriate plot of the scattering intensities obtained from the MALS provides detailed information on the tested polymer. An example represents the so-called Zimm plot, which

plots $\frac{K^*\cdot c}{R_\theta}$ against $\sin^2(\theta/2)$. R_g is then determined from the slope of the curve fit i.e., the angular dependence of the light scattering intensity. Furthermore, the molar mass and A_2, which is a measure of the solvent quality, can be determined from the y-intersection in case of $c \to 0$. If a non-equimolar slice is examined, the weight-average molar mass (M_w) is obtained, which may in practice lead to an overestimation of the molar masses of samples [60].

${R_g}^2$ is strongly influenced by branching in the polymer chain. Thus, combining SEC with LS has become a popular tool for branching analysis. Branching can be quantified by branching ratio (g) comparing ${R_g}^2$ of a branched polymer at a chosen molar mass (${{R_g}^2}_{Br,M}$) with ${R_g}^2$ of a linear reference sample at the same molar mass (${{R_g}^2}_{Lin,M}$), as shown in Equation (9) and as was outlined by Zimm and Stockmayer [34].

$$g = \frac{{{R_g}^2}_{Br,M}}{{{R_g}^2}_{Lin,M}} \tag{9}$$

From the branching ratio g information on the architecture of the branched materials can be derived. However, in case of LS ${R_g}^2$ can only be accurately determined for R_g>10 nm due to loss of angular scattering dependency. To overcome this limitation a VI is frequently employed additionally to LS and a concentration-sensitive detector resulting in TD-SEC. VI allows to determine the intrinsic viscosity ($[\eta]$) of individual SEC slices, which is defined as the quotient of the specific viscosity of a polymer solution (η_{sp}) and its concentration extrapolated to zero concentration (Equation (10)) [3].

$$[\eta] = \lim_{c\to 0} \frac{\eta_{sp}}{c} \tag{10}$$

$$\text{with: } \eta_{sp} = \frac{\eta_{pol} - \eta_0}{\eta_0} \tag{11}$$

η_{sp} is the specific viscosity, η_{pol} represents the viscosity of a polymer solution and η_0 is the viscosity of the pure solvent [3]. Furthermore, $[\eta]$ is related to the hydrodynamic volume of

the polymer in solution. Thus $[\eta] \cdot M$ of a polymer is plotted against V_R and the relation between $[\eta]$ and M is determined according to the Mark-Houwink-Kuhn equation (Equation (12)).

$$[\eta] = K \cdot M^{\alpha} \tag{12}$$

Furthermore, in accordance with ${R_g}^2$ $[\eta]$ is also influenced by branching in the chain, as was described by Zimm and Kilb [62]. Thus the branching ratio in case of η can be established in a similar way to ${R_g}^2$ as shown in Equation (13).

$$g' = \frac{[\eta]_{Br,M}}{[\eta]_{Lin,M}} \tag{13}$$

Generally, g' and g can be related with each other, however, conversion requires the viscosity shielding ratio (ϵ), which is affected by a number of variables such as solvent, temperature and molar mass (Equation (14)) [60].

$$g' = g^{\varepsilon} \tag{14}$$

TD-SEC has been widely applied for branching analysis, since it provides detailed and molar-mass-resolved information on branching of polymers [35, 36, 63-65]. However, polymer chains with different degrees of branching but of same hydrodynamic volume may coelute in the same SEC elution slice and, therefore, are simultaneously detected, which leads to misinterpretations of the calculated structural information [37, 66-68]. A scheme of the TD-SEC setup is given in Figure 7.

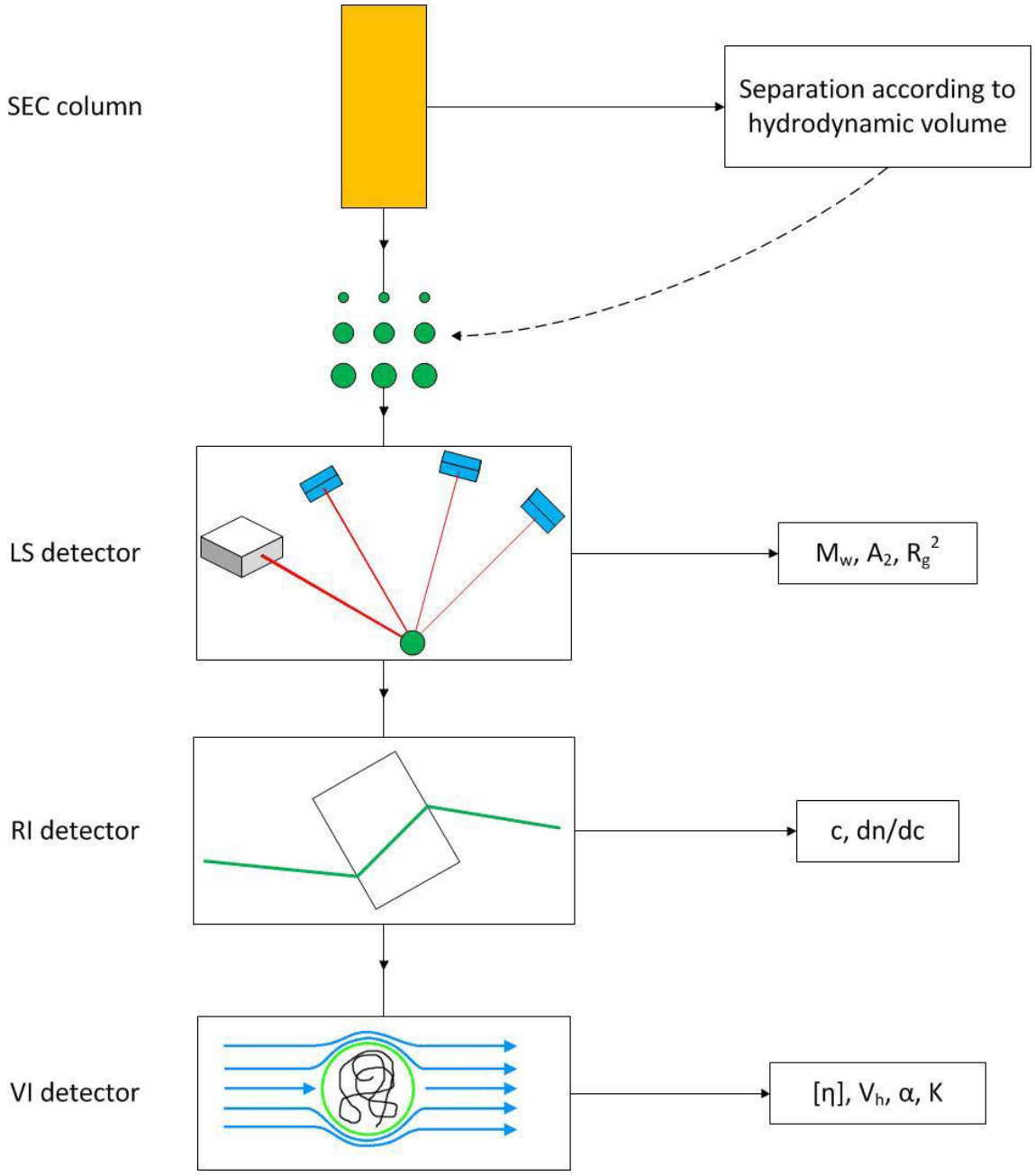

Figure 7: Schematic representation of a TD-SEC.

2.3 Liquid adsorption chromatography (LAC)

In case of liquid adsorption chromatography (LAC) the separation is based on enthalpic interactions of the macromolecules with the stationary phase [55]. Neglecting the entropic contributions Equation (1) is simplified to Equation (15).

$$K_{D,LAC} = exp\left(-\frac{\Delta H}{R \cdot T}\right) \tag{15}$$

$$V_R = V_Z + K_{LAC} \cdot V_p = V_Z + exp\left(-\frac{\Delta H}{R \cdot T}\right) \cdot V_p \tag{16}$$

Since adsorption is usually an exothermic process, ΔH is negative. The enthalpic interactions between polymer molecules and the stationary phase strongly depend on the thermodynamic quality of the solvent, or in chromatographic terms the eluent strength. While strong eluents suppress the interactions of the polymer chains with the stationary phase, weak eluents promote the interactions between the macromolecules and the stationary phase, and thus foster their adsorption [55]. In theory every repeating unit is able to interact with the stationary phase, which leads to a dependence of the chromatographic retention on the molar masses as well as the chemical composition of the polymer chains. Furthermore, macromolecules with high molar masses reveal very long retention times, since the number of repeating units, which interact with the stationary phase, is comparatively large [58, 69]. In order to shorten the analysis time and to avoid peak broadening due to diffusion processes the eluent strength is usually increased over the duration of the experiment, which can be realized by either application of gradients of mobile phase (solvent gradient interaction chromatography, SGIC) or temperature (temperature gradient interaction chromatography, TGIC) [6, 70].

The eluent composition at the injection of the sample corresponds to a weak eluent so that the polymer molecules adsorb on the stationary phase and, consequently, are retained in the column. The eluent strength is then continuously increased, so that the polymer molecules can desorb and then be eluted. As already mentioned, the eluent strength can be varied by the eluent composition (SGIC) on the one hand or by the temperature (TGIC) on the other hand, and both methods have found many different applications in polymer characterization. Examples for the separation of polymer blends and / or the corresponding block copolymers and

the determination of the comonomer distribution in statistical copolymers were comprehensively reviewed by Pasch and Trathnigg [6].

2.4 Liquid chromatography under critical conditions (LCCC)

At the transition from the entropy-dominated SEC to the enthalpy-dominated LAC a third mode exists, where the enthalpic and the entropic terms compensate each other. In that case the distribution coefficient ($K_{D,LCCC}$) becomes unity (Equation (17)) and, thus, the Gibbs free energy of the polymer backbone ($\Delta G_{backbone}$) is equal to 0, so that polymer molecules without any functional groups and with the same chemical structure elute independently of their molar mass (Figure 8) [6].

$$K_{D,LCCC} = exp\left(\frac{\Delta S_{backbone}}{R} - \frac{\Delta H_{backbone}}{R \cdot T}\right) = 1 \tag{17}$$

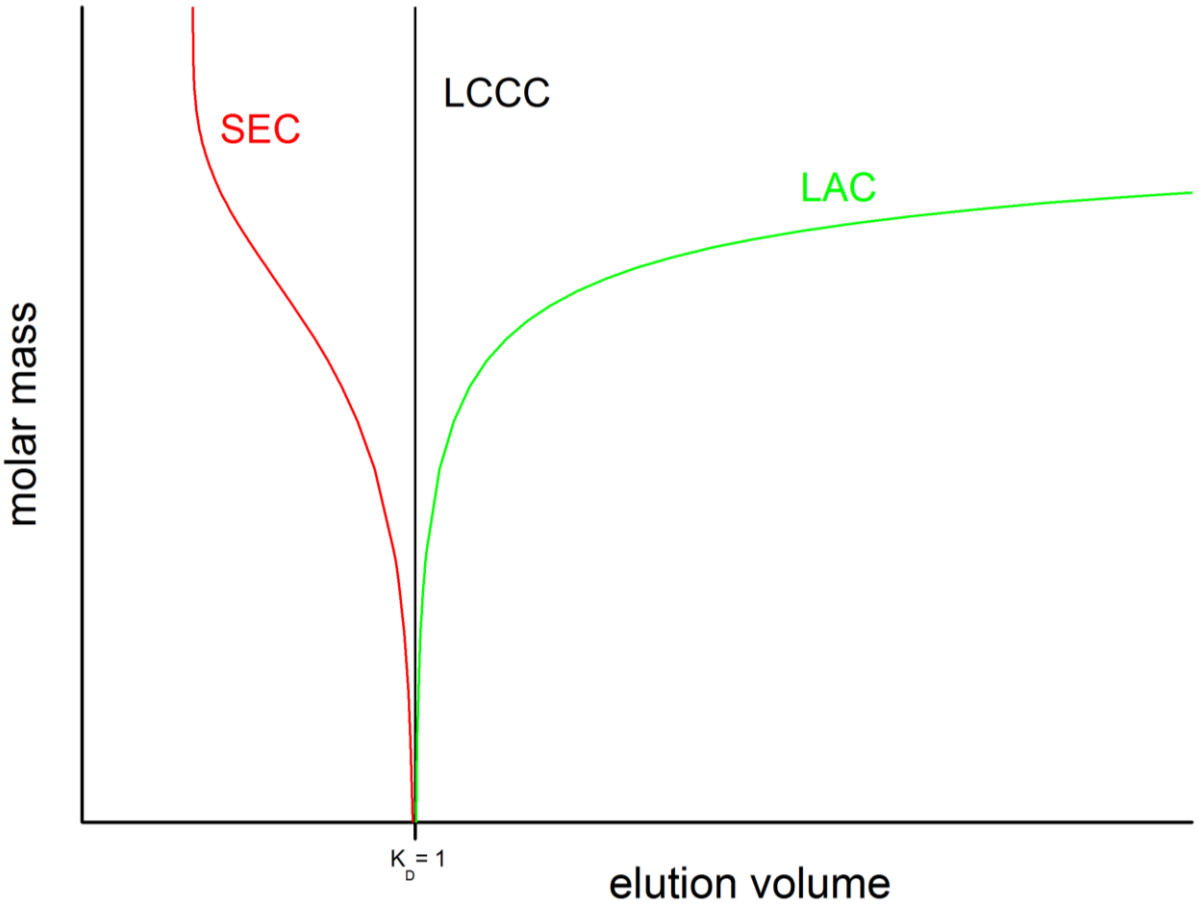

Figure 8: Schematic critical diagram. While the elution volume depends on the molar mass for LAC as well as for SEC mode, the elution is not affected by the molar mass in case of LCCC [6].

In contrast to SEC, where the separation is driven by changes in the hydrodynamic volume, and LAC, where the separation is dominated by molar mass and chemical composition, the elution in LCCC does not depend on the number of repeating units. Since LCCC occurs at an

exact thermodynamic equilibrium it is determined by a specific combination of stationary phase, temperature, and eluent composition for an analyzed polymer of a specified chemistry and microstructure (regio, stereo) [6]. However, not only the backbone but also end-groups of a polymer chain, that can also be represented by a second block in a block copolymer, contribute to the Gibbs free energy.

$$\Delta G = N \cdot \Delta G_{backbone} + \sum_{i} G_{i,end-group} \tag{18}$$

As $\Delta G_{backbone}$ is zero for LCCC the chromatographic separation is dominated by the end-groups (or a different block) of the polymer chains [71, 72]. Thus, LCCC is a very effective and an important method for investigating and quantifying the end group distributions or microstructure of polymers [47, 73-79]. Furthermore, it has found various applications for the identification of block copolymers [80, 81]. As branching in polymers may also lead to a variation of the numbers of functional (end-) groups, LCCC has also been applied to separate diverse polymer structures such as chains and stars with varying number of arms. Thus, LCCC could be employed to separate these different polymer architectures according to the number of functional groups and, consequently, according to number of branches [30, 82-85].

2.5 Two-dimensional liquid chromatography (2D-LC)

As described above, polymers are regularly distributed with regard to various molecular metrics such as molar mass, chemical composition or branching. A single chromatographic approach can theoretically separate according to only one of these molecular parameters and thus elucidate one of the polymer's distributions. However, usually chromatography concurrently separates according to different molecular parameters and, thus, interpretation of the obtained chromatograms is often complicated. For example, SEC separates according to hydrodynamic volume, which is affected by different other molecular parameters such as molar mass, degree of branching or chemical composition, which result in an overlaid separation principle. LAC, on the other hand, concurrently separates according to molar mass, microstructure and chemical composition. Therefore, applying only one characterization method it is impossible to gain comprehensive information on the molecular parameters of an analyzed polymer

Two-dimensional liquid chromatography (2D-LC), on the other hand, allows combining different orthogonal and complementary chromatographic methods within one experiment and provides more detailed information on the molecular metrics of an analyzed polymer material. For that purpose, the eluate, which has been separated in a first chromatographic dimension, is subsequently transferred into a second chromatographic dimension, which represents an orthogonal method. KILZ et al. [86] have been the first to report an automated multidimensional separation of polymers and since then 2D-LC has gained high popularity in the field of polymer analysis [49, 54, 87-90]. Although also off-line as well as stop-and-flow approaches exist, on-line 2D-LC using an automated transfer valve has found the most use. It benefits from both complete automation as well as quantitative sample transfer and, in the end, quantification of single components is possible, which allows for a more detailed investigation of the analyzed samples [91]. To interpret the outcomes 2D contour plots can be constructed. In these the corresponding detector response, which is acquired after the second dimension, is plotted color coded, while the axes of the contour plot correspond to the elution volumes or times in the first and second dimension, respectively (Figure 9).

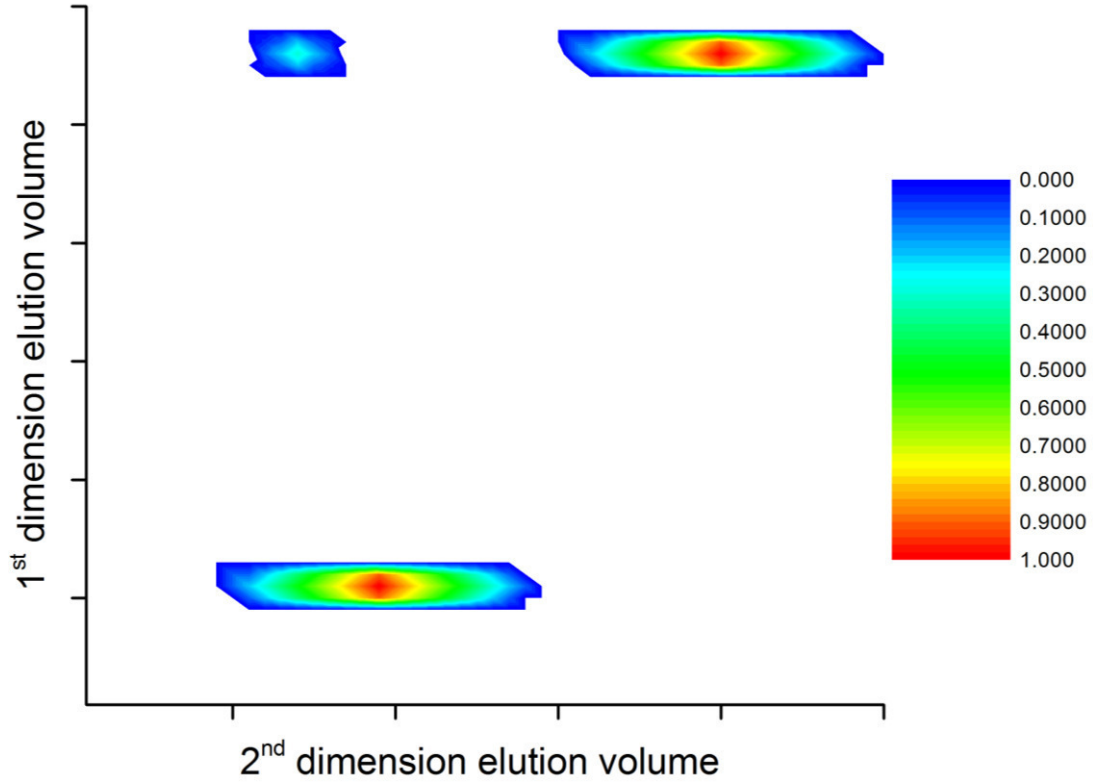

Figure 9: Schematic representation of a 2D contour plot. The detector responses are color-coded plotted against the corresponding elution volumes of the first and the second chromatographic dimension, respectively.

3 Results and discussion

3.1 Chromatographic investigations of PC using a PGC column[2]

3.1.1 Determination of the critical conditions in the eluent system $CHCl_3$/TCB and $CHCl_3$/DCB

As was outlined in section 2 the elution volume may be influenced by the molar mass of the analyzed sample depending on the chromatographic mode, namely LAC, LCCC or SEC. To establish LCCC conditions of PC on a PGC stationary phase, a specific combination of temperature and eluent composition has to be identified, at which the elution becomes independent of the molar mass of the polymer. Initially, an eluent system consisting of an adsorption promoting and desorption promoting eluent has to be selected. $CHCl_3$ is widely used as eluent for SEC measurements, as it is a good solvent for PC [92]. Although $CHCl_3$ has been stated as strong eluent for PGC earlier [93], adsorption of PC on PGC was observed. Thus, for the first time $CHCl_3$ could be applied as an adsorption promoting eluent for PGC in polymer analysis. On the other hand, dichlorobenzene (DCB) and trichlorobenzene (TCB) were used as desorption promoting eluents for PGC in a number of studies [47-49, 94]. Therefore, these were also tested in the present case and showed good desorption promoting efficiency for PC.

Five PC standard samples (PC1-5) with varying molar masses as listed in Table 9 were measured at a temperature of 25 °C with different isocratic eluent compositions of $CHCl_3$/TCB to analyze the dependence of the elution volume on the molar mass. The corresponding critical diagram for $CHCl_3$/TCB is depicted in Figure 10. The chromatograms of samples PC1-5, which were acquired at the critical conditions are shown in Figure 11.

[2] Parts of the displayed figures, tables, theoretical considerations and text segments, which are presented in this section, have been published by me as sole first author in N. Apel et al., J. Chromatogr. A, 1488, 77-84 (2017)

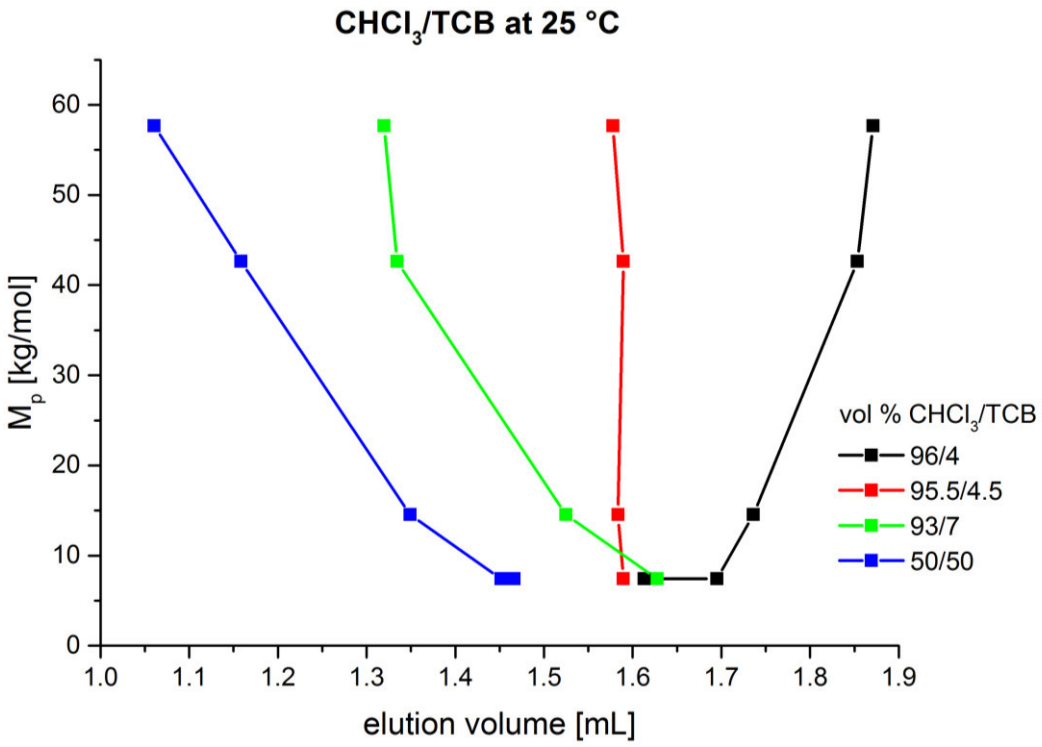

Figure 10: Critical diagram of PC in a PGC stationary phase in the mobile phase system $CHCl_3$/TCB at 25 °C. In order to plot the critical diagram the retention volumes of the first eluting peak of each sample were chosen, since some samples eluted in more than one peak. It has to be mentioned that the peaks of samples PC1 and PC2 overlap for the measurements with eluent compositions of 95.5/4.5 vol% and 93/7 vol% $CHCl_3$/TCB, so they seem to appear as a single point in the critical diagram [95].

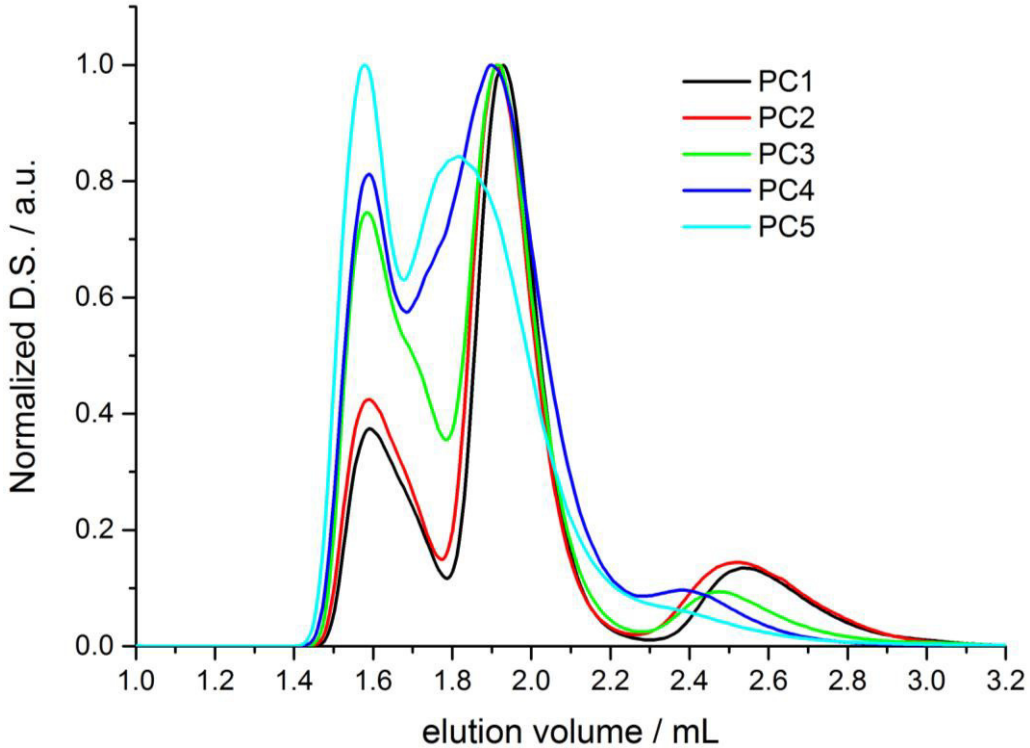

Figure 11: Overlaid chromatograms of PC1-PC5 at the critical conditions in a PGC stationary phase at 25 °C corresponding to an eluent composition of 95.5/4.5 vol% $CHCl_3$/TCB [95].

It becomes clear that for eluent compositions of 50/50 vol% and 93/7 vol% $CHCl_3$/TCB samples of higher molar masses elute earlier than those of low molar mass i.e., the PC samples elute in SEC mode for these conditions. Contrary to that, the molar mass dependence on the elution volume is reversed for an eluent composition of 96/4 vol% $CHCl_3$/TCB, which is indicative of LAC mode. The molar mass dependence of the elution volume vanishes at an eluent composition of 95.5/4.5 vol% $CHCl_3$/TCB i.e., the elution occurs at the critical point for that solvent composition.

In a similar manner the critical diagram can be established for the mobile phase system $CHCl_3$/DCB at a temperature of 25 °C, where critical conditions are found at an eluent composition of 85/15 vol% $CHCl_3$/DCB at 25 °C (Figure 12).

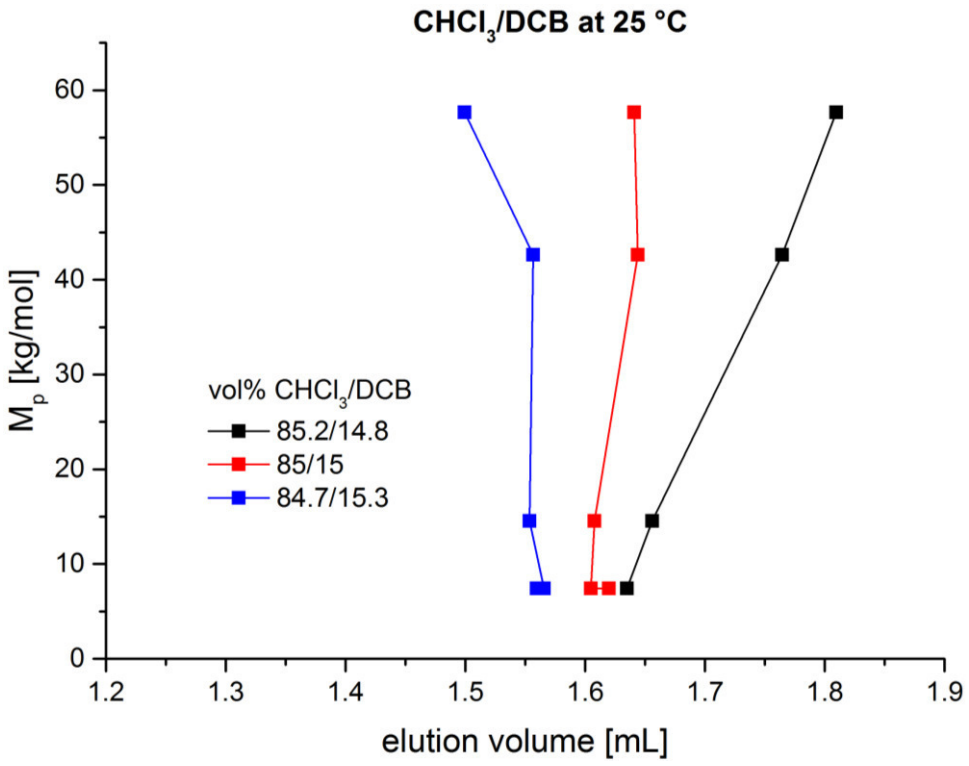

Figure 12: Critical diagram of PC in a PGC stationary phase in the mobile phase system $CHCl_3$/DCB at 25 °C [95].

The fact that the content of DCB, which serves as desorption promoting eluent, is distinctly higher (15 vol%) at the critical conditions than that of TCB (4.5 vol%) at the same temperature strongly indicates that TCB is a stronger desorption promoting eluent than DCB.

3.1.2 End-group separation at the critical conditions

As shown in Figure 11 for the eluent system $CHCl_3$/TCB the chromatograms of the commercial PC standards, which were used for the determination of the critical conditions, reveal distinct peaks. Hence, based on LCCC theory, it may be speculated that the peak splitting originates from heterogeneity with regard to end-groups. Furthermore, PC6, which is an additional standard sample and which has a weight-average molar mass close to that of PC1 but reveals a lower dispersity index, shows a distinct peak and only two small shoulders, as can be seen in Figure 13. Thus, it may be assumed that PC6 differs from the other samples with regard to the type of end-groups. To verify that MALDI-TOF-MS analyses of PC1 and PC6 were performed. The corresponding spectral subsets are presented in Figure 14 and Table 1 shows the structures, which could be identified from the MALDI-TOF-MS data.

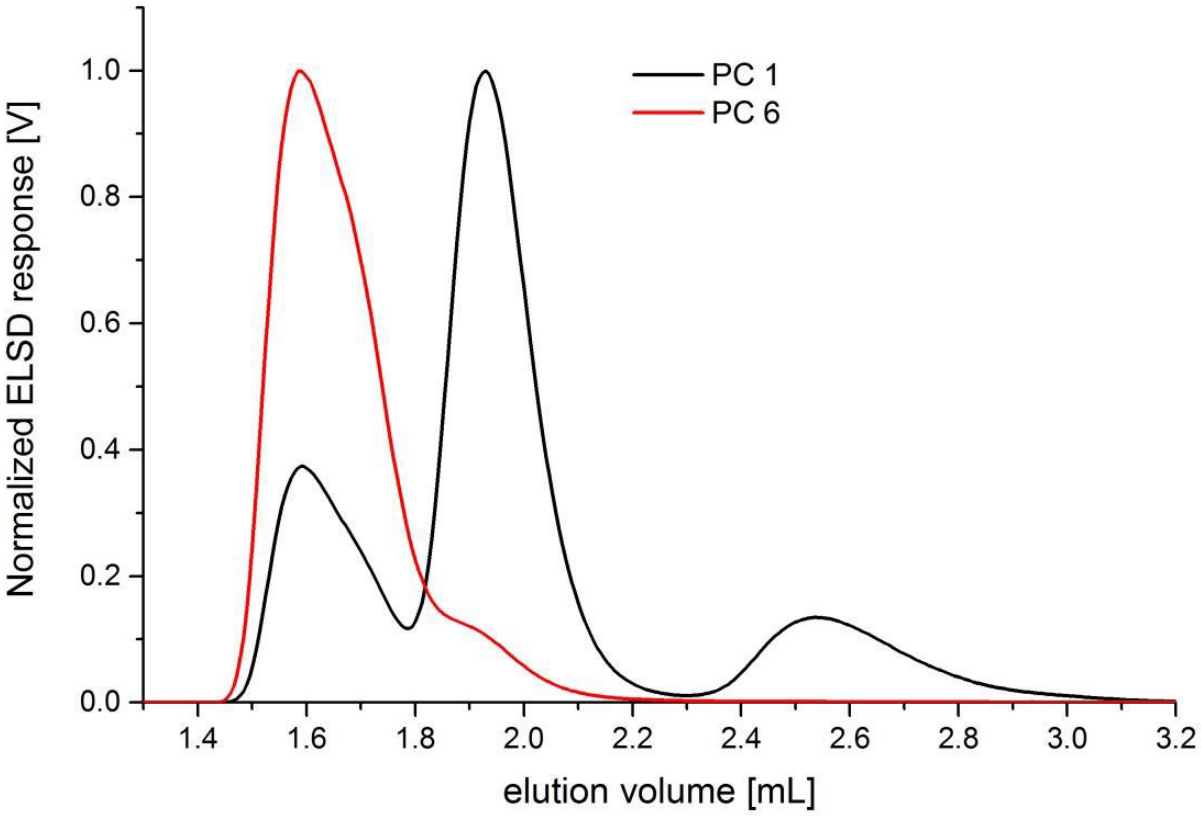

Figure 13: Overlaid chromatograms of PC1 and PC6 at the critical conditions (95.5/4.5 vol% $CHCl_3$/TCB) in a PGC stationary phase at 25 °C [95].

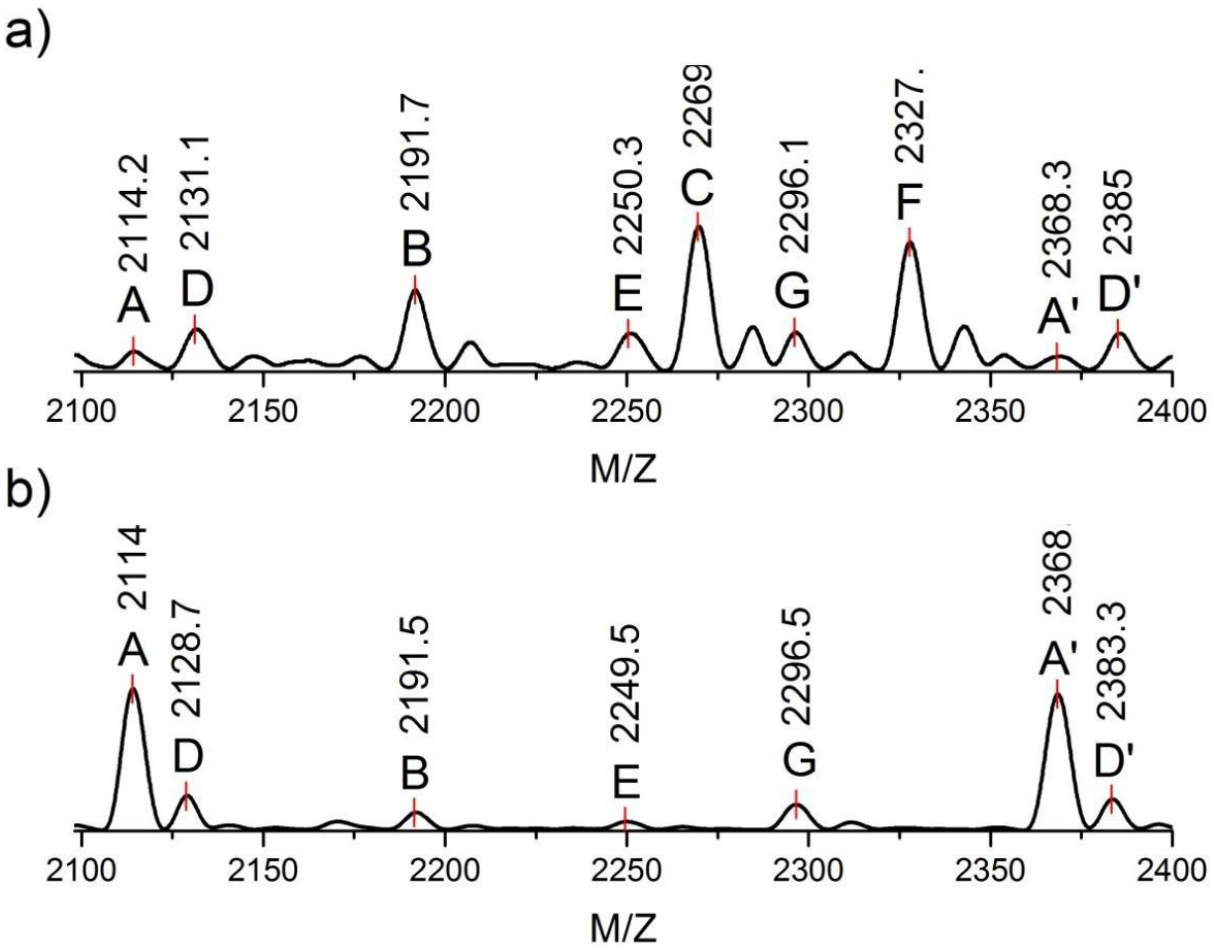

Figure 14: MALDI-TOF mass spectra of PC1 (a) and PC6 (b), revealing the different end-group compositions of PC1 and PC6 [95].

Table 1: Polymer structures as well as the oligomer masses detected in the mass spectra of PC1 and PC6 (Figure 14) [95].

Series in Figure 14	Polymer structure	Number of PC repeat units	Theoretical mass (Li^+ adduct) / Da
A A’	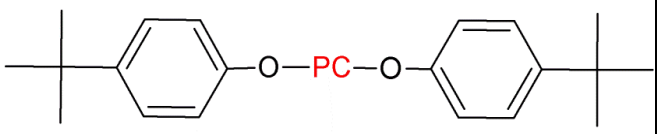	7 8	2113.2 2367,5
B	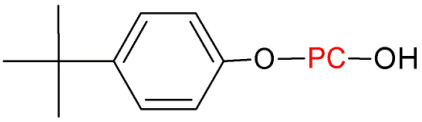	8	2191.3
C	HO—PC—OH	8	2269.4
D D‘	H_3C—O—PC—O—CH_3	8 9	2131.2 2385,4
E	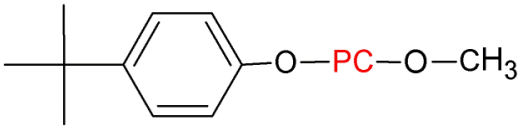	8	2249.3
F	H_3C—O—PC—OH	9	2327.4
G	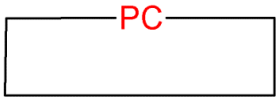	9	2295.4

Based on the MALDI-TOF mass spectra clear differences in the end-groups of PC1 and PC6 can be identified. The fully end-capped structure A clearly dominates in the spectrum of PC6 while other structures such as B, D and E can only be found in minute quantities. On the other hand, a variety of different end-groups is present in PC1. Only small amounts of the fully end-capped structure A and the statistically formed cyclic by-product G, which are usually present in all commercially available PCs and PC standards, can be identified. Interestingly, significant amounts of methoxy end-capped structure D were observed, which are untypical end-groups for PC. These might result from the PC synthesis from dimethyl carbonate and bisphenol A [96]. An alternative explanation is also the formation as a result of incomplete end-capping

during the production process and the subsequent precipitation in methanol, as has been described by KRICHELDORF et al. [97].

It might be speculated that samples, which contain distinct amounts of methoxy end-groups, are more prone towards degradation and, thus, a higher variety of end-groups is formed. PRYDE et al. [5] reported that the presence of uncapped species strongly influences the hydrolysis and thus the degradation of PC. As analyzed by IR and UV spectrometry this effect was explained by the formation of polar clusters of the hydroxyl end-groups within the PC matrix. Since polar clusters cause a higher water retention the polymer is more prone towards hydrolysis in that regions (Figure 15) [5].

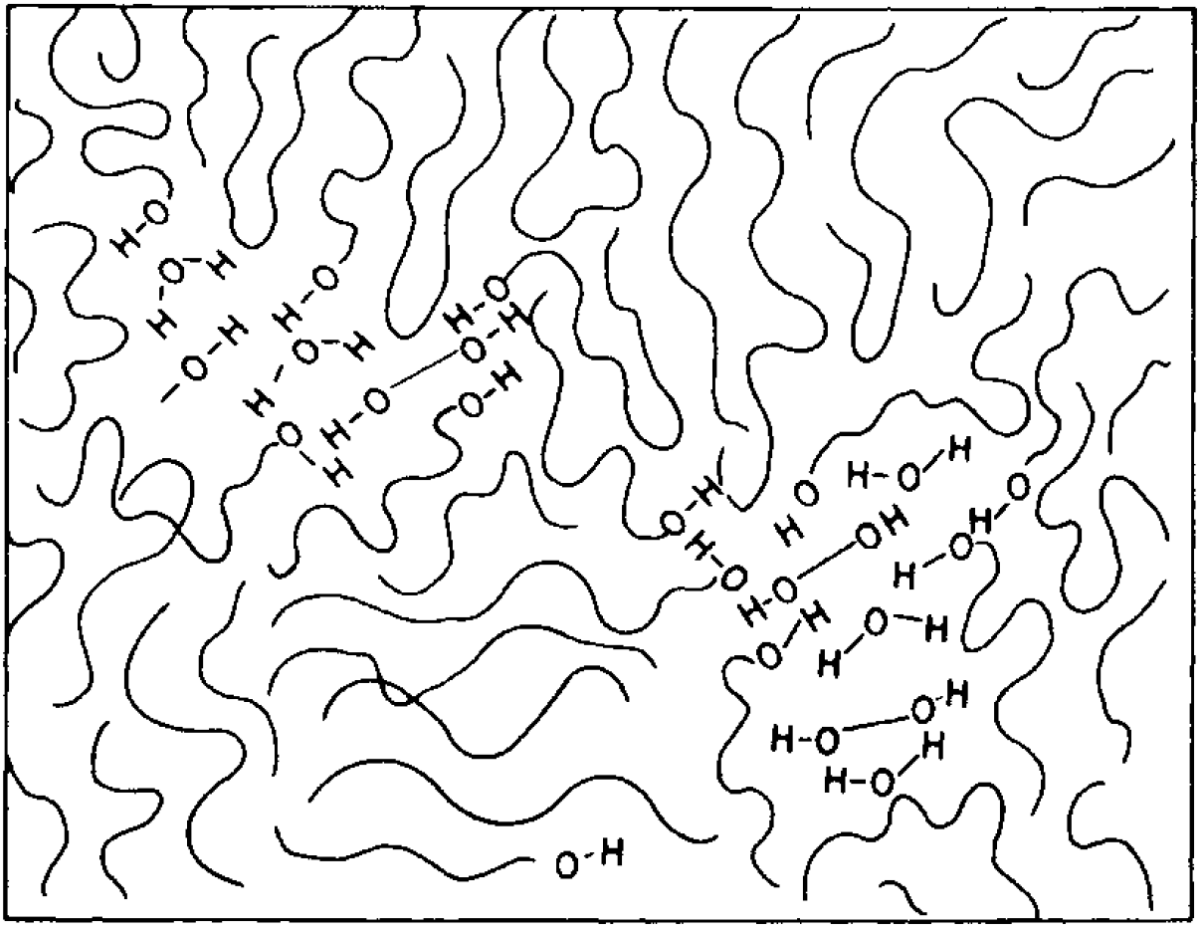

Figure 15: Schematic two-dimensional representation of the agglomeration of hydroxyl end-groups in a PC matrix. Figure taken from [5] Permission granted. © 1980 John Wiley & Sons, Inc..

The methoxy end-groups that could be identified for PC1 may also form polar clusters within the PC matrix. Thus, water can also be retained in these regions leading to higher degradation rates. This assumption is supported by the increased contents of B, C and F in PC1, which represent typical degradation products of PC due to hydrolysis and should only be present in mi-

nor amounts in PC standards [98-100]. Moreover, PC1 has a much broader MMD than PC6, which is indicated by a higher dispersity index (Table 9). That also confirms the occurrence of degradation in PC1, therefore, leading to a variety of different end-groups, as was demonstrated by MONTAUDO et al. [100].

In order to validate if the separated peaks that could be found at the critical conditions correspond to an end-group separation, the eluting fractions were isolated for sample PC1 at the critical conditions of $CHCl_3$/DCB and the collected material was analyzed after workup by MALDI-TOF-MS (Figure 16).

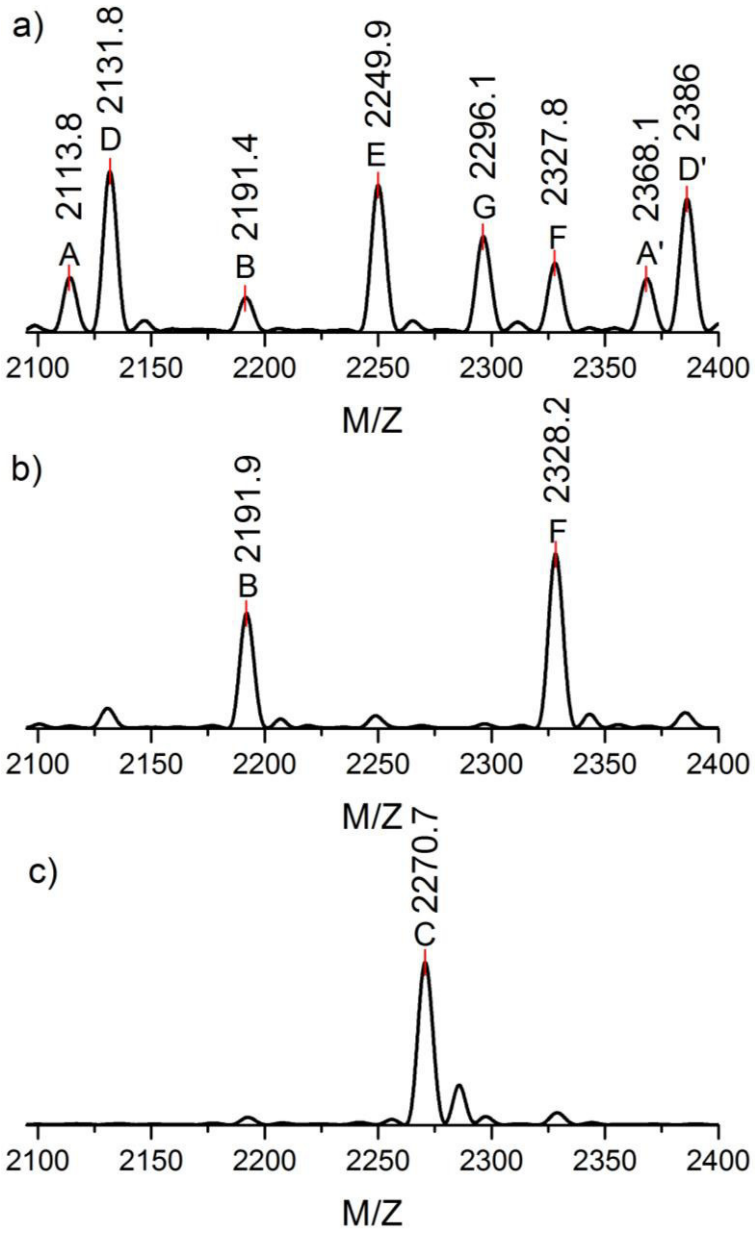

Figure 16: MALDI-TOF mass spectra of PC1 fractions corresponding to the three peaks observed in LCCC. a) first, b) second and c) third peak (Figure 13) [95].

The MS results confirm a separation according to end-groups: While A, D, E, G dominate in the first fraction (Figure 16 a), B and F can be found in minor quantities. As the latter are the sole structures in the second fraction (Figure 16 b), it might be speculated that these are present in the first fraction due to overlapping of the chromatographic peaks. On the other hand, fraction three shows only structure C (Figure 16 c). Thus, it can be confirmed that the LCCC separation in the PGC column is driven by the content of hydroxyl end-groups based on the polar retention effect on graphite. Unfortunately, the MALDI-TOF-MS analyses of the fractions could not show a separation of A, D, E and G. However, minute shoulders in the first peak at about 1.6 mL (Figure 13) indicate a limited separation. Since these species show a low polarity a separation based on the polar retention effect on graphite might be difficult. An exact quantification of the end-group levels is complicated by the fact that no baseline separation could be achieved.

3.1.3 Temperature influence on the end-group separation at critical conditions

To evaluate if end-group separation at critical conditions can be improved by varying the temperature the critical conditions for the eluent system $CHCl_3$/TCB were established at 5 °C and 57.5 °C, in an analogue procedure to the one described above for a temperature at 25 °C. The critical diagrams are shown in Figure 17.

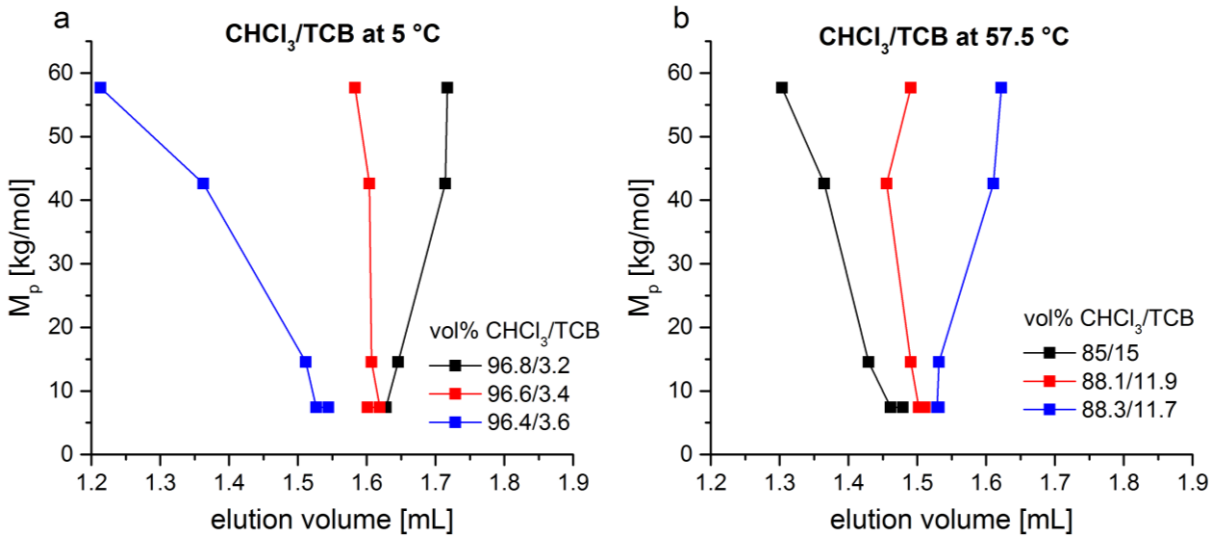

Figure 17: Critical diagrams of PC in a PGC stationary phase in the mobile phase system $CHCl_3$/DCB at a) 5 °C and b) 57.5 °C [95].

The eluent composition of the critical conditions at 5 °C was found to be 96.6/3.4 vol% $CHCl_3$/TCB, while at 57.5 °C LCCC was obtained at 88.1/11.9 vol% $CHCl_3$/TCB. In general, a temperature change influences the free Gibbs' energy (ΔG), which has to be maintained at zero to preserve LCCC mode. Hence, in order to compensate for the effect of temperature and to maintain LCCC the eluent composition has to be adjusted (Equation (17)) [101]. In the present case this means that the higher the temperature the higher the content of desorption promoting eluent, namely TCB, in order to achieve critical conditions. Contrary to that it is expected that an increase in temperature would lead to weaker interactions between the stationary phase and the analyte based on van't Hoff's equation, since adsorption is an exothermic process [58]. Yet one has to keep in mind that not only the interactions between the analyte and the stationary phase, but in addition those between the analyte and the eluent (preferential solvation) and between the stationary phase and the eluent (preferential adsorption) have to be taken into account to explain the observed shift in the mobile phase composition at the critical point [58].

In order to investigate how the temperature affects the separation with regard to hydroxyl end-groups at critical conditions a melt-produced PC sample (PC7, Table 9) was analyzed (Figure 18). As the end-capping in the melt process is incomplete, this sample contains additional hydroxyl end-groups and, thus, the separation efficiency can be better compared.

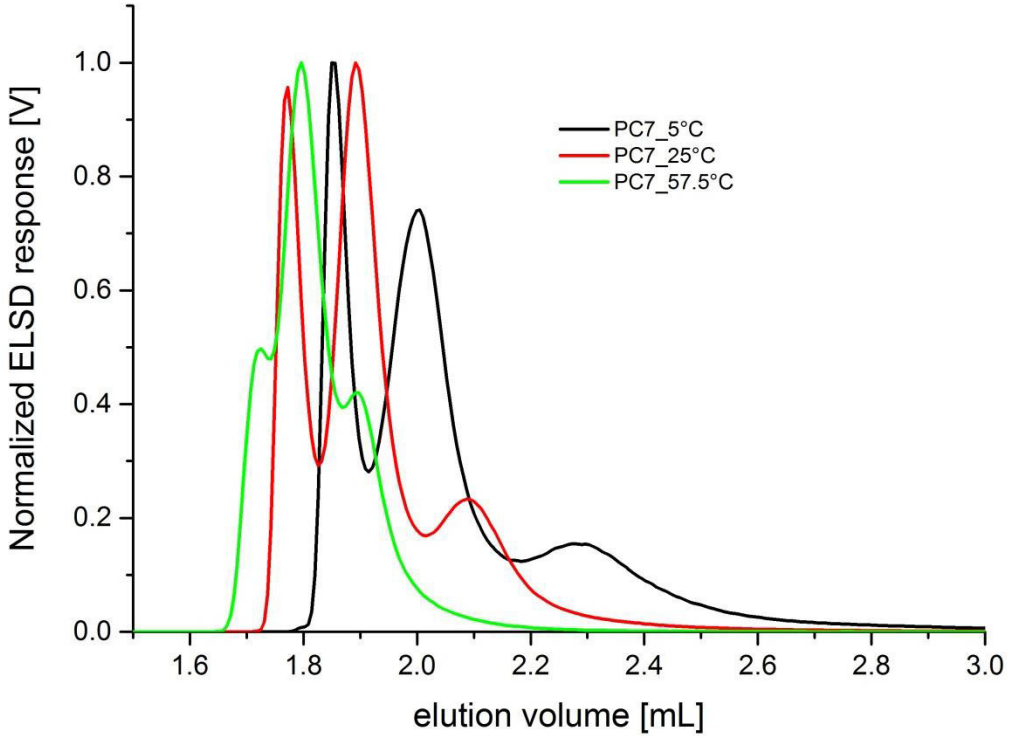

Figure 18: Chromatograms of PC 7, obtained at critical conditions at 5 °C (black curve), 25 °C (red curve) and 57.5 °C (green curve), respectively [95].

It is obvious that the best peak separation is achieved at a temperature of 5 °C (black curve), while the poorest peak separation appeared to be at a temperature of 57.5 °C (red curve). The better separation at lower temperatures might be explained by the higher contents of desorption promoting eluent (TCB) that are required to attain LCCC at elevated temperatures: It might be assumed that a higher TCB content in the mobile phase intensifies the interactions between the PGC and the TCB due to π-π stacking of the TCB on the PGC surface. Thus, the interactions between the end-groups of the PC and the stationary phase are suppressed, ultimately leading to a deterioration of the peak separation.

Besides, it can be recognized that the lower the applied temperature, the higher the elution volume of the first peak, indicating that the hold-up volume is not constant, which has also been observed by other authors and was explained by thermal expansion of the stationary phase [102].

3.1.4 Recovery rate determination

In the course of the studies presented in sections 3.1.1 to 3.1.3 it could be recognized that the eluent compositions required for critical conditions were not completely constant and that with ongoing time the elution volumes of the analytes increased. To compensate for that small adjustments in the eluent composition were required to maintain LCCC. In Figure 19 the effect of time (days elapsed since the column was placed in the oven) on the chromatogram of PC7 is shown as obtained under critical conditions.

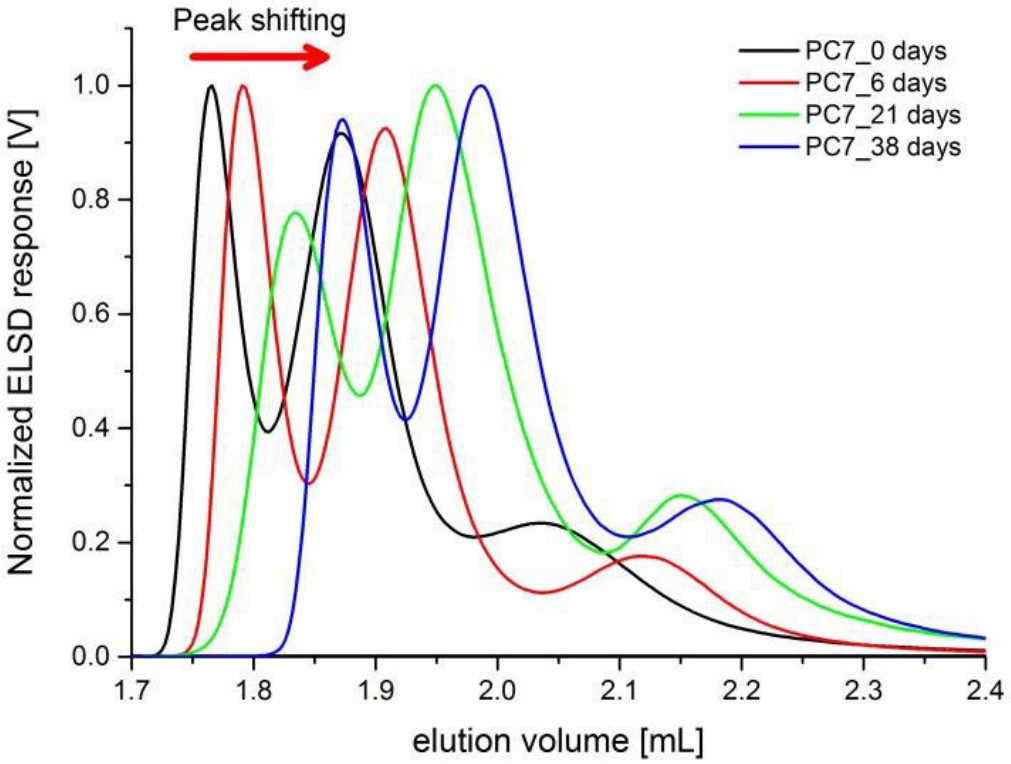

Figure 19: Progress of the peak-shifting phenomenon over time [95].

The observed peak shifting towards higher elution volumes upon prolonged use of the PGC column might be caused by several factors: On the one hand, the purity of TCB, which was used for the chromatographic analysis, is usually in the range of 99 %, and the content of impurities, such as other regio-isomers as well as chlorobenzene and dichlorobenzene, may vary from batch to batch. Furthermore, it might be speculated that small amounts of an injected PC sample are irreversibly adsorbed on the graphitic surface and, therefore, influence the elution behavior of subsequently injected samples. To probe this hypothesis the recovery rates were analyzed.

Unfortunately, a recovery rate determination by RI detection is complicated, since the refractive indices and the vapor pressures of $CHCl_3$ and TCB differ significantly. Hence, solvent and polymer sample signals strongly overlap, even when the samples are dissolved in the exact solvent composition corresponding to the eluent composition. An ELSD can also not be applied for recovery rate determination, as the detector signal depends in a non-linear mode on the polymer concentration as well as on the eluent composition [103]. Consequently, an IR detector was installed, which allows quantifying the characteristic carbonyl stretching vibration of PC at 1770 cm^{-1}, as can be seen in Figure 20, and thus, enables a solvent-independent detection.

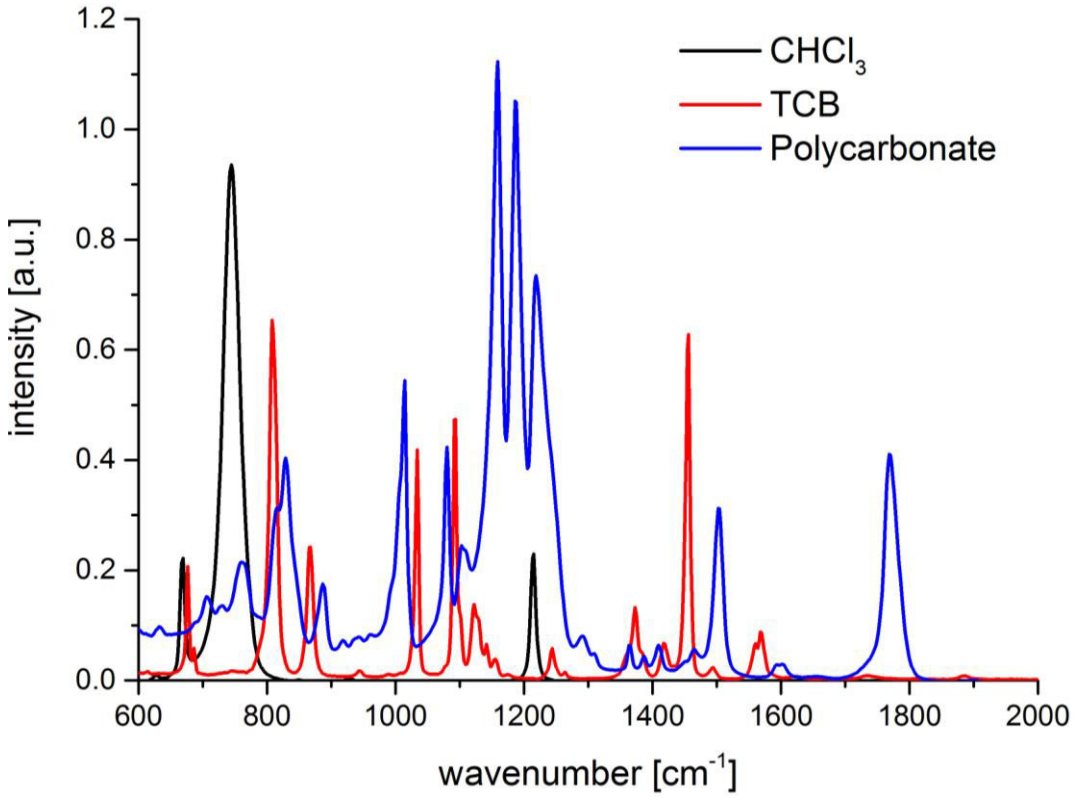

Figure 20: Overlaid ATR-FTIR spectra of $CHCl_3$, TCB and PC [95].

Figure 21 shows the IR spectra of PC and TCB in the distinctive range of the characteristic carbonyl stretching vibration of PC at 1770 cm^{-1}. To avoid overlapping with the small TCB peak in the range of 1730 cm^{-1} only half the peak is integrated, which is a common procedure for quantifications in FT-IR analysis [104]. The integration and baseline limits are listed in Table 2.

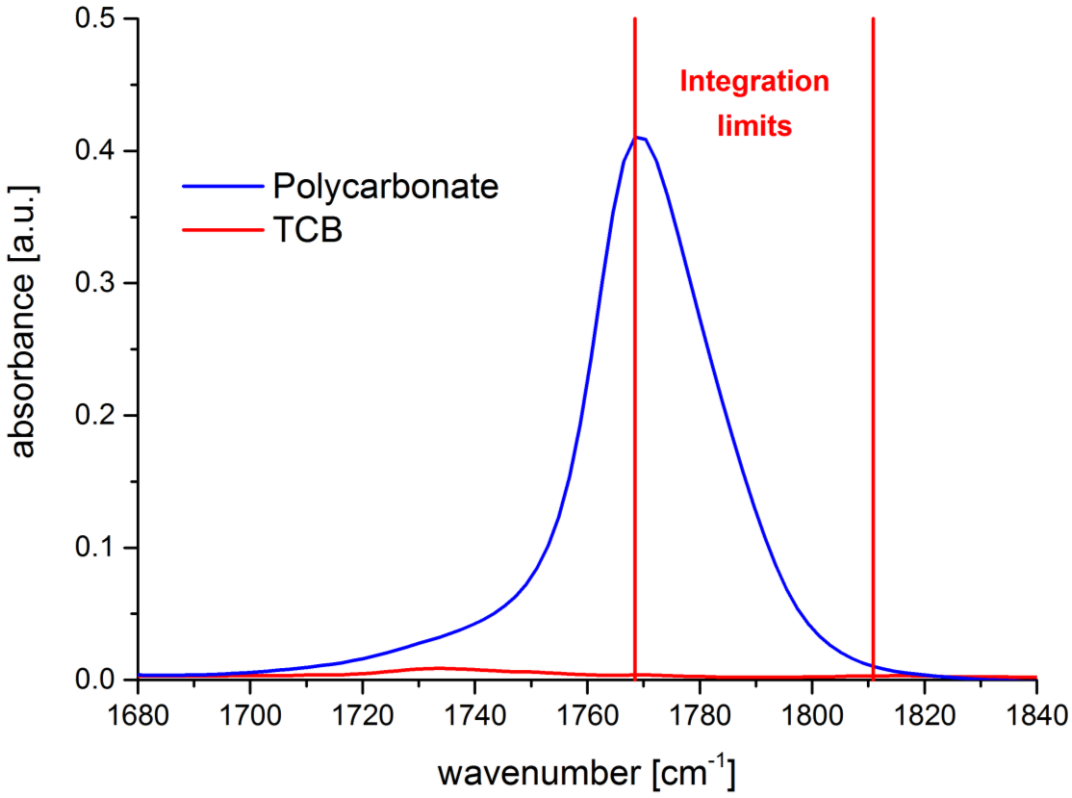

Figure 21: Section of the ATR-FTIR spectra of PC and TCB that are used for the determination of the PC recovery rate [95].

Table 2: Integration and baseline limits for the determination of the recovery rate with an FT-IR spectrometer [95].

Integration limits / cm^{-1}	baseline limits / cm^{-1}
1810 - 1770	1840 - 1690

In order to determine the recovery rate a calibration curve was constructed by installing a capillary instead of the PGC column and measuring the PC samples three times for different concentrations. Subsequently, the PGC column was re-installed and the procedure repeated. The single chromatograms are integrated and the calibration curve is plotted from the averaged values. This approach was then repeated for the other PC samples. A typical chromatogram is shown in Figure 22 while the calibration plot of PC5 is schematically depicted in Figure 23, respectively. The determined recovery rates of PC1, PC3 and PC5 are listed in Table 3. The standard deviation (Δ) was determined from three repeat measurements of each sample and at the different analyzed concentrations.

Table 3: Determination of the recovery rate using a FT-IR flow cell detector [95].

Sample	PC1	PC3	PC5
Recovery rate [%]	100	100	98
Δ [%]	13	12	12

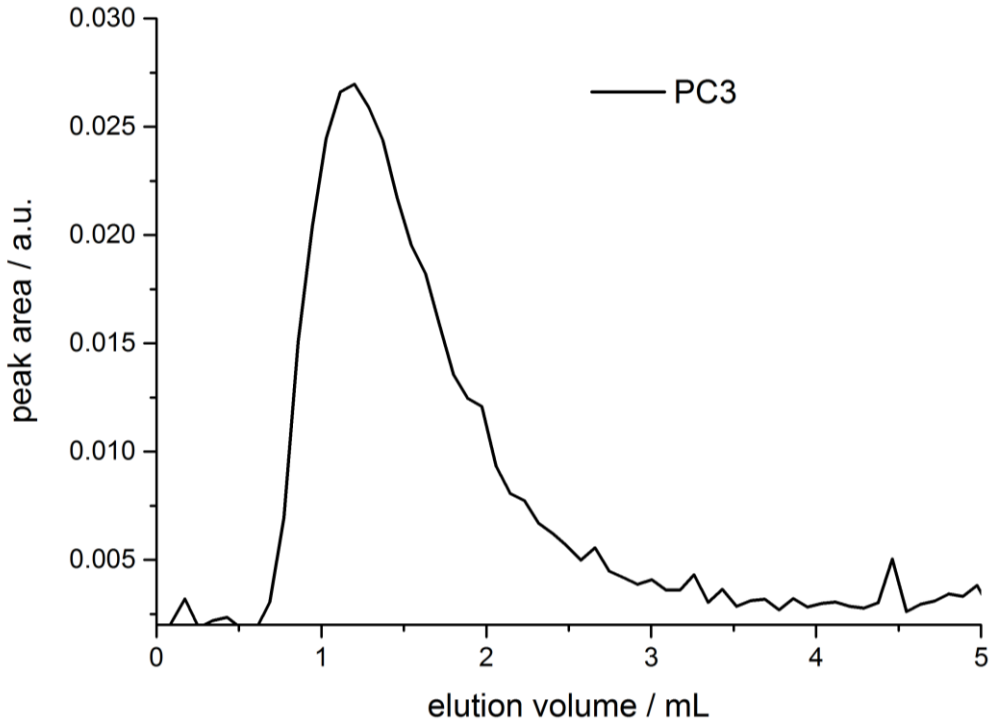

Figure 22: Obtained chromatogram, applying the integration and baseline limits as listed in Table 2 for all acquired spectra [95].

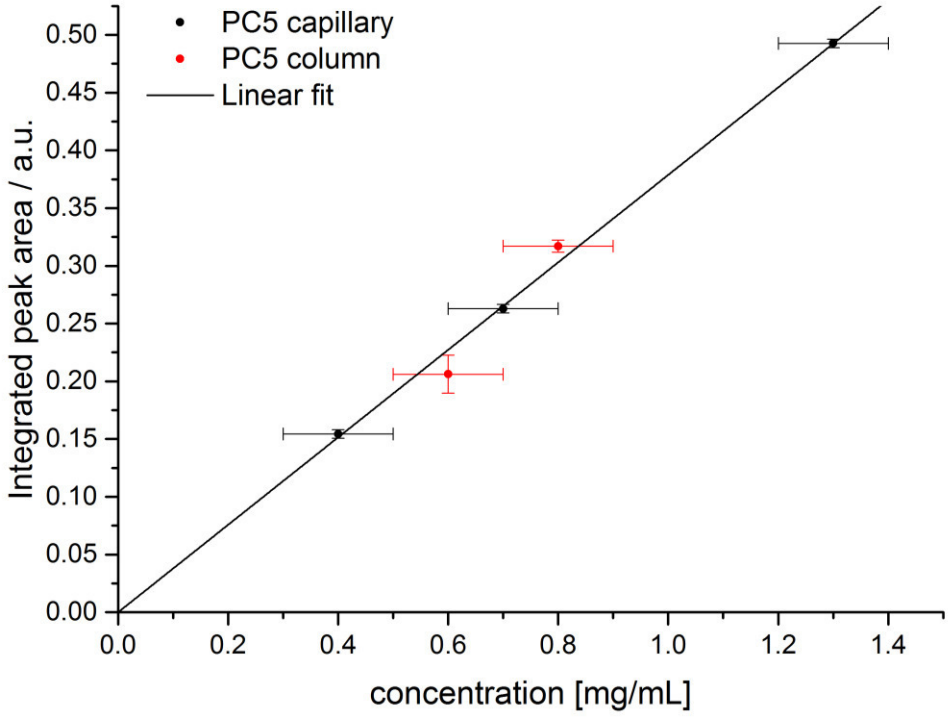

Figure 23: Determined calibration curve and obtained results with the installed column for PC5 [95].

PC1 and PC3 show recovery rates close to 100 %. Due to the high standard deviation that was determined from the three repeat measurements and the different concentrations the recovery rate for PC 5 statistically is also close to 100 %. Although the experiments indicate complete recovery, the formation of a mono- or multilayer of PC on the PGC surface may still not be ruled out. Similar observations were described for the adsorption of alkanes on graphitic surfaces by WAWKUSCHEWSKI et al. who showed that complex alkane mono- and multilayers were formed at the liquid/graphite interface [105]. As such mono- or multilayers of PC on the PGC surface can strongly influence the interactions between the stationary phase and the analyte, the retention as well as the critical eluent composition might be affected, which can explain the peak shifting phenomenon. Since PC mono- or multilayers can already be formed by minute amounts of PC, recovery rates of 100 % are not contradictious.

3.1.5 Influence of branching on the separation of PC at critical conditions

As outlined in section 2.4 and demonstrated in the previous sections for PC, LCCC basically separates according to the number of functional groups of a polymer chain. As branching of polymers may lead to a variation in the numbers of functional (end-) groups, LCCC might also be employed to separate branched PC according to the number of functional groups and, consequently, according to the number of branches in the polymer chain. In order to test this assumption a partially un-capped and branched PC sample (PC8, Table 9) was tested at critical conditions for PC. The corresponding chromatogram is depicted in Figure 24.

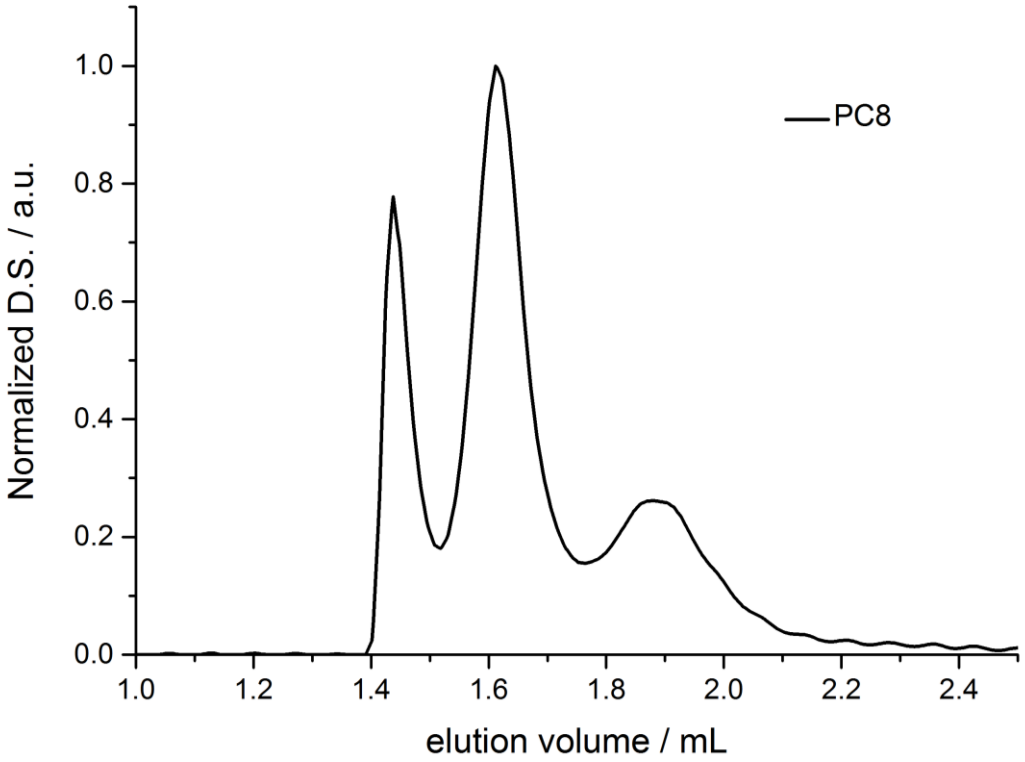

Figure 24: Chromatogram of PC8 at the critical conditions on a PGC stationary phase at 25 °C corresponding to an eluent composition of 95.5/4.5 vol% $CHCl_3$/TCB.

Unfortunately, the chromatogram of PC8 completely corresponds to the one of PC7 and it does not reveal any additional peaks, which might indicate a separation according to branched structures. Thus, although predicted by theory, critical conditions of PC on a PGC stationary phase are not a suitable way to achieve a separation according to branching. A possible explanation for that outcome might be that the separation in the present case is not only influenced by the number of hydroxyl end-groups, but the presence of the branching agent (THPE) affects the separation at critical conditions. Since the THPE is incorporated in the backbone of the polymer chain, $\Delta G_{backbone}$ might differ from 0 according to Equation (17)

and, hence, the conditions for LCCC are not fulfilled anymore. Thus, it might be speculated that elution for these branched polymer chains occurs in HPLC mode instead of LCCC, where the polymer is completely retained on the stationary phase. Consequently, their detection is not possible under these conditions.

3.1.6 Summary

Conditions for LCCC of PC were established on a PGC stationary phase applying the eluent systems $CHCl_3$/TCB and $CHCl_3$/DCB. A separation of PCs according to their end-group moiety was found, which could be confirmed by MALDI-TOF-MS analyses of the eluting fractions. The influence of temperature on the eluent composition at LCCC was examined and an improved end-group separation was observed at lower temperatures. It can be speculated that this outcome results from the reduced content of desorption promoting eluent that is required to establish LCCC at lower temperatures, thus, allowing enhanced interactions between the end-groups and the stationary phase at these conditions. However, no baseline separation of PC could be achieved according to end-groups, which complicates an exact quantification of the relative end-capping levels. The recovery was found to be in the range of 100 %. In order to probe if LCCC on a PGC stationary phase enables a separation of PC according to branching, a branched PC sample was analyzed. Although a separation according to end-capping could be achieved, no additional peaks were found and consequently no separation according to branched structures is indicated.

3.2 Chromatographic investigations of PC using a normal-phase column[3]

3.2.1 Solvent gradients at near-critical conditions (SG-NCC)

As outlined in section 3.1.5, LCCC with a PGC as stationary phase did not provide a separation of PC according to branched structures. Although critical conditions hold great potential for a separation of PC according to branching due to differences in the end-capping functionality, the observed peak shifting phenomenon as well as the potential formation of PC monolayers may complicate further investigations with the PGC columns. Therefore, it was decided to apply a normal-phase silica stationary phase, since that column material has been used for LCCC of PC in earlier studies.

COULIER et al [39, 40] established the critical conditions of PC on a normal-phase silica stationary phase applying a mobile phase with $CHCl_3$ and DEE as adsorption and desorption promoting eluents, respectively. Under these conditions a strong adsorption of the uncapped chains was found [39, 40]. In order to examine if these LC method is able to achieve a separation of PC according to branching the sample PC8 (branched and partially un-capped, Table 9) was measured under these conditions. The corresponding chromatogram is depicted in Figure 25.

[3] Parts of the displayed figures, tables, text segments and theoretical considerations, which are presented in this section, have been published or are about to be published by me as sole first author:

N. Apel et al.: "Separation of Branched Poly(bisphenol A carbonate) Structures by Solvent Gradient at Near-Critical Conditions and Two-Dimensional Liquid Chromatography", Submitted, 2018

N. Apel et al.: "Correlation between comprehensive 2D liquid chromatography and Monte-Carlo simulations for branched polymers", In Preparation, 2018

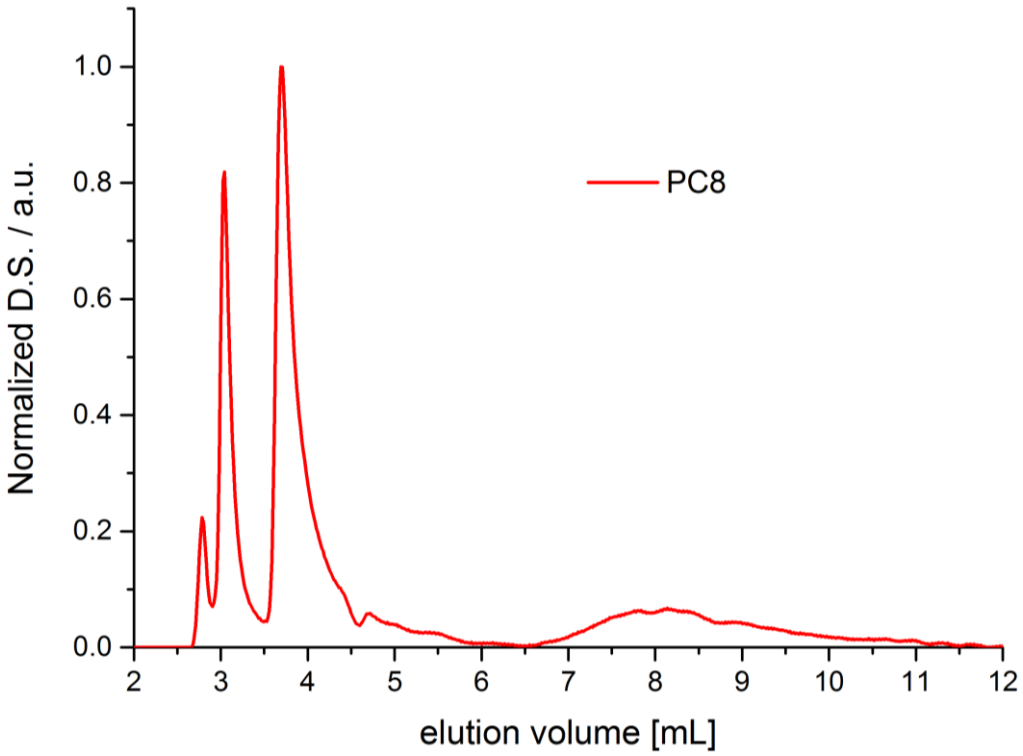

Figure 25: Chromatogram of sample PC8 at critical conditions of COULIER et al. [39, 40].

Based on the experiments of COULIER et al. it can be concluded that the two peaks eluting at about 3 mL correspond to fully end-capped PC and the cyclic species, while the peak at 4 mL represents the partially end-capped PC. The broad peak at 7-8 mL can be related to PC bearing two hydroxyl end-groups. Due to the strong peak broadening as well as the incomplete baseline separation the quantification of the corresponding structures is challenging. Furthermore, branched PC species that contain more than two hydroxyl end-groups may be retained longer than 12 min on the stationary phase and might elute in even broader peaks, which gives rise to resolution and sensitivity issues of these species. Thus, the method is not suitable for a separation according to branching based on number of functional end-groups.

On the other hand, the strong adsorption of the hydroxyl end-groups at the critical conditions on a normal-phase silica stationary phase bears high potential to separate PC according to branched structures. FALKENHAGEN et al. [106] developed the method of near-critical conditions (NCC), which could separate a poly(ethylene oxide) (PEO)-co-polymethylene (PM) model oligomer according to the PM chain length. For that purpose, the critical conditions of PEO were established in a first step. FALKENHAGEN et al. then found that slight changes towards adsorption mode simultaneously improved the characterization of chemical and molar mass heterogeneities and, thus, the identification of the PM chain-lengths in the PEO-co-PM oligomer was improved.

In the present study, to exploit the separation principle of LCCC, on the one hand, and to reduce issues related with resolution and band broadening, on the other hand, a novel chromatographic technique is applied, which is named solvent gradient at near-critical conditions (SG-NCC) and extends the NCC principle. For the application of the method in the present case, the LCCC determined by COULIER et al. served as a starting point.

COULIER et al. used $CHCl_3$ as adsorption promoting eluent and DEE as desorption promoting eluent. The latter has a low boiling point and is highly inflammable and, thus, causes safety concerns and issues in handling. During this study it could be found that the low boiling point of DEE complicated the mixing of the eluents, which caused problems in the reproducibility of the results. Therefore, it was decided to replace DEE by MTBE as desorption promoting eluent for further investigations with SG-NCC [107].

As the content of MTBE that is required to completely desorb PC from the normal-stationary phase is very low, in a first step, a 97.5/2.5 vol% $CHCl_3$/MTBE premixed solution was used as desorption promoting eluent. This allows exploiting the full scale of the gradient pump and, therefore, improving the accuracy and reliability of the applied eluent composition, which is an important consideration for the application in SG-NCC. Samples PC7-9, which differ in end-capping and degree of branching as shown in Table 9, are subjected to SG-NCC. The chromatograms of these samples are shown in Figure 26 applying a mobile phase gradient from $CHCl_3$ to a premixed $CHCl_3$/MTBE solution according to Table 10 on a silica column.

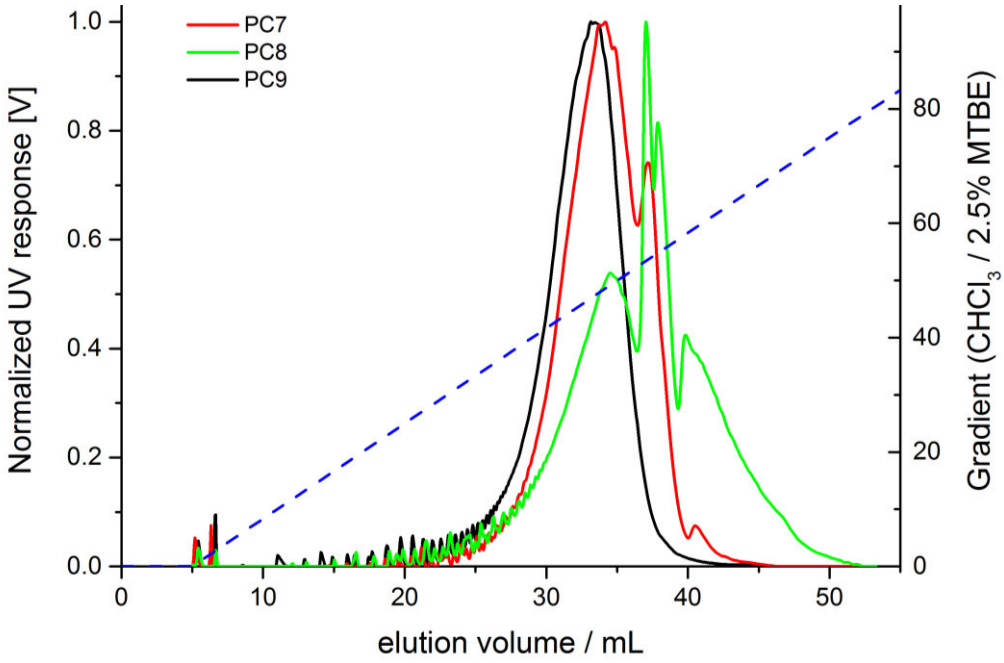

Figure 26: Chromatograms of PC7 (red), PC8 (green) and PC9 (black) in the applied mobile phase gradient $CHCl_3$→97.5 % $CHCl_3$/2.5 % MTBE. The dotted line shows the corresponding gradient [108].

Clear differences can be identified in the chromatograms of the different samples in SG-NCC. While PC9 (linear and end-capped) elutes in a single peak, PC7 (linear and partially un-capped) shows an additional peak at about 37 mL. Based on the differences in the degree of end-capping of the two samples it might be speculated that the additional peak corresponds to uncapped PC structures (C, D) which are illustrated in Table 4. Besides, another peak appears at about 40 mL. As will be discussed in section 3.2.3 this peak might originate from rearrangement reactions of the PC chains, which lead to the formation of additional functional groups along the PC chains.

Except for the additional peak at 37 mL, PC8 (branched and partially un-capped) reveals a further peak at about 38 mL and a long tail after 40 mL. Although the exact origin of these peaks is unclear at this point, based on the fact that PC8 is a branched sample it can be suspected that these conditions allow differentiating between branched and linear PC structures. Furthermore, the peaks of all samples reveal oscillation of the detector response in the elution range from 5 to 28 mL, indicating a separation of various oligomers, which shows that the chromatographic separation is also influenced by the molar mass as can be expected from theory (section 2.3).

In order to elucidate the origin of the additional peaks in the chromatograms of the PC samples the single peaks that occur in the chromatogram of PC8 were collected. After workup the collected fractions were analyzed by MALDI-TOF-MS. The fractions were collected as shown by the limits in Figure 27. MALDI-TOF mass-spectral subsets of the collected fractions are shown in Figure 28.

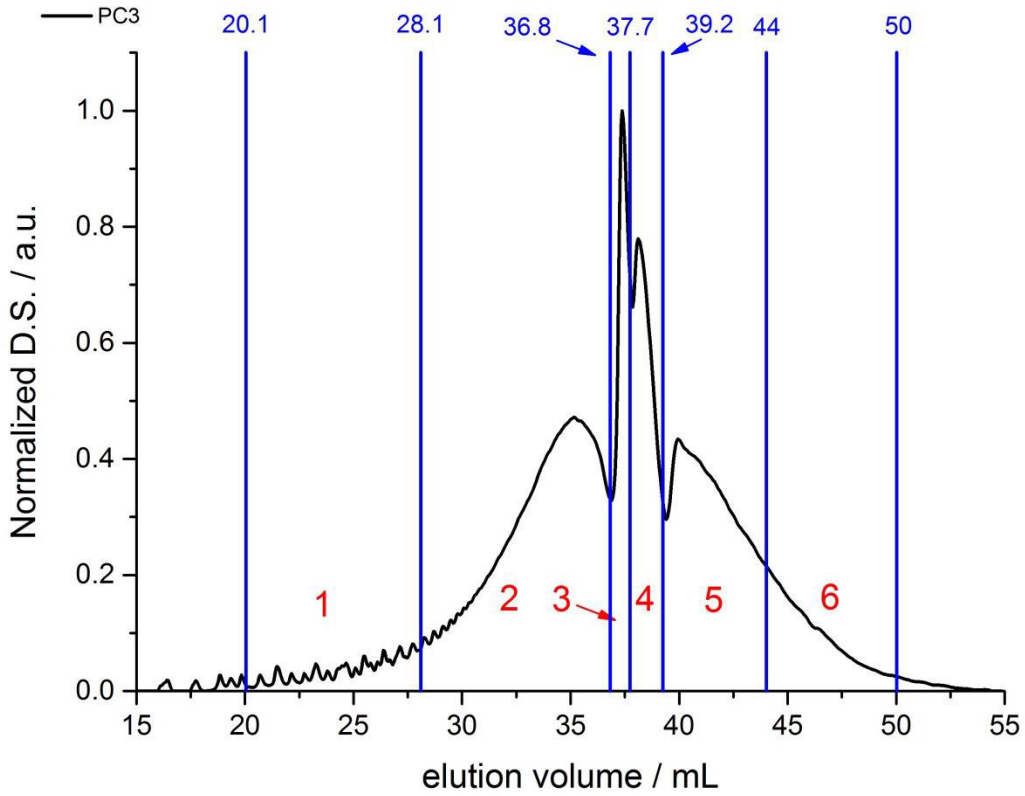

Figure 27: Limits of the collected fractions in the chromatogram of PC8, obtained in the mobile phase gradient $CHCl_3 \rightarrow CHCl_3$/2.5 % MTBE [108].

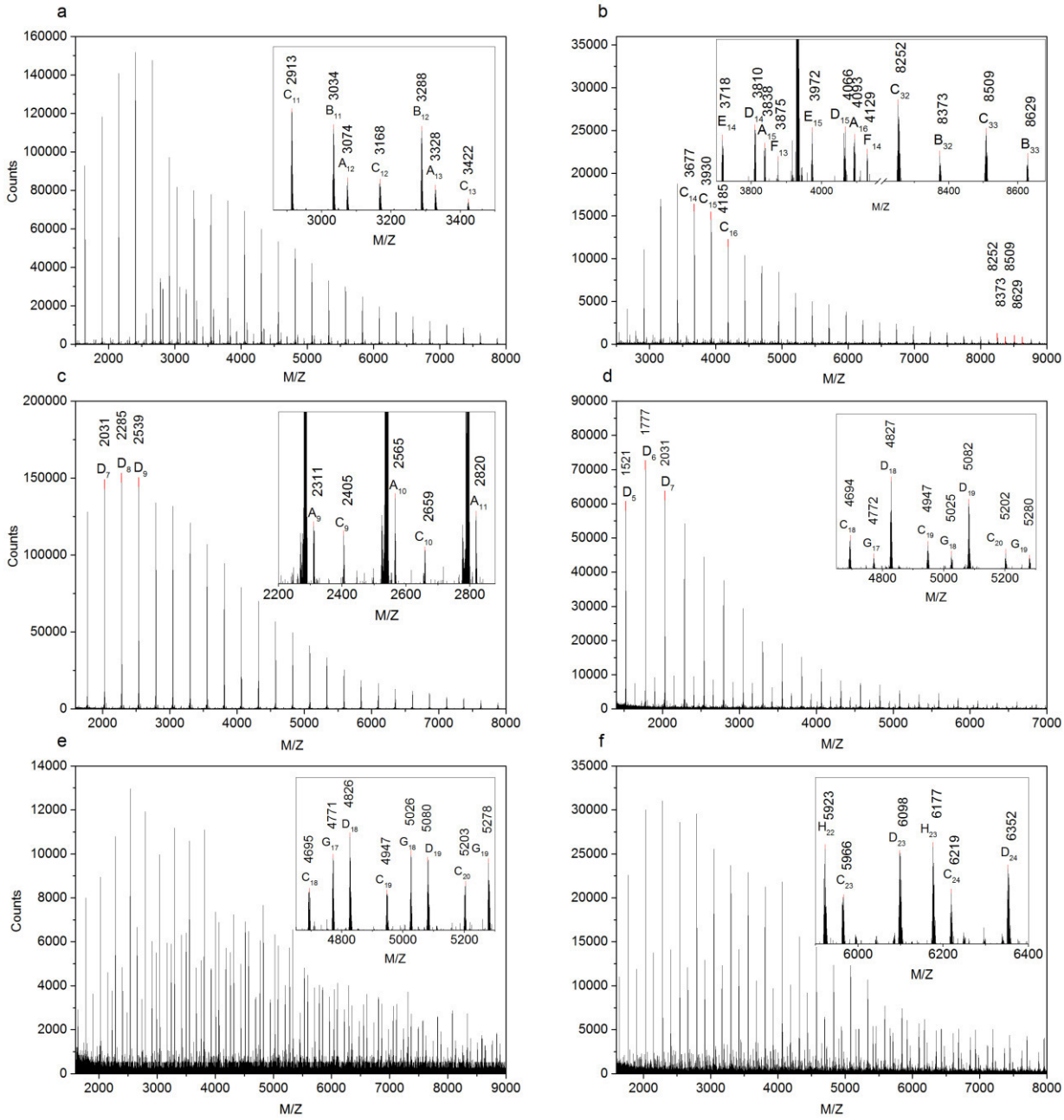

Figure 28: Mass spectra of fractions 1 to 6 (a-f). The structures, which could be identified in the mass spectra of the individual fractions, are shown in Table 4 [108].

Table 4: Polymer structures detected by MALDI-TOF-MS. Expected masses and the corresponding number of repeating units (n) are shown [108].

Mass series	Polymer structure	n	M^+ Na	Mass series	Polymer structure	n	M^+ Na
E	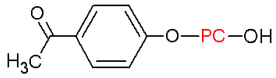	14 15 16	3718.9 3973.2 4227.4	**A**	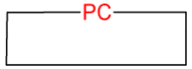	11 12 13	2820.0 3074.2 3837.0
F	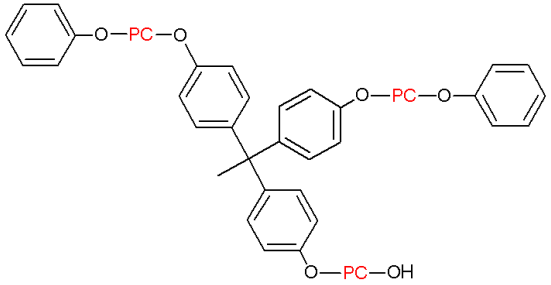	13 14 15	3875.0 4129.3 4383.6	**B**	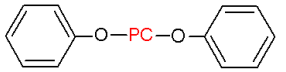	11 12 32	3034.2 3288.4 8373.8
G	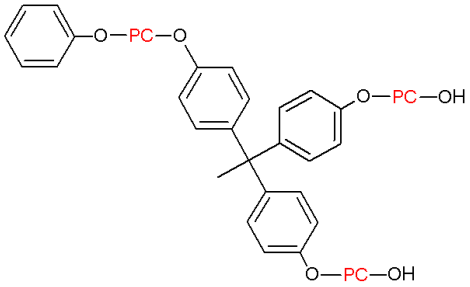	17 18 19	4772.0 5026.3 5280.6	**C**	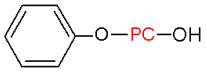	10 11 32	2659.8 2914.1 8253.7
H	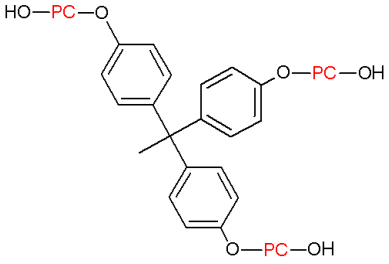	22 23 24	5923.3 6177.5 6431.8	**D**		18 19 23	4828.1 5082.4 6099.5

The linear fully phenol end-capped PC (B) is the main component in the mass spectrum of fraction 1 (Figure 28). Besides, the mass spectrum also shows linear PC with one hydroxyl end-group (C) and the statistically formed cyclic by-product (A) in the low molar mass range. Contrary to that, C dominates in the mass spectrum of fraction 2 (Figure 28 b), though small quantities of other structures such as A, E and F can be detected. In the mass spectra of fraction 3 (Figure 28 c), which correlates to the first additional peak at 37 mL in the chromatogram of PC8 (Figure 27), the fully uncapped PC (D) prevails. Therefore, this peak can be assigned to structure D, thus confirming that the developed SG-NCC method separates according to the number of hydroxyl end-groups in the different PC structures.

However, based on the theory of polymer chromatography an explanation why the SG-NCC method is able to separate according to PC end-groups is not straightforward. The applied composition of the mobile phase gradient is close to the critical conditions, which is indicated by the low difference in the eluent compositions that are required between complete adsorption ($CHCl_3$) and desorption of PC (97.5/2.5 vol% $CHCl_3$/MTBE) in SG-NCC. Thus, it might be speculated that at these near-critical conditions the interactions between the repeating units and the stationary phase are suppressed to such an extent that the interactions of the hydroxyl end-groups with the stationary phase dominate the separation.

In addition to separation according to end-groups, a separation according to various branched structures based on differences in the end-capping is indicated when using SG-NCC: While only small amounts of the branched PC structure with two hydroxyl and one phenol end-group (G) could be identified in fraction 4 its content is clearly higher in the mass spectrum of fraction 5 (Figure 28 e). Furthermore, branched PC with three hydroxyl end-groups (H) can be detected in the mass spectrum of fraction 6 (Figure 28 f), which provides evidence that the separation is determined by the number of end-groups. However, no structures containing more than one THPE unit could be identified in the fractions by MALDI-TOF-MS. A possible explanation for that outcome might be that these structures reveal distinctly higher molar masses, as will be discussed in section 3.2.5 in more detail. Since a sensitivity drop of MALDI-TOF-MS could be recognized for detection of molar masses higher than 10 kDa, such structures could not be traced in the present case.

In order to confirm that apart from a separation according to end-groups the SG-NCC method enables a separation according to different branched structures the collected fractions were hydrolyzed and the products were analyzed by LC, which allows quantification of THPE and, thus, identification of the degree of branching in each fraction. The corresponding results are listed in Table 5.

Table 5: Quantification of THPE in PC8 fractions after hydrolysis. Standard deviation of 0.009 % was determined for the THPE quantification [108].

Sample	Fraction 1	Fraction 2	Fraction 3	Fraction 4	Fraction 5	Fraction 6
THPE / mole%	0.033	0.336	0.218	0.826	1.229	0.979

It becomes clear that the determined THPE proportions and the MALDI-TOF-MS analyses are in line. Fractions 1 and 3, in which no branched structures could be identified in the mass spectra, also reveal the lowest THPE amounts. On the other hand, higher THPE contents were determined for fractions 2 and especially 4 to 6, which revealed distinct signals in their mass spectra specific for branched structures. Therefore, the presented fractionation approach of sample PC 3 and the subsequent MALDI-TOF-MS and LC analyses clearly prove that the separation in the applied SG-NCC method is governed by the end-capping of the different PC species. In this sense this correlates with a separation according to branched structures. However, as shown in Figure 26 and by the MALDI-TOF mass-spectra subsets, the individual peaks in the chromatogram strongly overlap and, thus, the developed method is not capable to fully separate various structures.

3.2.2 Off-line two-dimensional chromatography with triple detection

Hyphenating the developed SG-NCC with a separation according to molar mass (SEC) to an on-line 2D-LC offers opportunities to further improve the separation. As information on branching is desired, useful insights can be obtained by using triple detection. Initially, the collected fractions (section 3.2.1) were analyzed by TD-SEC in an off-line manner.

For PC, as a polycondensate polymer, relatively low weight-average molar masses in the range of several tens-of-thousand Dalton are characteristic. Thus, an accurate measurement of $R_g{}^2$ by LS in a TD-SEC experiment to analyze the degree of branching is complicated as described in section 2.2. Consequently, $[\eta]$ by VI was determined to gain information on the branching.

In a first step, the practicability of the TD-SEC is demonstrated measuring the bulk samples PC9 (linear, cf. Figure 29 a) and PC8 (branched, cf. Figure 30) as references for later correlation with the fractions. The Mark-Houwink-plot of the linear sample, which allows the calculation of Mark-Houwink parameters is given in Figure 29 b and a comparison with literature values is provided in Table 6.

Table 6: Comparison of experimentally determined and literature Mark-Houwink parameters. The Mark-Houwink parameters were fitted in the molar mass range from 10,000 to 70,000 Da [109].

α_{exp}	K_{exp} / mL/g	α_{lit}	K_{lit} / mL/g
0.74	0.0291	0.74	0.0301

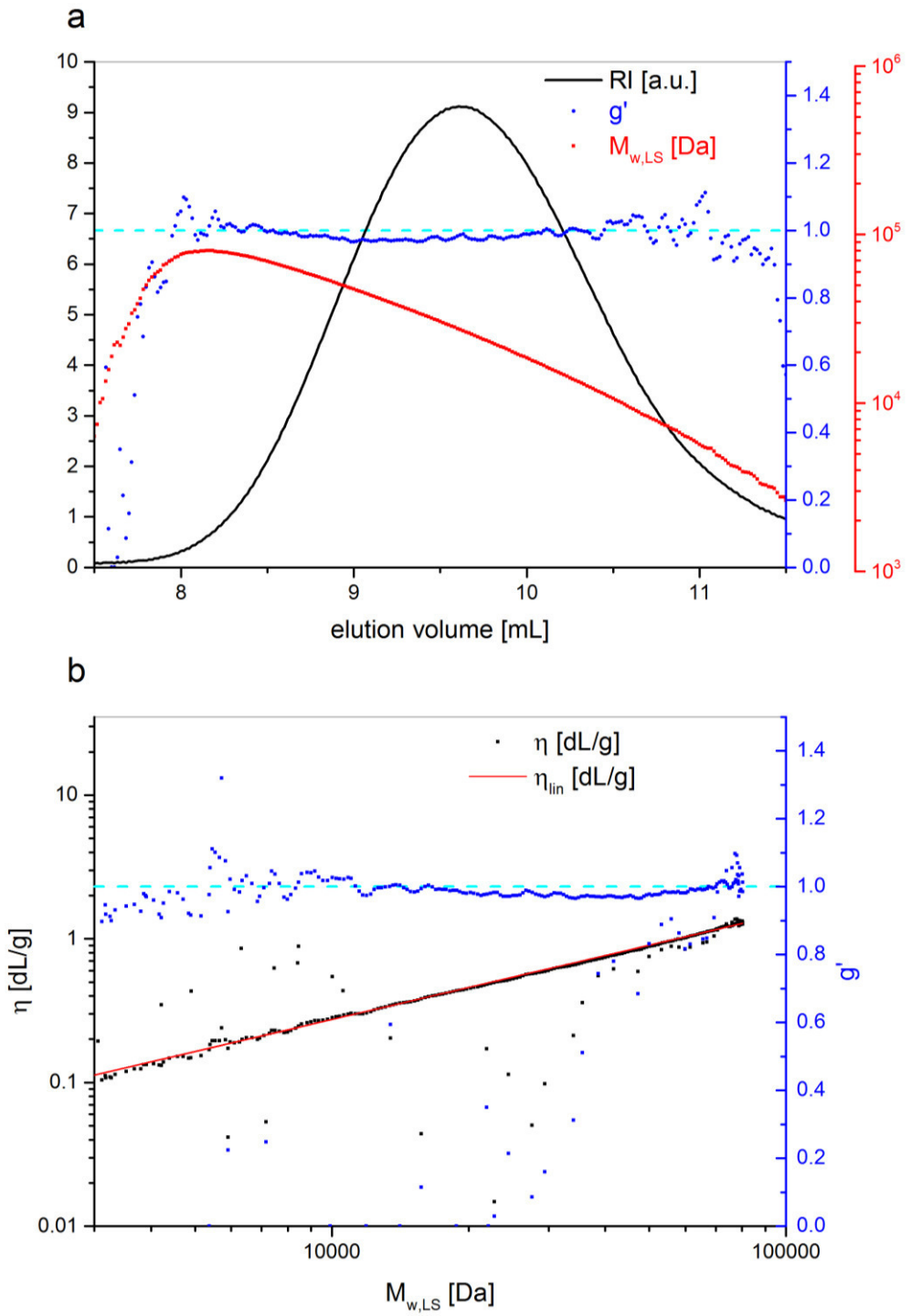

Figure 29: a) Chromatogram of PC9 obtained from TD-SEC. Except for the RI response (black) also $M_{w,LS}$ (red) and g' (blue) are illustrated. b) Mark-Houwink plot as well as g' of the linear sample [109].

The results lead to the conclusion that the Mark-Houwink parameters from literature and the experimental ones are in excellent agreement, thus confirming that the setup parameters of the TD-SEC were well chosen. It also can be seen that g' is equal to 1 for almost the entire molar mass range, which is expected for a linear sample. Deviation from 1 at very low elution volumes (high molar masses) can be explained by low detector responses in these ranges.

Further evidence for this explanation is also provided by the drop in the determined molar masses at elution volumes below 8 mL.

Since $[\eta]$ is affected by the degree of branching of a sample, g' approaches lower values for TD-SEC of a branched PC sample. To demonstrate that fact the TD-SEC chromatogram of the branched sample PC8 is shown in Figure 30.

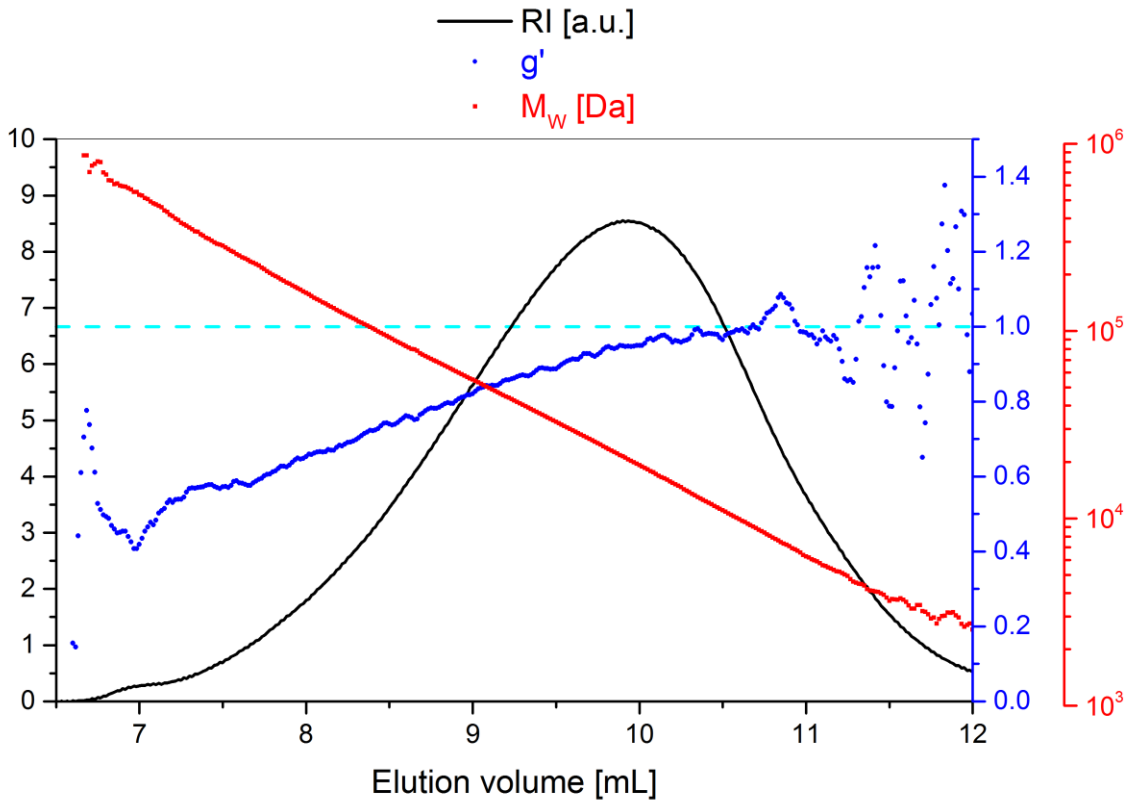

Figure 30: Chromatogram of PC8 obtained from TD-SEC. Except for the RI response (black) also $M_{w,LS}$ (red) and g' (blue) are illustrated.

As expected, when approaching higher molar masses (and accordingly lower elution volumes) a drop in g' can be recognized, which indicates a higher degree of branching. Since the degree of branching can be related to the THPE content in a PC chain, this outcome can be well explained by the increased probability for multiple incorporation of THPE units in longer polymer chains. However, it is also well known that coelution of branched and linear polymer chains occurs [3]. A branched and a linear PC chain may differ in their molar mass but hold the same hydrodynamic volume and, thus coelute in SEC, since SEC separates according to hydrodynamic volume. This coelution might lead to misinterpretations of the derived structural information and, therefore, the obtained results have to be treated carefully [66].

After the feasibility of TD-SEC for the branching analysis of PC samples was shown, in a next step, the fractions that were collected in section 3.2.1 were measured by TD-SEC. The chromatograms of fractions 2-6 are shown in Figure 31. Due to the low quantities no TD measurements of fraction 1 could be performed.

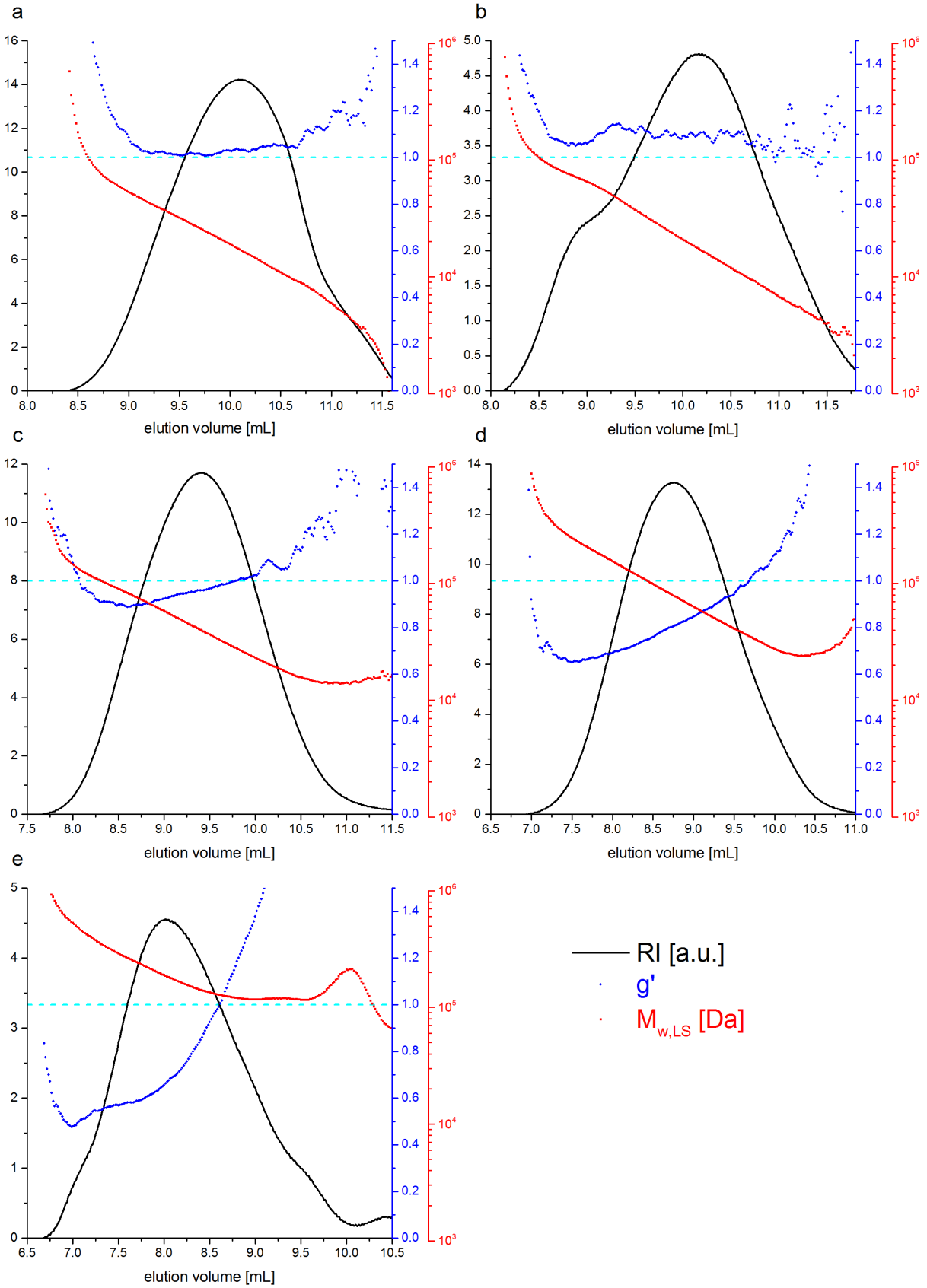

Figure 31: Chromatograms of fractions 2-6 (a-e) of sample PC8 obtained in TD-SEC. Except for the RI response (black) also $M_{w,LS}$ (red) and g' (blue) are illustrated.

According to the results from MALDI-TOF-MS (Figure 28 a-f) and the THPE quantification by LC (Table 5) fraction 1 consists of almost exclusively linear PC species, while fraction 2 comprises small amounts of THPE. On the other hand, fractions 4-6 reveal higher THPE contents and, thus, the degree of branching should be distinctly increased. These findings can be confirmed by the TD-SEC chromatograms and the corresponding g' plots of the various fractions (Figure 31 a-e).

The TD-SEC chromatograms of fractions 2 and 3 (Figure 31 a-b) exhibit *g'* values close to 1 over almost the entire elution volume range and deviations at the peripheries of the chromatograms might be explained by the low detector responses. Interestingly, *g'* is almost equal to 1 for fraction 2, although a drop is expected based on the determined THPE content (Table 5). However, compared to the other fractions the THPE content is lower suggesting that the linear species predominate in this fraction increasing the average *g'* value. Besides, it might be speculated that, although the PC chains bear THPE units, the caused branching does not affect the hydrodynamic volume i.e., the branches are fairly short. Hence, TD-SEC measurements confirm that fractions 2 and 3 mainly consist of linear macromolecules. Furthermore, these outcomes already prove that a coelution of linear and branched species leads to misinterpretation of the results.

A clear drop of *g'* can be observed for fractions 4-6 (Figure 31 c-e) approaching lower elution volumes (higher molar masses), which confirms the presence of branched macromolecules in these fractions determined by MALDI-TOF-MS and THPE quantification (Table 4, Table 5). Interestingly, fraction 6 shows the lowest *g'* values, which indicates the highest degree of branching, though the determined THPE content is reduced compared to fraction 5. A possible explanation for that outcome might be that fraction 6 shows distinctly higher molar masses in the TD-SEC chromatogram (Figure 31 e). On the basis of a statistical THPE incorporation the probability should be increased that a polymer chain bears a THPE unit at higher molar masses and, hence, the degree of branching is enhanced. However, the higher the molar masses the lower the molar fraction of a single THPE unit, thus, the THPE contents are reduced although higher degrees of branching are present.

3.2.3 On-line two-dimensional chromatography (2D-LC)

After off-line 2D-LC could successfully be applied analyzing the fractions collected from the developed SG-NCC method by TD-SEC, in a next step, an on-line 2D-LC method is of interest. On-line 2D-LC using an automated transfer valve has been widely practiced in chromatographic analysis [49, 54, 87-90]. It benefits from both complete automation as well as quantitative sample transfer and, in the end, quantification of single components is possible, which allows for a more detailed investigation of the analyzed samples.

To establish on-line 2D-LC the experimental parameters have to be adjusted in order to synchronize the two chromatographic dimensions. A high-speed SEC column is installed in the second dimension, which allows flow rates up to 5 mL/min and acquisition times of 2 min per run. Since the volume of the transfer loops is 200 μL, a flow rate of 0.01 mL/min in the first dimension instead of 1 mL/min is required to ensure a complete analysis of the sample. Consequently, the mobile phase gradient of the SG-NCC is extended from 60 min to 600 min to preserve the slope of the gradient. The corresponding color coded 2D contour plots of PC7-9 under the described experimental 2D-LC conditions are shown in Figure 32 a-c.

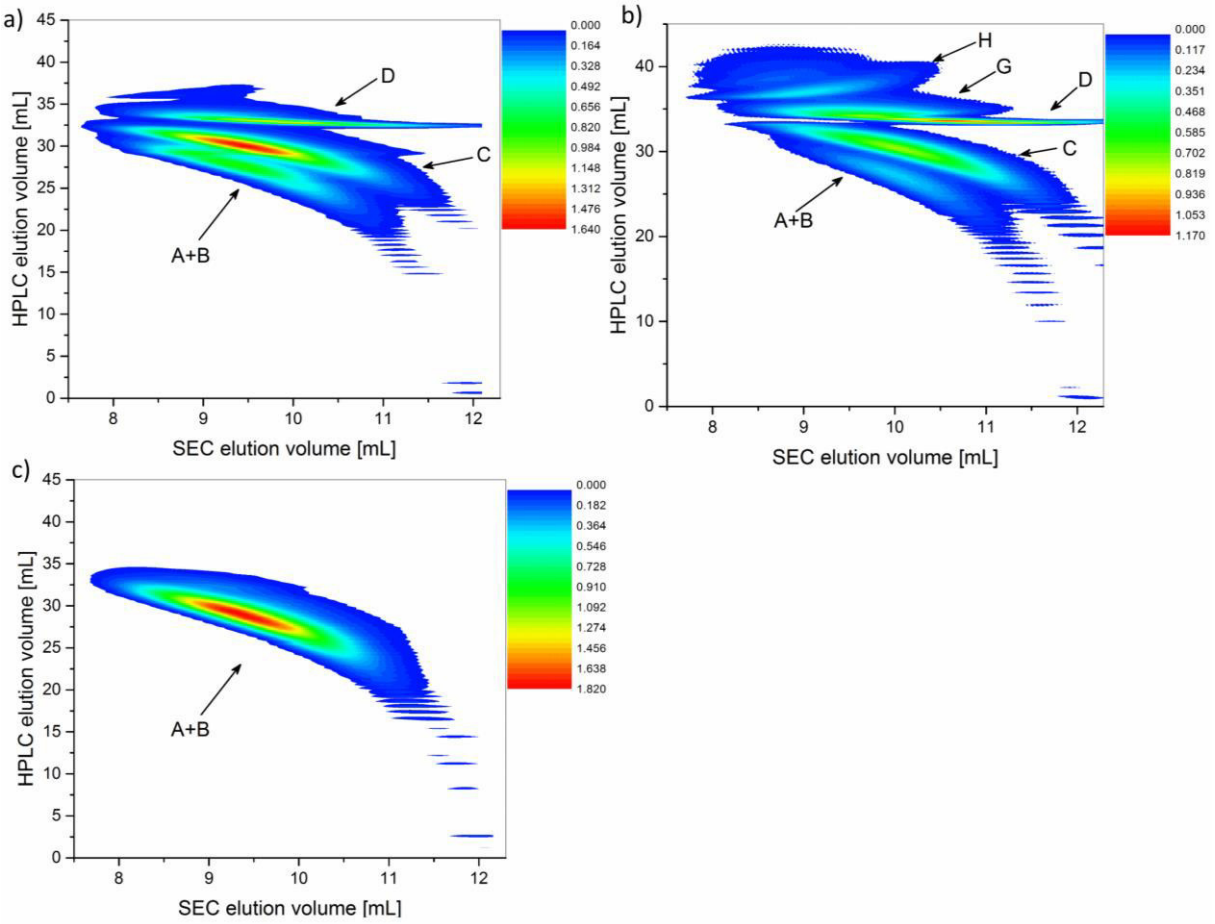

Figure 32: 2D contour plots of samples PC7-9 (a-c) obtained from 2D-LC analyses with SG-NCC in the first and SEC in the second dimension. The assignment of the spots corresponds to the labeling in Table 4. The UV response is plotted color coded in arbitrary units, where low concentrations are represented by a blue color and high concentrations by a red color [108].

The 2D contour plots reveal clear differences between PC7-9. The 2D-LC contour plot of PC7 (linear and partially un-capped) shows three distinct spots, which can be assigned to structures B, C and D, respectively (Table 4). Furthermore, an additional spot, which could already be detected in the SG-NCC analysis of PC2, appears at an HPLC elution volume from 35 to 38 mL and may correspond to small amounts of branched structures. A possible explanation for the presence of small amounts of branched structures in this sample might be rearrangement reactions, which are well known for PC [98-100]. As the resulting products contain free hydroxyl groups, branching during the production process might be possible.

As can be expected from Figure 26 the contour plot of PC9 (linear and fully end-capped) exhibits one distinct spot corresponding to structure B, which by far dominates this sample. Besides, also the cyclic structure (A) is present, which is statistically formed during the PC synthesis [110]. However, the contour plot does not exhibit any separation between structures A

and B, which is also indicated by the MALDI-TOF-MS analyses, since structure A could be identified in a number of analyzed fractions.

Contrary to PC7 the contour plot of PC8 (branched and partially un-capped) reveals distinct spots at HPLC elution volumes ranging from 35 mL to 41 mL. Considering the chromatograms of the first dimension and the MALDI-TOF-MS analyses of the fractions it becomes clear that these additional spots correspond to branched structures including G and H as shown in the mass spectra (Figure 28 e and f).

Thus, it can clearly be proved that the employed 2D-LC method with SG-NCC in the first dimension allows separating not only according to end-groups but also according to branching based on differences in end-capping. As the 2D contour plots reveal distinct spots in the corresponding elution range a separation between the individual branched structures can also be achieved. However, based on the 2D contour plots of the linear samples PC7 and 9 it is expected that the branched structures G and H elute between 33-37 mL. Furthermore, apart from these structures, which could be identified by MALDI-TOF-MS, the presence of more complex branched structures with more than more THPE unit in the polymer backbone is assumed. A possible reason for this outcome might be provided the minor quantities of these structures. Moreover, based on the SEC elution range for these species it can be hypothesized that the molar masses of spot 6 and large parts of spots 4 and 5 exceed the detection limit of MALDI-TOF-MS in the present case. Therefore, polymer chains and structures in the corresponding molar mass range cannot be detected. To validate this assumption, the corresponding SEC column was calibrated with PS standards and, subsequently, the molar masses of the different spots were determined as listed in Table 7. As spots 3+4 could not be well separated in the 2D contour plot they were treated as one peak for the quantifications.

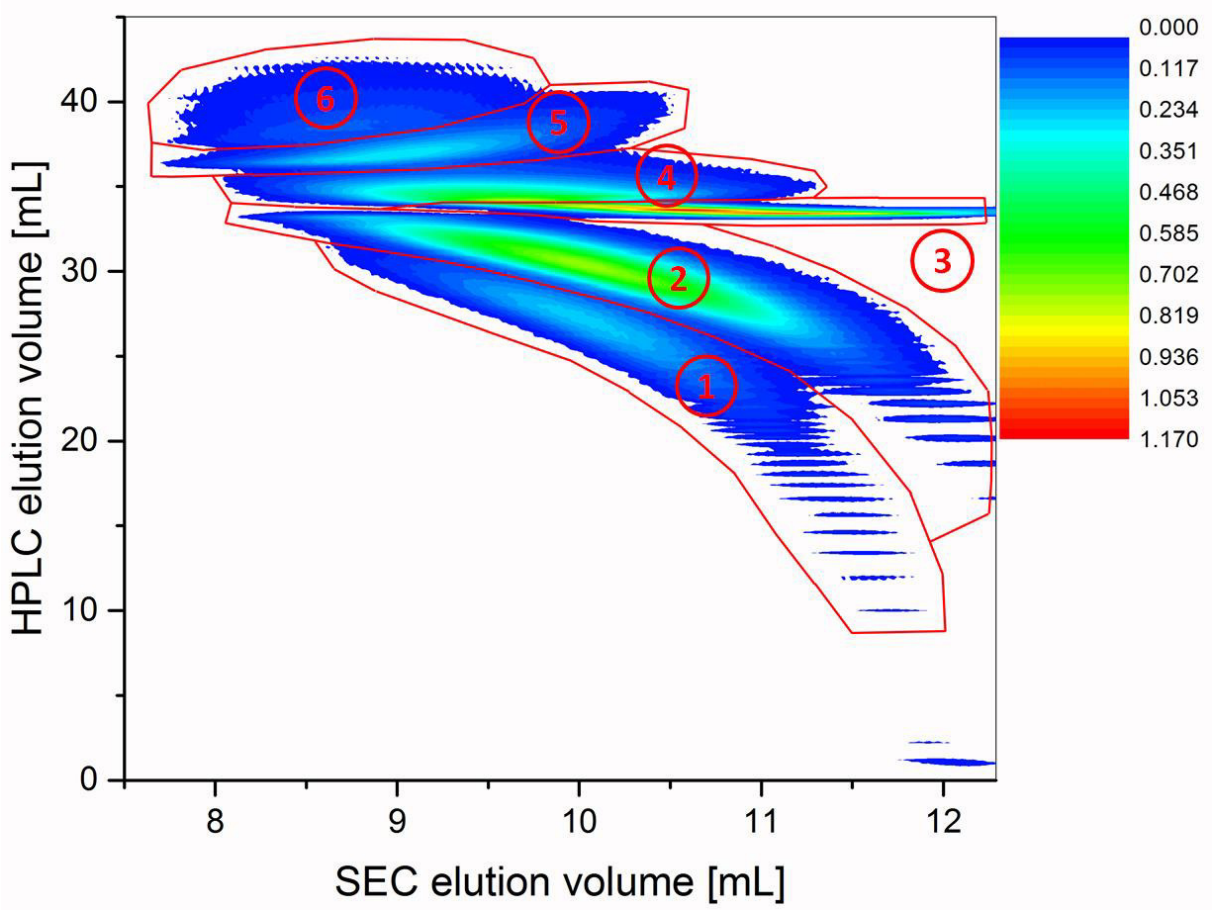

Figure 33: 2D contour plot of PC8 with the defined spots, which are used to calculate the integral fractions and molar masses [108].

Table 7: Integral fractions and molar masses of the different spots as defined in the 2D contour plot of PC8 in Figure 33 [108].

Peak No.	Integrated area / %	M_n / Da*	M_w / Da*
1	10.4	11,600	28,900
2	37.4	9,300	30,100
3+4	26.5	9,300	38,500
5	9.4	67,600	94,100
6	16.3	161,500	273,600

*Column calibrated with PS standards

Even though the SEC column was calibrated with PS standards and, therefore, the determined molar masses differ from the actual ones the resulting number- and weight-average molar masses of the single spots differ dramatically. While molar masses obtained for spots 1 and 2

are similar, the weight average molar masses of spot 3+4 are clearly higher. This might be caused by the overlapping of the linear structure D with the branched structures, which show higher molar masses. Furthermore, spots 5+6 exhibit distinctly higher molar masses which prohibit the identification of individual PC species by MALDI-TOF-MS. A more detailed spot analysis will be provided in section 3.2.5.

3.2.4 Reversed elution order

An interesting aspect from the chromatographic point of view, which could be identified in the contour plot of PC8 (Figure 32 b and Figure 33), is the elution behavior of spots 5 and 6. It is theoretically expected that low molar mass chains exhibit lower elution volumes in SG-NCC, which acts as first dimension in the present case [69, 111-113]. However, a reversed elution behavior (i.e longer chains have lower retention in SG-NCC compared to shorter chains) can be observed for spots 5 and 6 in the contour plot of PC8 (Figure 33). In this context, the 2D contour plot of PC8 clearly reveals similarities with a so-called critical diagram [114]. In order to illustrate that, a typical critical diagram is compared with the 2D contour plot of PC8 in Figure 34.

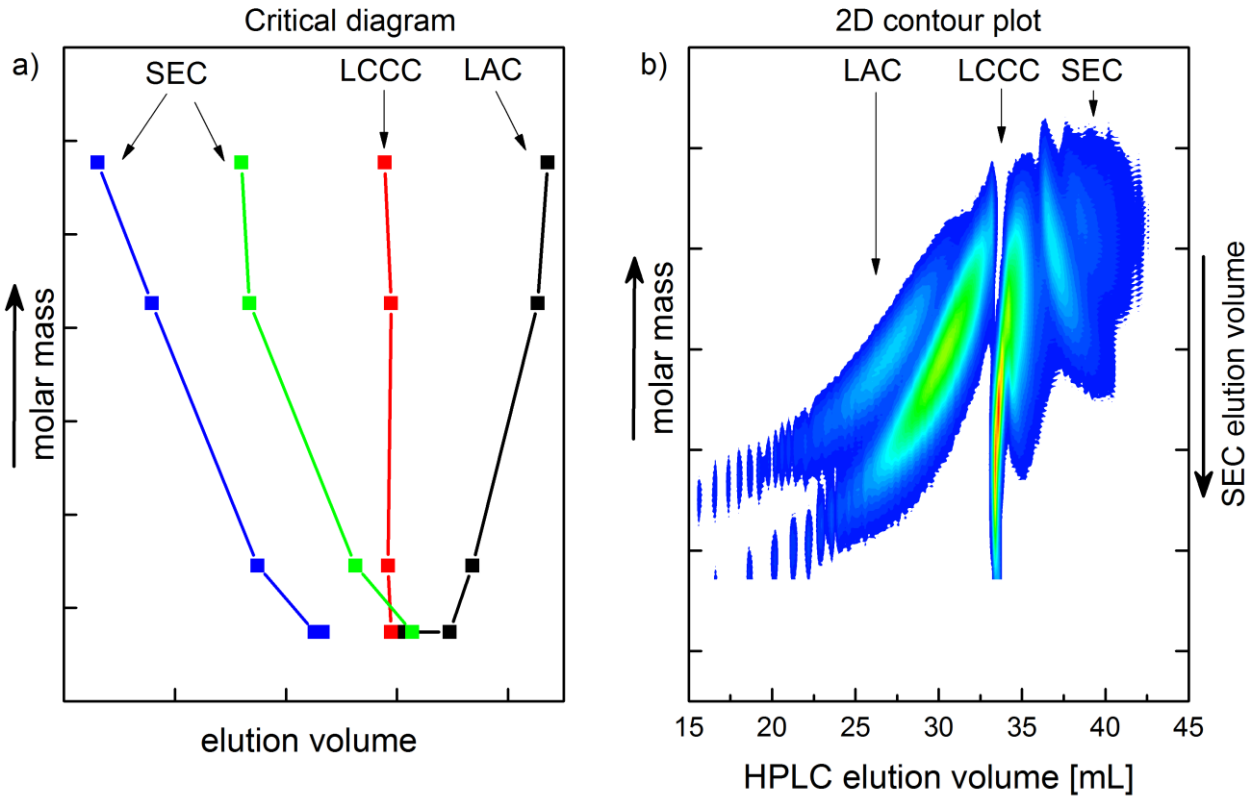

Figure 34: Comparison of a) a critical diagram [95] with b) the 2D contour plot of PC8. The axes of the HPLC and the SEC elution volume were swapped to illustrate the similarity with the critical diagram [108].

As can be seen in the critical diagram (Figure 34 a) LAC is characterized by higher elution volumes for higher molar masses, whereas in SEC mode the higher the molar mass the smaller the elution volume. At the transition point from LAC to SEC, the LCCC mode occurs, which manifests as a molar mass- independent elution volume.

The elution behavior, which can be identified in the critical diagram for the different chromatographic modes can be transferred to the 2D contour plot of PC8 (Figure 34 b): While the fully end-capped (B) and the single end-capped (C) PCs (spots 1+2) elute in LAC mode (higher molar mass→higher elution volume) the elution of linear uncapped PC (D) and the branched PC with two hydroxyl groups (G) (spots 3+4 in Figure 33) is not affected by molar mass and, therefore, occurs in LCCC mode. The branched PC species in spots 5+6 (Figure 33), including the branched PC with three hydroxyl end-groups (H), display SEC elution behavior (higher molar mass→smaller elution volume), which was described as reversed elution order by ADRIAN et al. [90].

The experiments and theoretical considerations of RADKE et al.[84] and BIELA et al.[85], who analyzed star-shaped and hydroxyl terminated polylactides (PLA) with variable number of arms on a silica column, might provide an explanation for the observed reversed elution order. Among others, PLAs were synthesized with variable number of arms while the overall number of hydroxyl groups in a polymer chain was kept constant. The additional hydroxyl groups were located in the core of the star molecules. Based on the principal theory of LCCC the elution volume of these stars should not differ as long as the number of hydroxyl groups remains constant, since the separation ought to be based on the differences in the number of the functional hydroxyl groups.

Contrary to that expectation, RADKE et al. found, that the retention volume changed for PLA stars with different numbers of arms although their number of hydroxyl groups was kept constant. The LCCC experiments revealed that the star with the lowest number of arms and, hence, the highest number of hydroxyl groups located in the core of the polymer eluted last. Thus, RADKE et al. concluded that the separation in LCCC is not solely based on the number of functional groups but is also affected by the way these functional groups are arranged within the polymer chain. Hence, they suspected that an agglomeration of functional groups at a specific location along the polymer chain results in extended interactions and consequently higher elution volumes. Furthermore, they were able to develop a theoretical model for the description of this observation, which could confirm the LCCC experiments. It could be concluded that the higher the number of core functional groups the higher the interaction with the stationary phase. These findings might also be applied to explain the reversed elution order, which was observed for the branched as well as uncapped PC structures in the present study.

It can be assumed that the hydroxyl groups of branched PC macromolecules with higher molar masses are further apart from each other and agglomeration is less probable. Contrary to

that, the probability of hydroxyl group agglomeration in case of branched polymer chains with lower molar masses is enlarged, as the hydroxyl groups may be located close to each other, which might be comparable with the core functional groups found by RADKE et al.. To illustrate this fact, two polymer chains containing a single branch with each chain end hydroxyl terminated are schematically represented in Figure 35.

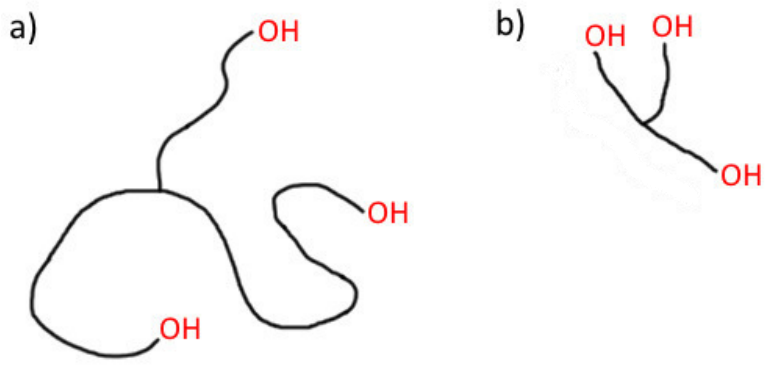

Figure 35: Schematic representation of two PC macromolecules with hydroxyl end-groups to illustrate the differences in the end-group distances between a polymer chain with a) a high molar mass and b) low molar mass [108].

Therefore, based on the theory of RADKE et al., lower-molar mass chains exhibit higher overall interaction energy. Consequently, they also elute later in LCCC compared with their high molar mass analogues and, thus, this can explain the reversed elution order of the branched PC structures containing more than one hydroxyl group. One might correctly object that the employed method does not fulfill the requirements of LCCC, which was the subject in the publication of RADKE et al.. However, the MALDI-TOF-MS results and the obtained 2D contour plots clearly confirm that the method presented here mainly separates according to end-groups. Since the mobile phase gradient applies an eluent ratio, which is close to the critical composition ($CHCl_3$→97.5/2.5 vol% $CHCl_3$/MTBE), the findings of RADKE are well applicable.

3.2.5 On-line two-dimensional chromatography with triple-detection (2D-LC with TD)

With the developed on-line 2D-LC method a separation of individual linear and branched PC structures was possible in the analyzed PC samples. However, although relative molar masses can be calculated, no information on the absolute molar masses as well as the structure of the branched PC species can be derived. In that context, coupling of the 2D-LC method with TD holds potential, since it enables the measurement of absolute molar masses as well as the elucidation of structural information in a single experiment. Furthermore, the hyphenation can solve coelution issues, which occur in case of TD-SEC, as the linear and branched PC species are separated in the 2D-LC method.

On-line 2D-LC with TD requires a further and precise optimization of the experimental parameters to firstly avoid loss of analyte and secondly gain maximum separation performance [91]. In order to identify the optimal experimental parameters, the limitations of the TD unit that was installed downstream of the 2D-LC setup have to be taken into account. According to the application notes of the TD unit, the backpressure of the VI must not exceed 100 kPa to prevent damage on the capillaries [115]. Thus, the maximum employed flow rate of the second dimension is confined to less than 1.8 mL/min in the present case, and to be on the safe side it was decided to apply a flow rate of 1.5 mL/min in the second dimension.

Besides, a four capillary VI with a Wheatstone bridge-like fluid flow setup was employed in the unit (Figure 36). Thus, a hold-up column was installed in the VI creating a delay of the analyzed polymer eluate along one side of Wheatstone bridge. This imbalance causes a pressure drop between the capillaries, which is then detected. The hold-up column induces a so-called “breakthrough” peak, eluting about 15 mL after the original sample in the present case, which is illustrated in Figure 37 [60].

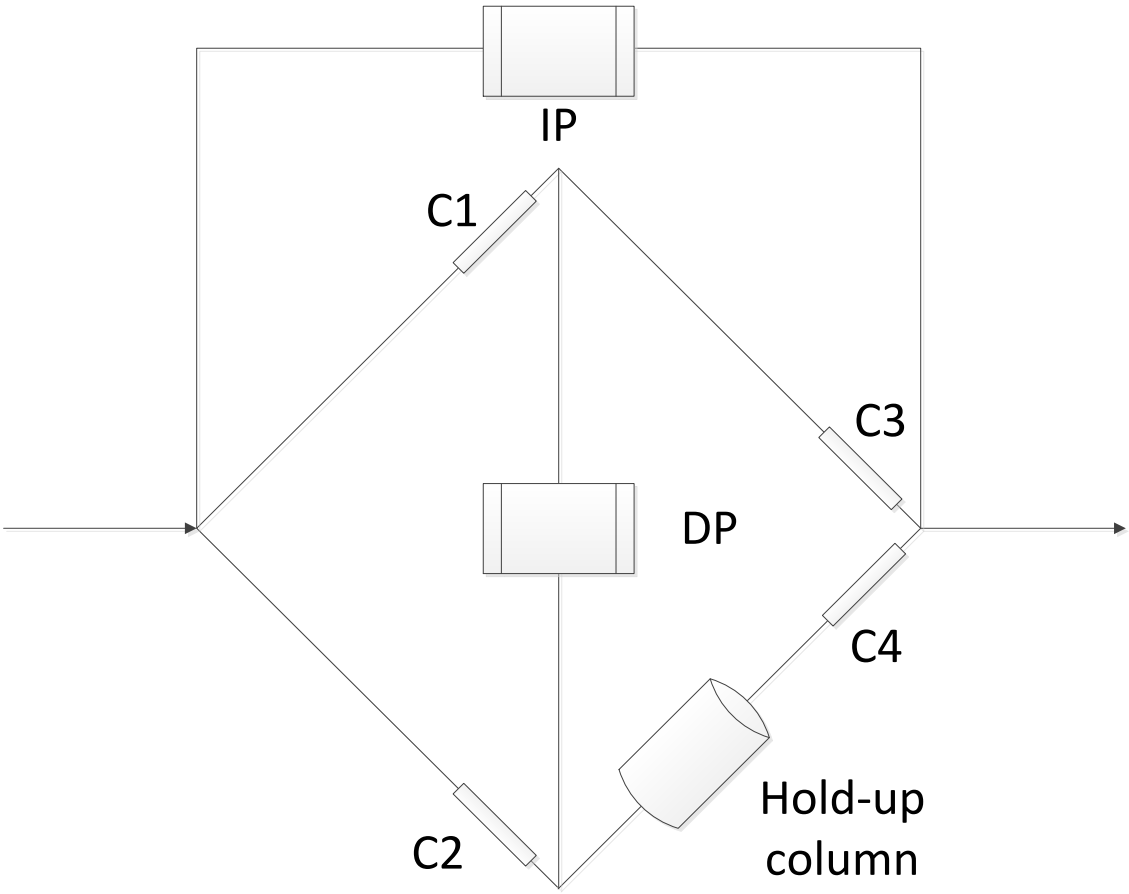

Figure 36: Schematic representation of a viscometer with a Wheatstone bridge-like fluid flow setup.

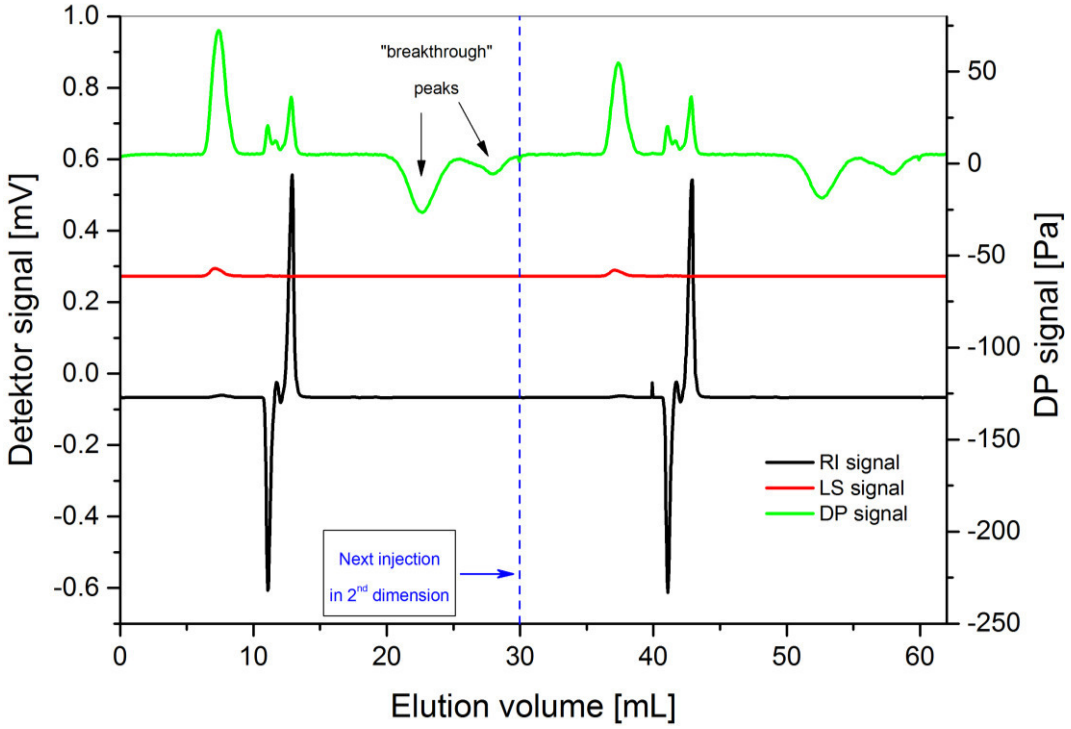

Figure 37: Detector responses for the TD-SEC measurement of two subsequently injected samples in a 2D-LC analysis. The acquisition time of one sample was set to 20 min at a flow rate of 1.5 mL/min. The "breakthrough" peaks occur at elution volumes of about 22 and 28 mL [109].

Furthermore, not only the polymer sample itself but also the solvent plug of each inject causes a “breakthrough” peak. This observation can be explained by the composition of the solvent from the first dimension, which is injected into the second dimension. Since a solvent gradient is applied in the first dimension, the solvent, which is injected into the second dimension, consists of a mixture of $CHCl_3$ and MTBE instead of pure $CHCl_3$. Thus, a significant solvent plug is transported with the flow to the VI and the RI detector and, consequently, the acquisition time for a single injection in the second dimension has to be extended to 20 min in order to prevent an overlap of consecutive injections.

Due to acquisition times in the second dimension (20 min) and the volume of the transfer valve loops (200 μL) the flow rate of the first dimension has to be reduced from 0.1 mL/min to 0.01 mL/min to ensure that the complete sample is analyzed without any losses. Apart from the flow rate also the slope of the solvent gradient has to be adjusted: For previous 2D-LC analyses a mobile phase gradient $CHCl_3$ → 97.5/2.5 vol% $CHCl_3$/MTBE with a duration of 600 min at a flow rate of 0.1 mL/min was applied. When decreasing the flow rate to 0.01 mL/min it was decided keep the compositional window of the mobile phase ($CHCl_3$ to 97.5/2.5 vol% $CHCl_3$/MTBE), yet extend the duration only to 3000 min instead of 6000 min in order to limit the overall measurement time. The color coded contour plots of sample PC8 for the RI, LS, and VI responses are shown in Figure 38 to Figure 40. Spots that could be identified in the 2D contour plots are highlighted in the contour plot of the RI response (Figure 38).

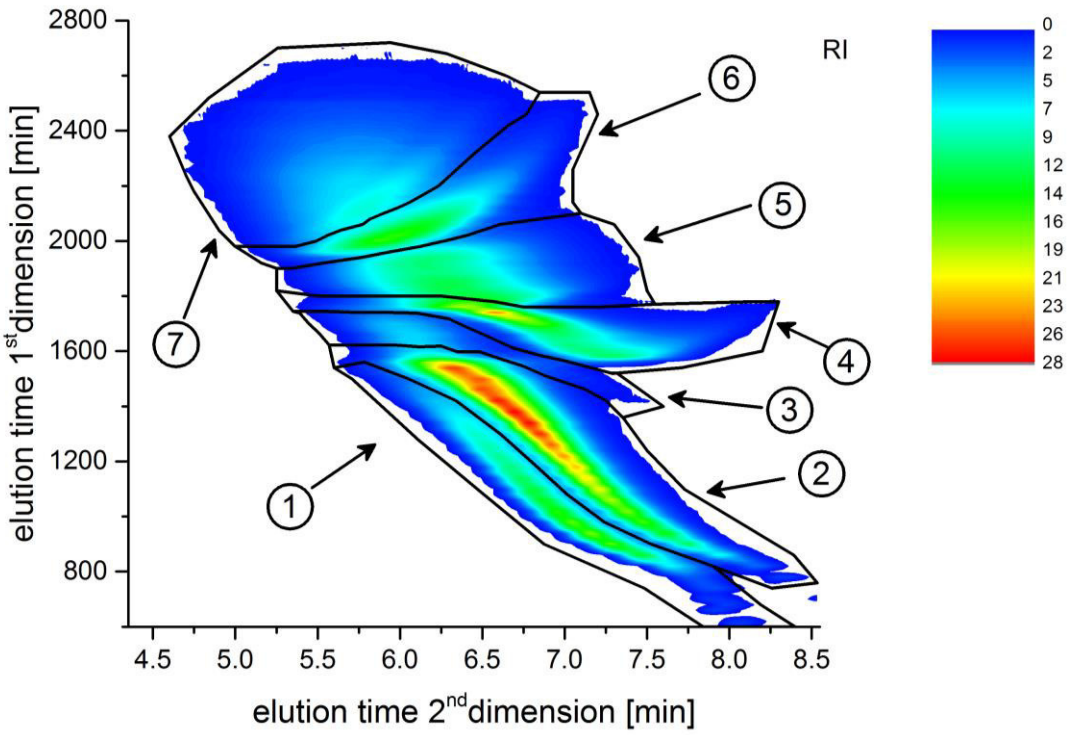

Figure 38: 2D contour plot of the RI response obtained from the MDS detector [109].

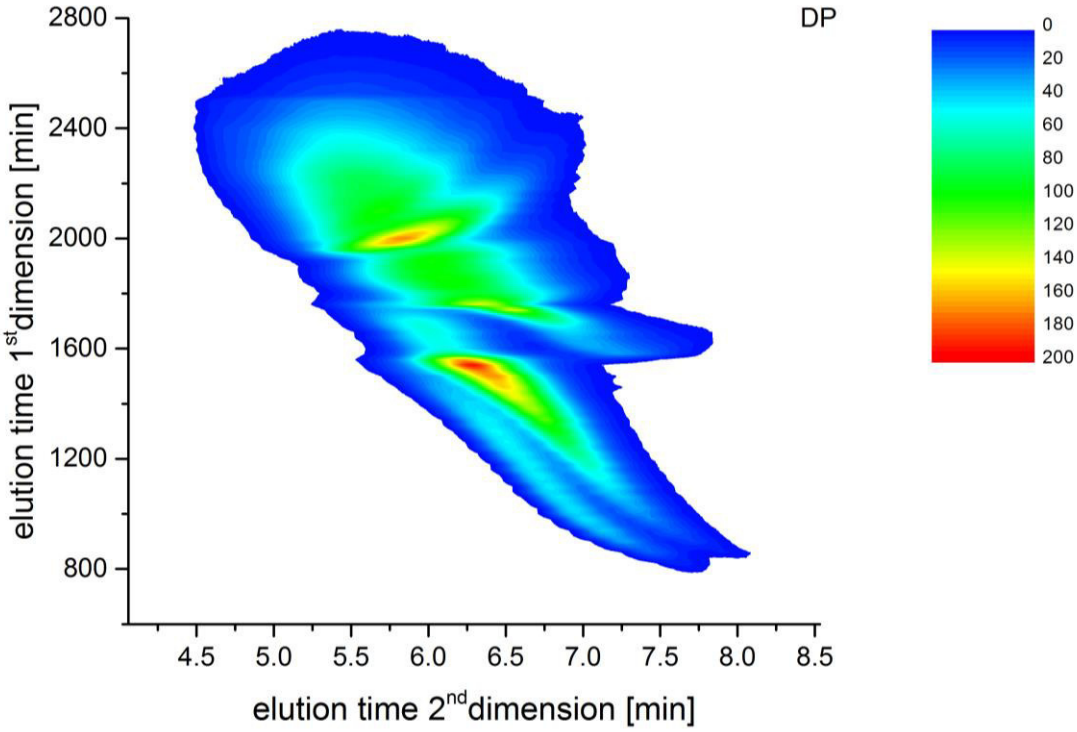

Figure 39: 2D contour plot of the DP response obtained from the MDS detector [109].

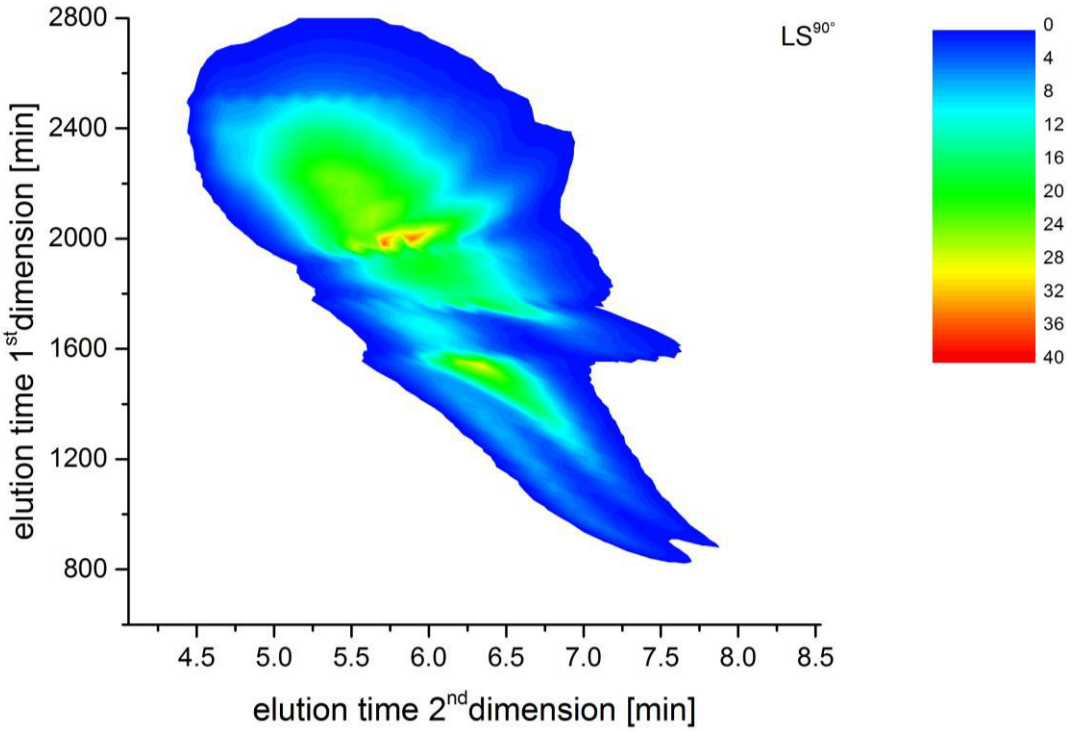

Figure 40: 2D contour plot of the LS^{90° response obtained from the MDS detector [109].

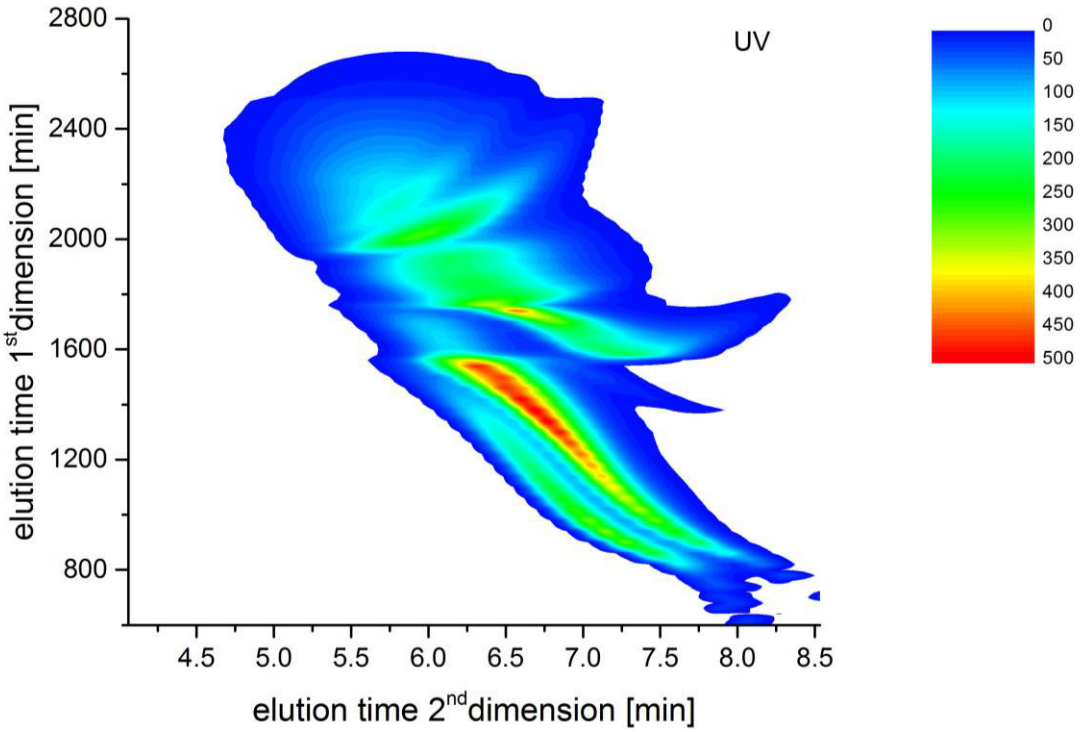

Figure 41: 2D contour plot of the UV response obtained from the UV detector [109].

Furthermore, the UV response is shown in Figure 41, as it exhibited a higher sensitivity than the RI response in the present case. Namely, the presence of an additional area (spot 3) at an elution volume of about 1400 min in the first dimension, which could not be detected in earlier experiments presented in section 3.2.3, is indicated by the UV response. This spot can hardly be detected by the RI response as will be discussed later.

Although the UV detector revealed a higher sensitivity, the RI detector was used as concentration-sensitive detector for the calculation of $M_{w,LS}$ and g', since it is located between the LS and VI detector, while the UV detector is located upstream of all other detectors. Thus, using the UV as concentration-sensitive detector would unnecessarily increase the interdetector volume, which is a potential source for errors when calculating $M_{w,LS}$ and g' [116].

It can clearly be recognized that the 2D contour plots that are obtained with the present setup correspond to those shown in section 3.2.3. Hence, it can be concluded that the separation efficiency of the 2D-LC setup is barely affected by the lower flow rate in the first dimension. Besides, differences between the 2D contour plots of UV and RI compared with those of LS and VI become visible, since the latter detectors are more sensitive towards higher molar masses. The different 2D contour plots of the RI, LS and VI responses enable the establishment of a 2D contour plot of g', which is shown in Figure 42.

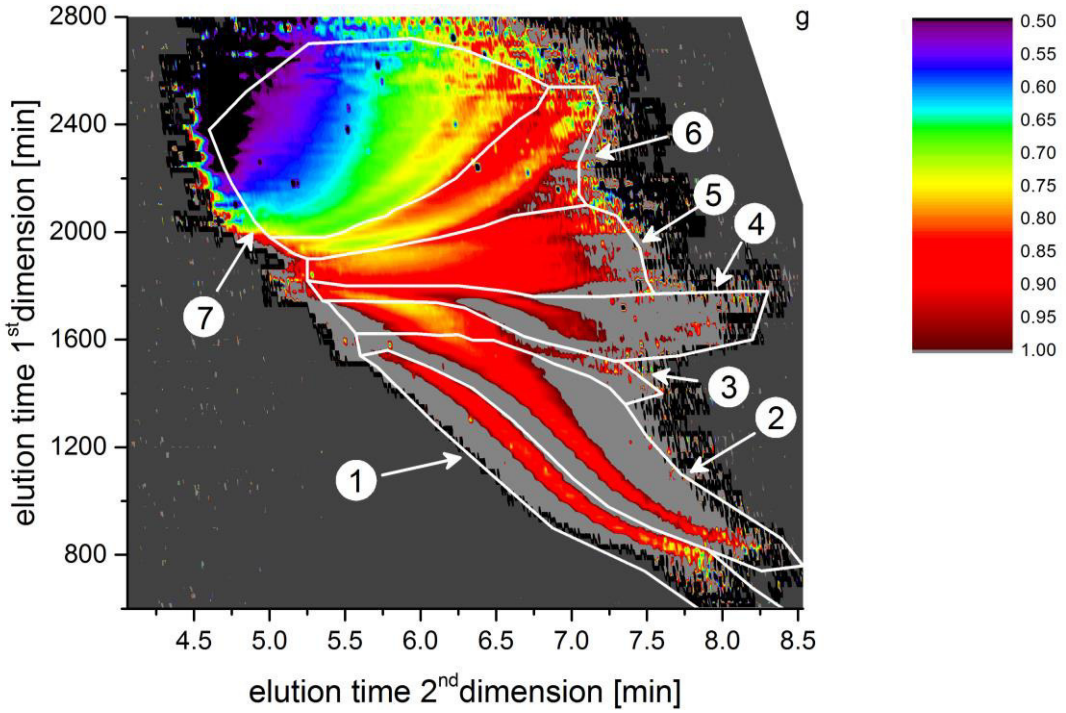

Figure 42: 2D contour plot of g' resulting from the 2D contour plots of the RI, LS and VI responses [109].

The MALDI analysis and THPE quantification of fractions 1-3 suggest that g' is equal or close to 1 at elution times from 800 to 1700 min (spots 1-2) in the first dimension, as linear chains should prevail. It can be recognized that g' is slightly shifted towards lower values in the center of the peaks while g' exceeds 1 (grey scale) at the outskirts. This observation might be explained by interdetector band broadening, which frequently occurs in multi-detector analyses [116]. As the analyzed polymer chains that are detected in the corresponding elution range are almost equimolar, band broadening influences the determined g'. However, the overall g' values at the corresponding elution times are close to 1. Thus, the expectation that linear chains prevail can basically be confirmed.

Furthermore, a drop in g' can be observed in the elution range from 1500 to 1700 min (spot 3), which is an indication for the presence of branched structures. As already discussed in section 3.2.1, the THPE quantification of the fraction in this elution range suggested the presence of minor amounts of branching. Based on the separation principle it is assumed that the branched species present in this elution range are either completely end-capped or exhibit only one hydroxyl end-group. This is also confirmed by the MALDI-TOF-MS analysis, where structure F (branched PC with one hydroxyl end-group) could be detected in the corresponding elution range. Moreover, the fact that spot 3 is more distinctly discernable in the UV response than in the RI response indicates the higher sensitivity of this detector.

In the elution range from 1800 to 2800 min (spot 5-7) the progression of g' for individual and isolated branched structures can be especially well tracked. In addition to fraction analysis, where no isolated branched species could be detected, individual spots in the 2D contour plot of g' can be linked to various branched structures. Thus, hyphenating 2D-LC to TD enables the observation of differences of g' for specific linear and branched species, while conventional TD-SEC only provides information on the overall degree of branching for distinct hydrodynamic volumes, where linear and branched species might overlap. Hence, compared to TD-SEC analysis of the bulk samples and the fractions, the approach shown here supplies detailed knowledge on the frequency of branching for individual branched PC structures versus molar mass, which may help to establish the architecture of these species. Furthermore, the content and the MMD of the individual spots can be determined, as demonstrated in Table 8.

Table 8: Integral fractions of the different spots as defined in the 2D contour plot of PC8 in Figure 38 [109].

Spot (Structure)	**1 (linear)**	**2 (linear)**	**3 (branched)**	**4 (linear)**	**5 (branched)**	**6 (branched)**	**7 (branched)**
Integrated area / %	11.79	28.04	4.54	10.22	15.68	14.89	14.34
$\boldsymbol{M_n}$ **/ kDa**	8.8	11.7	39.8	11.6	33.1	46.7	96.6
$\boldsymbol{M_w}$ **/ kDa**	16.3	20.2	54.1	22.1	42.5	61.2	130.8

It becomes clear, that the integrated areas are in line with those determined by conventional 2D-LC (Table 7). However, deviations in the obtained molar masses can be observed. This outcome can be explained by the differences in the calculations of on-line 2D-LC with and without TD. While the molar masses listed in Table 7 are presented in polystyrene (PS) units, the molar masses listed in Table 8 are determined by the LS detector, which provides absolute molar masses. Thus, the values listed in Table 8 represent the more accurate molar masses. In a next step, these outcomes can be exploited to deepen the knowledge on the structural composition of branched PC as will be discussed in section 3.2.6.

3.2.6 Monte-Carlo simulations

The results stated in the previous section can be further strengthened by MC models, which are able to describe the statistics of the polymerization of branched PC and have been shown to be close to experimental outcomes [26]. For that purpose, a method and algorithm described by HILLEGERS et al. [117-120] was used in the present case. The polymer is built up from a mixture of monomers bearing reactive groups of a hydroxyl and a phenyl end-group. Specifically, in order to simulate the branched polymer a tri-OH functional branching agent is added to the monomer mixture. The probability of choosing one monomer is proportional to its molar fraction in the recipe, and the two end-groups i.e., the hydroxyl and the phenyl moiety react with each other (the possibility of two hydroxyl or phenyl reacting with each other is excluded). The reaction was performed according to the Metropolis rule [121]. It must also be noted that no end-capers or chain stoppers were added to the simulation, the simulation was stopped at a conversion of 0.987 to achieve the same molar mass as that of the samples given in Table 9. Other assumptions include: (1) all groups are equally reactive and accessible, (2) no cyclics are formed, (3) there are no side reactions, and (5) the condensation by-product is removed. It is important to note that this approach only simulates the equilibrium polymerization products at a given degree of conversion and not the reaction kinetics.

The generated ensemble comprises the structure of each molecule. With such detailed information not only several statistical quantities can be calculated, but also other structural information can be obtained, which is not accessible with other approaches. As an example, the MMDs of branched and linear structures can be calculated by MC models and compared with the MMDs determined by 2D-LC with TD. As shown in Figure 43, high molar mass chains exhibit significantly larger numbers of branching points in a MC simulation than lower molar mass ones. Hence, it can be concluded that the molar masses of linear chains are distinctly lower. Thus, these predictions from MC models are well in line with the experimentally obtained results listed in Table 8.

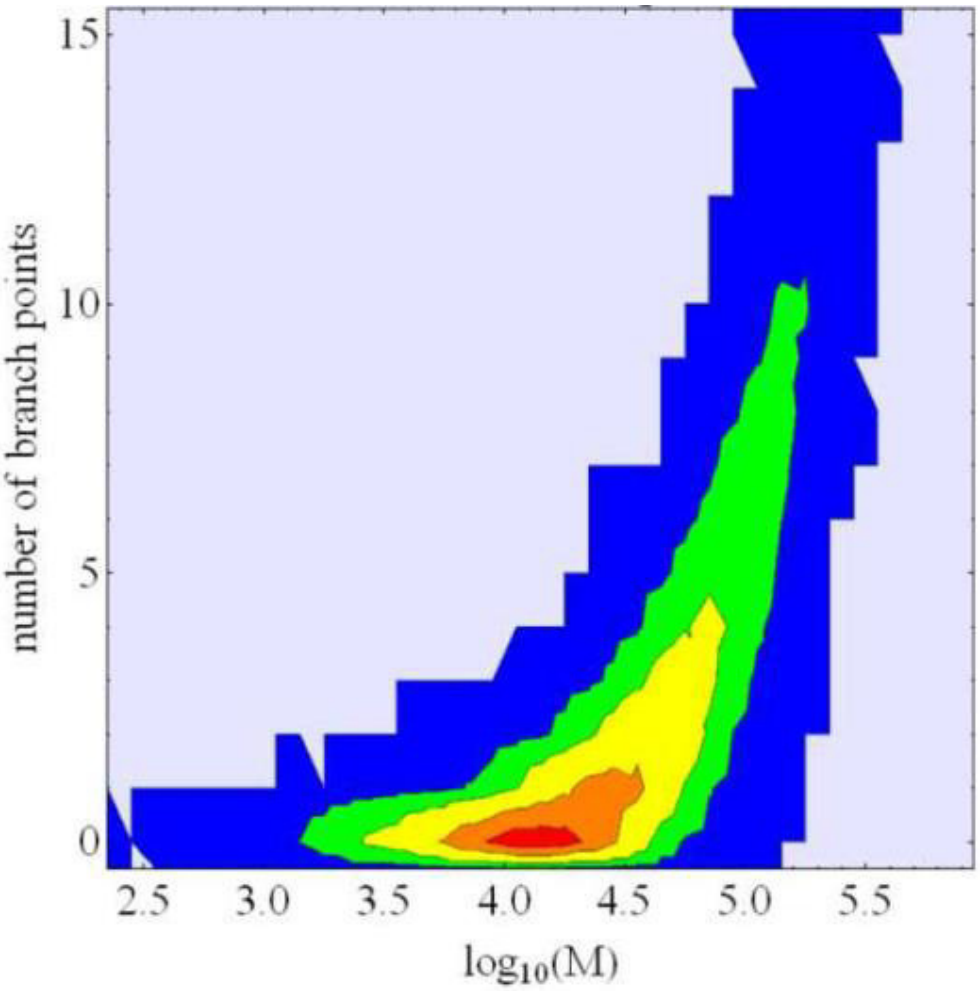

Figure 43: Distribution of branching points along the molar mass for branched PC. The appropriate calculation was performed by Vaidyanath RAMAKRISHNAN, SABIC, Bergen op Zoom, the Netherlands [109].

Furthermore, the percentages of linear and branched structures formed during the synthesis can be calculated from the 2D-LC with TD and compared with those predicted by MC models. As the proportions of branched structures strongly dependent on the conversion rates, as shown in Figure 44, they have to be determined initially.

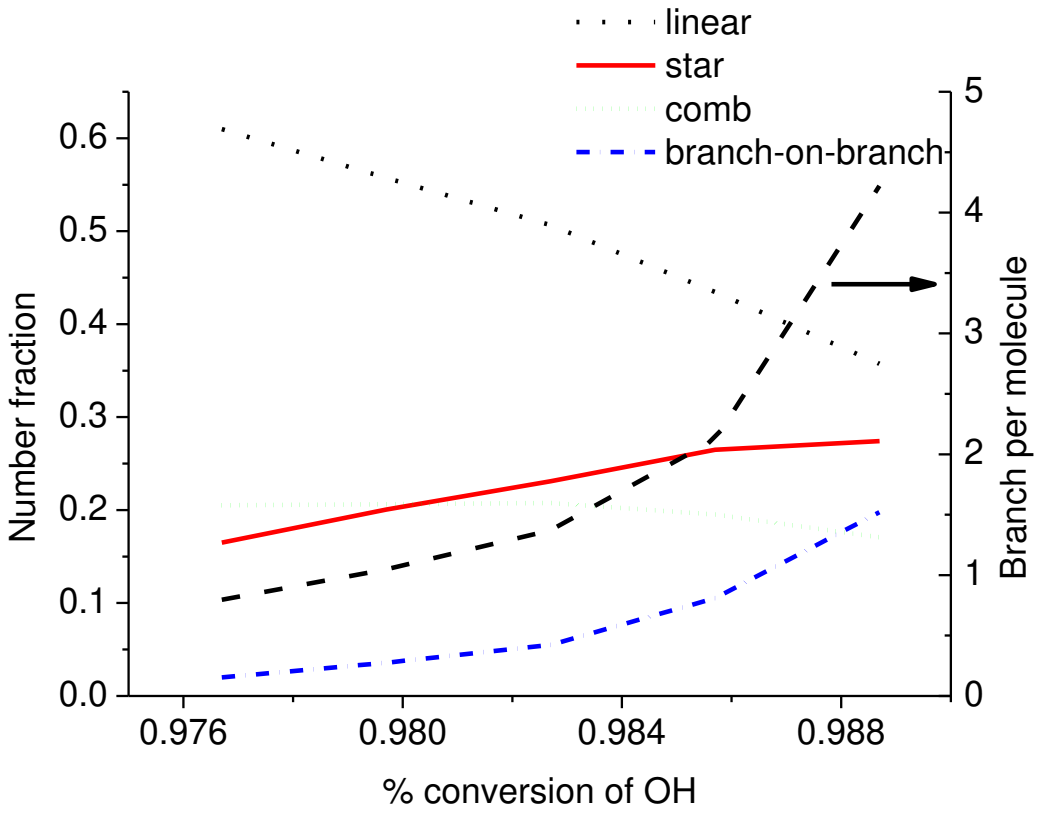

Figure 44: Distribution of structures formed during the polymerization of the branched PC depending on the conversion rate. The appropriate calculation was performed by Vaidyanath RAMAKRISHNAN, SABIC, Bergen op Zoom, the Netherlands [109].

Since the conversion rate decisively affects the MMD, the optimum conversion rate is obtained by comparison with a MMD as determined by TD-SEC, which has already been depicted in section 3.2.2. The corresponding overlay of the two molar mass distributions, which is shown in Figure 45 reveals good correlation. Hence, the optimum conversion rate is determined at a value of 0.987, where a percentage of 44 % linear structures is obtained. In comparison, the experimental data provide approximately 50 % linear structures. This outcome demonstrates that the two methods provide comparable results and, thus, MC yields plausible values despite small deviations.

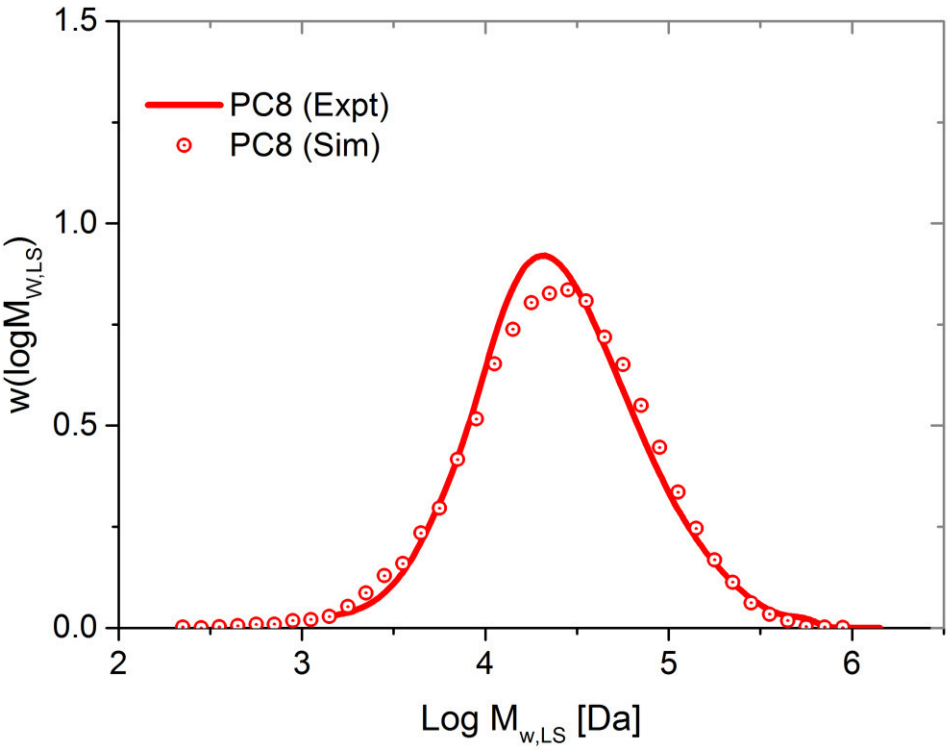

Figure 45: MMD of branched PC8, determined by TD-SEC and MC simulation. Solid lines represent experimental data and the symbols show MC simulation. The appropriate calculation was performed by Vaidyanath RAMAKRISHNAN, SABIC, Bergen op Zoom, the Netherlands [109].

3.2.7 Summary

As LCCC could not achieve a separation of PC according to branching based on differences in the end-group moiety, a novel chromatographic method, namely SG-NCC was developed following the chromatographic method NCC developed by FALKENHAGEN [106]. For that purpose, SGIC was applied in a mobile phase composition range around the point of LCCC on a normal-phase silica stationary phase. Thus, it was aimed at a separation of PC according to end-groups and branching. In order to understand the separation mechanism, fractions of a branched sample were collected. To that end, the fractions were analyzed by MALDI-TOF-MS as well as TD-SEC, and the THPE contents in the single fractions were quantified.

Coelution of branched and linear PC species could be identified, which complicated the interpretation of the TD-SEC results. In order overcome these issues, the chromatographic method was extended to on-line 2D-LC with the developed SG-NCC in the first dimension and SEC as second dimension.

A reversed elution order was observed for some of the branched species in the 2D-LC analyses, which can be explained by the arrangement of the hydroxyl end-groups along the branched chains. As a PC separation according to linear and branched structures could be attained, the developed 2D-LC was augmented by TD and, thus, coelution issues could be overcome. Since TD-SEC allows determining absolute molar masses, detailed information on the molar masses as well as proportions of specific spots in the 2D contour plot were determined. Moreover, for the first time a 2D contour plot of the branching ratio g' could be established from the TD data and, thus, structural information on the individual linear and branched species was extracted.

The experimental outcomes could be exploited to investigate the predictive power of MC models, which are able to simulate statistics of the polymerization of branched PC. Thus, the MMDs and the contents of different structures in a branched PC sample, as determined by the developed 2D-LC with TD method, were compared with MC simulations. Good agreement between the content as well as MMDs determined by 2D-LC with TD and the ones predicted by MC were found and deviations could be explained by model assumptions of the MC simulation as well as incomplete separation in 2D contour plot.

4 Conclusions

The processing and application properties of polymers in general and of Poly(bisphenol A carbonate) (PC) in particular strongly depend on their composition (molar mass distribution, architecture, chemical moiety). Thus, a comprehensive knowledge of the molecular parameters is required for a rational material development. However, the overall structure of polymer chains is a difficult-to-access function with regard to molar mass distribution (MMD) on the one hand and the complex chain architecture on the other hand. Unfortunately, there are no comprehensive characterization methods available that can extract information on the structure of branched PCs so far. Therefore, the aim of this work was the development of a liquid chromatographic method that allows a PC separation according to chain structure types and quantification with regard to molar masses as well as proportions of these species.

In the first part of this thesis, the critical conditions of PC on a PGC stationary phase were established applying the eluent systems $CHCl_3$/TCB and $CHCl_3$/DCB. At these conditions a separation of PC according to the number of hydroxyl end-groups was observed, which was confirmed by MALDI-TOF-MS analysis of the eluting fractions. Analysis of a branched PC sample revealed that a separation of branched structures based on the hydroxyl end-groups could not be achieved with the developed method. Furthermore, a gradual change in the separation selectivity was observed over time, which was explained by the formation of polymer monolayers on the stationary phase and thus necessitated a continuous adjustment of the mobile phase composition. However, in contrast to methods already known in the literature, the presented method was suitable for the identification of linear PC structures with two hydroxyl end-groups. Thus, the developed method can be used to investigate PC degradation products, which might be formed upon hydrolysis or oxidation during the application period of the material. Furthermore, the method may be highly valuable to monitor the end-capping during the PC synthesis, which is used to control the molar masses on the one hand and on the other hand protects the polymer chains from degradation.

Taking into account the drawbacks of porous graphitic carbon as stationary phase for the separation of PC, a normal-phase silica stationary phase was chosen as alternative. However, working at conditions for LCCC also did not lead to the desired PC separation according to branching. Thus, a novel chromatographic approach was developed where the mobile phase composition is varied around the critical point by a solvent gradient (solvent gradient at near-critical conditions, SG-NCC). To elucidate the underlying separation mechanism, a branched sample was subjected to SG-NCCC and the eluting fractions were collected. These were analyzed by MALDI-TOF-MS and TD-SEC, and the THPE contents in the individual fractions were

quantified. Thus, it could be confirmed that the method indeed separated according to molar masses, hydroxyl end-groups as well as branching. In order to improve the separation performance the developed method was hyphenated with a separation according to molar mass to an on-line 2D-LC (SG-NCC × SEC). In the corresponding 2D contour plots individual linear and branched structures could be identified and their content could be determined by a quantitative detector.

Based on theory of liquid adsorption chromatography an earlier elution of polymer chains with lower molar masses was expected, as the number of repeating units defines the interaction strength. However, a reversal of that elution order was observed in the SG-NCC chromatogram when moving from linear to branched chains. This phenomenon could be explained by end-group effects described in the literature [84], which may affect the strength of the interactions with the stationary phase depending on their arrangement along the chain.

In order to further characterize the branched and linear structures that could be separated by the developed 2D-LC analysis the method was augmented by TD and additional insights into the polymer chain structure could be obtained. Moreover, for the first time, the degree of branching was investigated in a 2D-LC experiment, the corresponding 2D contour plot could be established and the individual structures were quantified. Furthermore, the absolute molar mass distribution of the specific spots was extracted. Therefore, 2D-LC with TD offered an experimental opportunity to determine the detailed polymer chain composition in a branched PC sample for the first time.

This method could be exploited to investigate the predictive power of statistical Monte-Carlo (MC) simulation models. MC models have been developed aiming at a statistical determination of the chain structure of branched PC in order to predict the resulting material processing properties. However, MC simulations are based on empirical data evaluations and involve a number of model assumptions.

The chain structures of branched PC predicted by MC simulations were compared with experimental data that are accessible by the newly developed 2D-LC with TD. For that purpose, the MMDs as well as proportions of linear and branched structures in a PC sample could be quantified by LC and the outcomes were compared with MC simulations. The results revealed fair agreement and deviations could be explained by assumptions in the MC models.

In order to improve the predictive power of the MC simulations, additional branched PC samples differing in degree of branching and molar masses might be investigated in further studies. The determined proportions of branched and linear structures may be compared with the

outcomes of MC models and the MC simulation should be further optimized, if required. Furthermore, the information on the degree of branching that could be determined in the 2D-LC with TD might be correlated with chain structures derived from MC simulations. In that way, the comprehension on the structure composition of branched PC might be deepened, the predictive power of rheological simulations could be improved and tailor-made synthesis of branched PC materials may be developed.

5 Zusammenfassung und Schlussfolgerungen

Die Verarbeitungs- und Anwendungseigenschaften von Polymeren im Allgemeinen, und von PC im Besonderen, hängen stark von deren Aufbau (Molmassenverteilung, Architektur, chemische Zusammensetzung) ab. Daher ist eine genaue Kenntnis dieser molekularen Parameter eine notwendige Voraussetzung für eine sinnvolle Materialentwicklung.

Der genaue strukturelle Aufbau der Polymerketten stellt jedoch eine schwer zugängliche Funktion mit Blick auf Molmassenverteilungen auf der einen Seite und der komplexen Kettenarchitektur auf der anderen Seite dar. Leider gibt es bis heute keine Charakterisierungsmethoden, die den komplexen strukturellen Aufbau verzweigten PCs aufklären können.

Ziel der vorliegenden Arbeit war daher die Entwicklung einer flüssigchromatographischen Methode, die eine Trennung von PC nach komplexen Kettenstrukturen ermöglicht. Des Weiteren sollen diese Kettenstrukturen hinsichtlich ihrer Anteile und Molmassen quantifiziert werden.

Im ersten Teil der Arbeit wurden zu diesem Zweck die kritischen Bedingungen von PC in einer PGC-Säule unter der Verwendung der Eluentensysteme $CHCl_3$/TCB und $CHCl_3$/DCB bestimmt. Bei diesen Bedingungen konnte eine Trennung von PC nach der Anzahl der Hydroxyl-Endgruppen beobachtet werden, was durch das Sammeln der eluierenden Fraktionen der entsprechenden Signale und anschließende MALDI-TOF-MS-Analysen bestätigt werden konnte. Die Untersuchung einer verzweigten PC-Probe zeigte, dass eine Trennung verzweigter Strukturen auf Grundlage der Hydroxyl-Endgruppen mit der entwickelten Methode nicht möglich war. Des Weiteren konnte ein graduelle Veränderung der Selektivität der Trennung beobachtet werden, die durch die Bildung monomolekularen Schichten auf der stationären Phase erklärt werden konnte und eine stete Anpassung der Zusammensetzung der mobilen Phase benötigte. Allerdings eignete sich die Methode im Gegensatz zu bereits in der Literatur beschrieben zur Identifikation linearer PC-Strukturen mit zwei Hydroxyl-Endgruppen. Die entwickelte Methode stellt somit eine Möglichkeit zur Untersuchung von Abbauprodukten in PC-Materialien dar, die sich aufgrund von Hydrolyse- oder Oxidationsreaktionen während der Anwendungsphase bilden. Des Weiteren gestattet die Methode während der Synthese eine Überwachung der Terminierung, die einerseits benötigt wird, um die Molmassenverteilung des entstehenden Materials zu kontrollieren und andererseits die Polymerketten vor Abbau schützt.

Unter Beachtung der Nachteile von PGC als stationärer Phase zur Trennung von PC wurde eine Normalphasensäule als Alternative gewählt. Allerdings führte das Arbeiten unter kriti-

schen Bedingungen nicht zu der gewünschten Trennung von verzweigtem PC. Daher wurde eine neue chromatographische Methode entwickelt, bei der die Zusammensetzung der mobilen Phase in der Nähe der kritischen durch die Verwendung von Lösungsmittelgradienten variiert wurde (SG-NCC). Um den zugrundeliegenden Trennmechanismus aufzuklären, wurde eine verzweigte Probe unter der neuentwickelten SG-NCC-Methode aufgetrennt und die eluierenden Fraktionen gesammelt. Die Untersuchung der Fraktionen mittels MALDI-TOF-MS, TD-SEC und die Bestimmung der THPE-Gehalte in den einzelnen Fraktionen bestätigte, dass eine Trennung sowohl nach Molmassen, Hydroxyl-Endgruppen und Verzweigungen vorlag. Um die Trennleistung zu erhöhen, wurde die entwickelte Methode mit einer Trennung nach Molmassen zu einer online 2D-LC (SG-NCC × SEC)erweitert. In den entsprechenden 2D-Konturplots konnten einzelne lineare und verzweigte Strukturen durch einen quantitativen Detektor identifiziert.

Auf der Grundlage der Theorie der Wechselwirkungsflüssigchromatographie wird für Polymere mit kleineren Molmassen auch eine entsprechend frühere Elution erwartet, da die Anzahl der Wiederholungseinheiten die Stärke der Wechselwirkungen bestimmt. Im Gegensatz dazu konnte in dem SG-NCC-Chromatogramm eine Umkehr der Elutionsreihenfolge beim Übergang von den linearen zu den verzweigten Ketten beobachtet werden. Diese Beobachtung konnte durch in der Literatur beschriebene Endgruppeneffekte erklärt werden, die die Stärke der Wechselwirkungen zwischen Kette und stationärer Phase in Abhängigkeit ihrer Positionierung entlang der Kette beeinflussen können.

Um die verzweigten und linearen Strukturen die durch die entwickelte 2D-LC Analyse getrennt werden konnten, detaillierter zu charakterisieren, wurde die Methode durch einen Dreifachdetektor (TD) erweitert, so dass die Untersuchung des strukturellen Kettenaufbaus des PC verbessert werden konnte. So konnte erstmalig der Verzweigungsgrad in einem 2D-LC-Experiment untersucht und der entsprechende 2D-Konturplot bestimmt werden. Des Weiteren konnten die einzelnen Strukturen quantifiziert und deren absolute Molmassenverteilungen ermittelt werden. Daher bietet die beschriebene Methode zum ersten Mal eine experimentelle Option zur Untersuchung des strukturellen Kettenaufbaus verzweigten PCs.

Dies konnte dazu verwendet werde, den Vorhersagekraft statistischer Monte-Carlo (MC) Simulationsmodelle zu überprüfen. MC-Modelle sind im vorliegenden Fall mit dem Ziel entwickelt worden, den strukturellen Kettenaufbau verzweigten PCs durch statistische Methoden zu bestimmen und so die resultierenden rheologischen Verarbeitungseigenschaften des Materials vorherzusagen. Allerdings basieren diese MC-Simulationen auf empirischen Daten und umfassen eine Reihe an Modellannahmen.

Diese Kettenstrukturen des verzweigten PCs, die durch MC-Simulationen vorhergesagt werden, wurden mit experimentellen Daten vergleichen, die durch die neuentwickelte 2D-LC-Methode und die Kopplung mit TD erstmals zugänglich sind. Zu diesem Zweck wurden die Molmassenverteilungen und Anteile der linearen und der verzweigten Strukturen in einer PC-Probe mittels Flüssigchromatographie quantifiziert und mit denjenigen von MC-Simulationen verglichen. Die Ergebnisse lieferten ein hohes Maß an Übereinstimmungen und auftretende Abweichungen konnten durch die Modellannahmen der MC-Simulationen erklärt werden.

Um die Vorhersagekraft der MC-Simulationen zu optimieren, sollten in weiteren Untersuchungen zusätzliche verzweigte PC-Proben, die sich hinsichtlich ihrer Verzweigungsgrade und Molmassen unterscheiden, charakterisiert werden. Die jeweils ermittelten Anteile an verzweigten und linearen Strukturen könnten mit den Ergebnissen der MC-Simulationen verglichen und diese entsprechend optimiert werden. Des Weiteren könnten die Informationen über den Verzweigungsgrad, die durch die Kopplung des Dreifachdetektors mit der 2D-LC-Methode gewonnen werden, mit denjenigen korreliert werden, die aus den MC-Simulationen abgeleitet werden können. Auf diese Weise könnte das Verständnis des strukturellen Aufbaus verzweigten PCs vertieft, die Vorhersagekraft rheologischer Simulationen verbessert und letztendlich maßgeschneiderte Reaktionsführungen entwickelt werden.

6 Experimental part

6.1 Polymer samples

PC standards PC1 to PC 6 were purchased from Polymer Standards Services (PSS), Mainz, Germany. Although the average molar masses as well as end-capping were provided by PSS, the incomplete end-capping as described in section 3.1.2 indicates degradation of the standards. For that reason the number average (M_n), weight average (M_w), and peak (M_p) molar masses, specified in Table 9, were determined by SEC with $CHCl_3$ as eluent. For this purpose, a PLgel Mixed B column, Agilent, Waldbronn, Germany, was installed and calibrated with polystyrene standards, purchased from PSS. The SEC analyses were performed at a temperature of 25 °C. The average molar masses of PC were calculated from a Mark-Houwink calibration [122] using the Mark-Houwink parameters for PS, α=0,794, K=0,0049 mL/g [123], and for PC, α=0,74, K=0,0301 mL/g [92].

Samples PC7 to PC9 were provided by SABIC, Bergen op Zoom, the Netherlands. Their number average (M_n) and weight average (M_w) molar masses of samples provided by SABIC (PC7-9), as determined by SEC with TD, are also listed in Table 9. The experimental setup and details of the analyses are stated in section 6.3.5. End-capping of the sample was analyzed by ^{1}H-NMR according to the method described by KIM et al [124]. THPE contents were determined as stated in section 6.5.

Table 9: PC samples and their molecular characteristics, which were used in the present study.

Sample	M_n / kDa	M_w / kDa	M_p / kDa	Specified End-capping	End-capping level	Content THPE / %
PC1	1.6	7.7	7.4	*t*-Butylphenol	Low	-
PC2	2.0	8.1	7.4	*t*-Butylphenol	Low	-
PC3	3.0	15.3	14.6	*t*-Butylphenol	Low	-
PC4	12.2	48.2	42.6	*t*-Butylphenol	Low	-
PC5	18.4	71.9	57.7	*t*-Butylphenol	Low	-
PC6	2.8	7.9	7.2	*t*-Butylphenol	High	-
PC7	17.4	28.8	-	Phenol	Low	-
PC8	15.1	43.8	-	Phenol	Low	0.86 %
PC9	12.2	29.0	-	Phenol	High	-

6.2 Solvents and chemical substances

Chloroform ($CHCl_3$), stabilized with 0.002 % 2-methyl-2-butene, trichlorobezene (TCB), diethylether (DEE), methyl *tert*-butyl ether (MTBE) and 1,4-dioxane were purchased from Merck, Darmstadt, Germany.

Dithranol (97 %), trans-2-[3-(4-*tert*-Butylphenyl)-2-methyl-2-propenylidene]malononitrile (DCTB) and sodium trifluoroacetate (NaTFAc) were obtained from Sigma Aldrich, Zwijndrecht, the Netherlands.

Lithium chloride (LiCl) anhydrous (99 %), dichloromethane (DCM) and potassium hydroxide (KOH) were supplied from Acros Organics, Geel, Belgium.

Tetrahydrofuran (THF), methanol, glacial acetic acid, ammonium formate (NH_4HCO_2), formic acid (FA) and acetonitrile (ACN) were purchased by Fisher Scientific, Fair Lawn, NJ, USA.

Water was supplied from Merck Millipore, Billerica, MA, USA, under the trademark MilliQ®.

6.3 Chromatographic equipment and methods

6.3.1 Liquid chromatography under critical conditions in PGC stationary phase (LCCC)

The chromatographic measurements were conducted using an Agilent 1100 series HPLC system consisting of a vacuum degasser, a quaternary gradient pump, an auto-sampler and a column oven with temperature control. The mixed mobile phase ($CHCl_3$ as adsorption promoting eluent and TCB as desorption promoting eluent) was prepared using the gradient pump of the HPLC system. In order to attain critical conditions, the mobile phase composition was changed in steps of 0.1 vol% and corresponding PC standards were subsequently injected. The temperature was set to 5 °C, 25 °C or 57.5 °C. Data were collected using WinGPC software from PSS. Data were processed by OriginLab© 9.1 from OriginLab Co., Northampton, MA, USA.

An evaporative light scattering detector (ELSD) model PL-ELS 1000, Polymer Laboratories, Church Stretton, UK, was used with a nebulizer temperature of 160 °C, an evaporation temperature of 260 °C and a nitrogen flow rate of 1.5 L/min.

A Hypercarb™ column (100 x 4.6 mm L. x I.D., particle diameter 5 μm, pore size 250 Å; obtained from ThermoFisher Scientific, Dreieich, Germany) was installed and thermostated in the column oven.

In order to accurately and reproducibly collect fractions the fractionation process was automated. A 12-port VICI™ valve from Valco Instruments, Houston, TX, USA was used. The switching of the valve was triggered by an output relay, which was controlled by the WinGPC software. For this purpose, a time table was loaded in the relay options of the software allowing a precise collection of the fractions after each sample injection. The valve was turned after 1.4 mL, 1.75 mL and 2.3 mL obtaining three fractions, which were subsequently analyzed by MALDI-TOF-MS as outlined in section 6.4.

6.3.2 Recovery rate determination

IR spectra of $CHCl_3$, TCB and PC were acquired on a Nicolet™ 8700 Fourier transform infrared (FTIR) spectrometer, Thermo Scientific, Waltham, MA, USA.

A Nicolet™ iS™ FTIR spectrometer (Thermo Scientific) equipped with an on-line flow cell was used as detector for the recovery rate determinations. Initially, the Hypercarb™ column was replaced by a steal capillary (INOX316) with a length of 400 mm and 0.5 mm I.D. and samples PC1, PC3 and PC5 were injected at a flow rate of 0.7 mL/min. A mobile phase of 95.5/4.5 vol% $CHCl_3$/TCB was used. Subsequently, the Hypercarb™ column was reinstalled and the samples were measured again under the same conditions. All measurements were performed three times and the average values of the peak areas were calculated using the characteristic carbonyl stretching vibration of PC at 1770 cm^{-1}. The standard deviation was determined using the statistical method of the propagation of uncertainty [125].

6.3.3 Solvent gradients at near-critical conditions (SG-NCC) in a normal-phase stationary phase

In addition to the chromatographic setup as stated in section 6.3.1 an Agilent 1100 series variable wavelength detector (UV detector) was used for the SG-NCC analyses. A normal-phase Nucleosil® column 250 x 4.0 mm (L. x I.D.), 7 μm, 1000 Å, obtained from Macherey-Nagel (Düren, Germany) was thermostated in the Agilent column oven at 45 °C. The wavelength of the UV detector was set to 254 nm. $CHCl_3$ acted as adsorption promoting eluent and MTBE served as desorption promoting eluent. As the content of MTBE, which was required to completely desorb the PC from the silica column, was very low, a 97.5/2.5 vol% $CHCl_3$/MTBE solution was used as desorption promoting eluent, which was premixed before its application. This allowed exploiting the full flow rate scale of the gradient pump and, therefore, improving the accuracy and reliability of the applied eluent composition.

The samples PC7-9 were analyzed in a 60-min-linear mobile phase gradient from $CHCl_3$ to 97.5/2.5 vol% $CHCl_3$/MTBE, starting 5 min after the injection at a flow rate of 1 mL/min. Details of the applied gradient are listed in Table 10. WinGPC was used for data acquisition. Data were processed by OriginLab© 9.1.

Table 10: Mobile phase gradient, which was applied for the separation of PCs in the newly developed SG-NCC.

Time / min	**$CHCl_3$ / vol%**	**97.5/2.5 % $CHCl_3$/ MTBE / vol%**
0	100	0
5	100	0
65	0	100

A 12-port VICI™ valve from Valco Instruments was used to collect the fractions. At the valve outlets vials were placed to collect the eluate in different fractions. An output relay, which was operated by the WinGPC software, triggered the switching of the valve. Sample PC8 was repeatedly injected and analyzed in the SG-NCC as described in section 3.2.1. 6 fractions were obtained as shown in Figure 27 turning the valve after 20.1 mL, 28.1 mL, 36.8 mL, 37.7 mL, 39.2 mL, 44.0 mL and 50.0 mL. The corresponding time table was loaded in the relay options of the WinGPC software, which allowed precisely switching the valve after each sample injection. The fractions were analyzed by MALDI-TOF-MS as outlined in section 6.4.2, TD-SEC as stated in section 6.3.5 and the THPE was quantified as described in section 6.5.

6.3.4 On-line two-dimensional liquid chromatography (2D-LC)

In the first dimension (SG-NCC) the same conditions as described in section 6.3.3 were used except for the flow rate and the mobile phase gradient. The flow rate was reduced from 1 mL/min to 0.1 mL/min in order to synchronize with the second dimension (SEC). Consequently, the duration of the mobile phase gradient had to be increased from 60 min to 600 min, since the slope of the gradient was related to the dimension of volume rather than to the one of time. Thus, the gradient slope of the SG-NCC and the first dimension of the 2D-LC were identical.

An electronically controlled 8-port VICI^{TM} valve from Valco Instruments equipped with two loops of 200 μL each was applied to connect the two chromatographic dimensions. The switching operation of the valve was triggered by an output relay which was controlled by WinGPC software.

In the second dimension an Agilent 1100 series HPLC system was used as well, consisting of a vacuum degasser, an isocratic pump, a column oven and a UV detector set at 254 nm. A HighSpeed SDV column (SEC) 50 x 20 mm (L x I.D.), 5 μm, 10,000 Å from PSS was thermostated at 30 °C in the column oven. $CHCl_3$ was used as eluent and the flow rate was set to 5 mL/min. The schematic workflow of the 2D-LC setup is given in Figure 46. Data were acquired by WinGPC software and processed by OriginLab© 9.1.

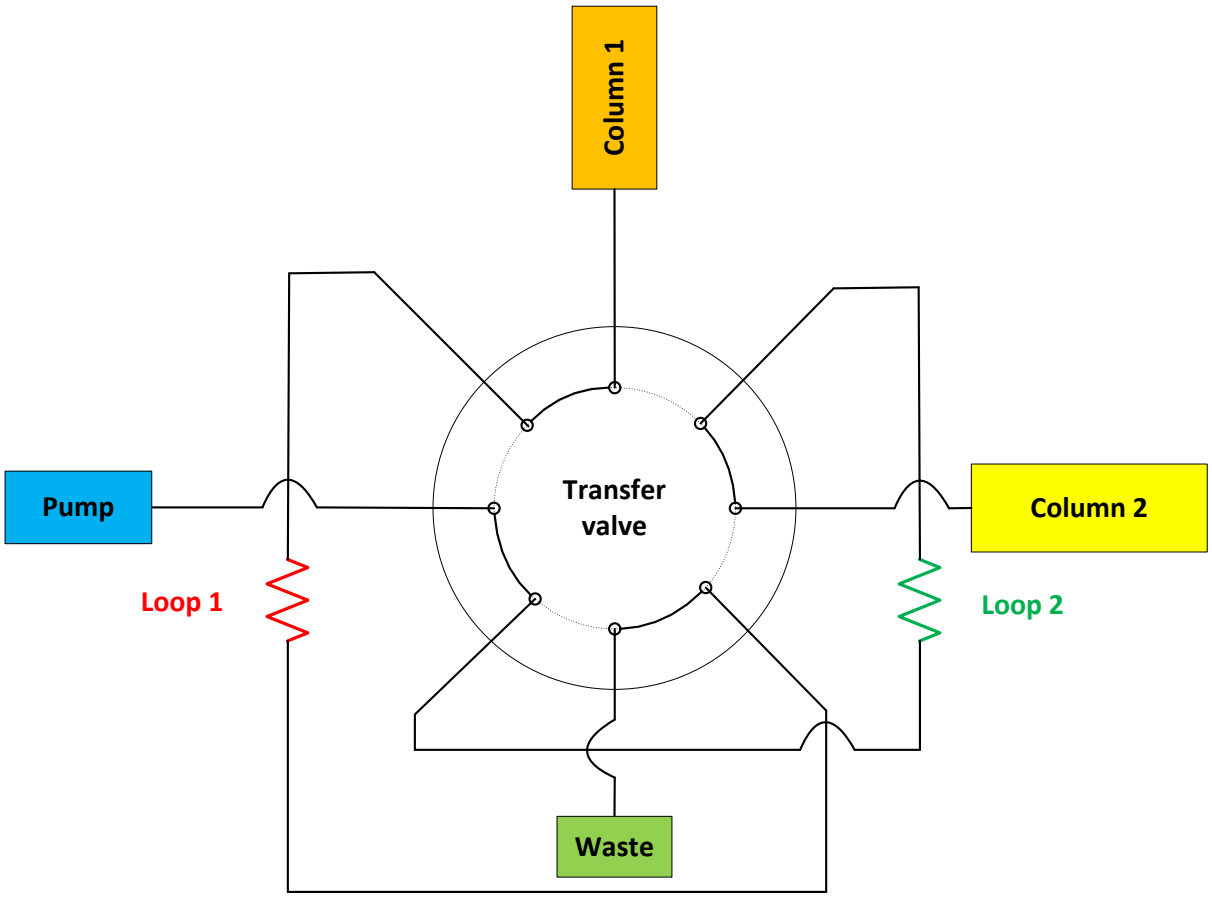

Figure 46: Schematic representation of the 2D-LC valve component.

6.3.5 Triple-detection size-exclusion chromatography (TD-SEC)

An Agilent 1260 series HPLC system from Agilent consisting of a vacuum degasser, an isocratic pump, an auto-sampler and a column oven, was used for all TD-SEC measurements. A UV detector (254 nm) and an Agilent 1260 Infinity Multi-detector suite (MDS) were applied as detectors. The MDS was equipped with a differential RI detector (λ=658 nm), a dual angle (15°, 90°) LS detector (λ=658 nm) and a four-capillary VI, which are arranged in series. A dn/dc of 0.155 mL/g was determined for PC at λ=658 nm and 30 °C. A PSS SDV column, 300 x 8 mm (L. x I.D.), 5 μm, 10,000 Å, obtained from PSS was installed.

Samples were dissolved in $CHCl_3$ preparing a solution with a concentration of 1-2 mg/mL. A flow rate of 1.0 mL/min was applied. The instrument calibration was performed with a PS standard (M_w=98 kDa, Đ$_M$=1.02). Data were collected and processed using Agilent GPC/SEC software and OriginLab© 9.1.

6.3.6 On-line two-dimensional liquid chromatography with triple-detection (2D-LC with TD)

In the first dimension (SG-NCC) the same Agilent 1100 series HPLC system was used as described in section 6.3.3. A normal-phase Nucleosil® column 250 x 4.0 mm (L. x I.D.), 7 μm, 1000 Å, obtained from Macherey-Nagel was thermostated in the Agilent column oven at 45 °C. The same eluents were applied as stated in section 6.3.3.

An electronically controlled 8-port VICI™ valve from Valco Instruments equipped with two loops of 200 μL each was installed to connect the two chromatographic dimensions. The switching operation of the valve was triggered by an output relay which was controlled by WinGPC software from PSS. The process flow diagram of the electronic switching control is provided in Figure 47.

To determine the optimum experimental parameters of the 2D-LC setup, the application notes of the TD unit, namely the occurrence of a “breakthrough” peak and the limitation of the flow rate in order to avoid that the backpressure in the VI might exceed 100 kPa, had to be considered [115]. As described in section 3.2.5 a flow rate of 1.5 mL/min was applied in the second dimension. Accordingly, to ensure a complete analysis in the 2D-LC setup the experimental parameters of the first dimension had also to be adjusted. Considering the volume of the loops of the transfer valve (200 μL) and the acquisition times in the second dimension (20 min) the flow rate of the first dimension had to be set to 0.01 mL/min to ensure the analysis of the complete sample without any losses. A flow rate of 0.01 mL/min might lead to a deterioration of the separation performance. However, as could be shown in the corresponding 2D contour plots (Figure 38 to Figure 41), the separation of the different PC structures was still achieved with the present setup and deterioration of the performance could hardly be recognized.

Apart from the flow rate also the slope of the solvent gradient had to be adjusted. As stated in section 6.3.4 for previous 2D-LC analysis a mobile phase gradient from $CHCl_3$ to 97.5/2.5 vol% $CHCl_3$/MTBE with a duration of 600 min at a flow rate of 0.1 mL/min had been applied. When decreasing the flow rate to 0.01 mL/min it was decided to apply a mobile phase gradient from $CHCl_3$ to 97.5/2.5 vol% $CHCl_3$/MTBE over 3000 min instead of 6000 min in order to limit the overall measurement time. Samples were dissolved in $CHCl_3$ preparing a solution with a concentration of 100 mg/mL.

Data of the second dimension were collected and processed using Agilent GPC/SEC software from Agilent and OriginLab© 9.1.

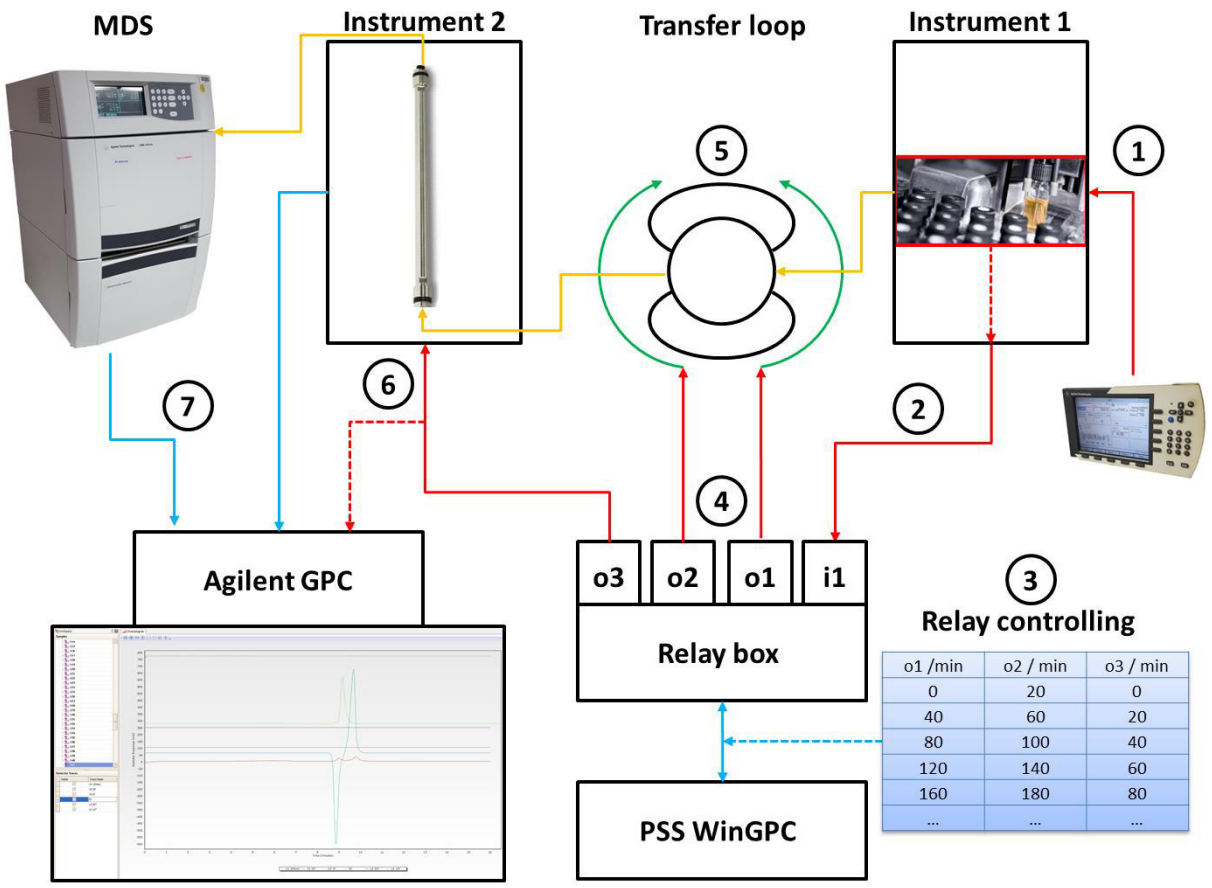

Figure 47: Process flow diagram of the 2D-LC-TD-SEC analyses. PSS WinGPC software is used for controlling of the transfer valve while data are collected by Agilent GPC software.

6.4 MALDI-TOF-MS

6.4.1 Analysis of samples related with section 3.1

An Axima-Tof2^{TM} system, Shimadzu, Kyoto, Japan, was used for the MALDI-TOF-MS analyses. Samples PC1 and PC6 were dissolved in 1,4-dioxane (concentration about 4 mg/mL). 1,4-dioxane was used as solvent instead of THF in order to prevent formation of peroxides. 15 μL of the solution were mixed with 15 μL of a dithranol solution (concentration 10 mg/mL in 1,4-dioxane). Subsequently, 7.5 μL of an aqueous LiCl solution (concentration 10 mg/mL) were added and the mixture was deposited on a MALDI target. The solvent was evaporated in air, and the target was subsequently placed into the spectrometer and irradiated by an UV laser (wavelength 337 nm). The laser focus on the target was shifted after every shot and 150 shots were accumulated and averaged for one analysis. An acceleration voltage of 20 kV was applied.

6.4.2 Analysis of samples related with section 3.2

A JMS-S3000 MALDI-TOF-MS from JEOL, Tokyo, Japan was used for analysis of the corresponding fractions. Fractions 1-6 were diluted in DCM (concentration about 5 mg/mL). The solution was mixed with DCTB serving as MALDI matrix in DCM (concentration 10 mg/mL) and NaTFAc in THF (concentration 6 mg/mL) at a 10/100/10 ratio. After spotting the mixture onto a MALDI target the solvent was evaporated in air, and the target was placed into the mass spectrometer and irradiated by an UV laser (wavelength 337 nm). The laser focus on the target was shifted after every shot and 150 shots were accumulated and averaged per analysis. An acceleration voltage of 20 kV was applied.

6.5 THPE quantification by liquid chromatography

1 mg of PC11 and each fraction were weighed in a separate customary HPLC vial using a micro balance. 50 μL DCM were added and the vial was placed on a shaking bench for 20 min. Subsequently, 30 μL of 10 % KOH solution in methanol were added to hydrolyze the carbonate linkages of the polymer and the solution was shaken for 30 s. 20 μL of glacial acetic acid were added to neutralize the solution.

The samples prepared in this way were analyzed by an Ultimate 3000 chromatograph from Thermo Scientific, Waltham, MA, USA, comprising a degasser, a quaternary pump, an autosampler, a column oven and a diode array detector (DAD). 1 μL of each analyte was injected onto a Poroshell EC-C18 (150 x 2.1 mm L x I.D.), 2.7 μm revered-phase silica column from Agilent thermostated at 35 °C, while a flow rate of 0.25 mL/min was applied. A mobile phase gradient from water containing 10 mM NH_4HCO_2 and 0.1 % FA to ACN was applied according to Table 11.

In order to quantify the THPE content in the different fractions calibration standards with exactly known contents of THPE were measured and a calibration curve was plotted for the areas under the peaks obtained for the DAD response at 280 nm. All measurements were performed three times and an error of 0.009 % THPE was calculated for the quantification.

Table 11: Mobile phase gradient of the LC, which was applied for the quantification of THPE in the different PC fractions.

Time / min	H_2O + 10 mM NH_4HCO_2 + 0.1 % FA / vol%	ACN / vol%
0	95	5
3	70	30
14	60	40
15	0	100
20	0	100

7 References

[1] H. Elias, Makromoleküle, Band 1, Hüthig und Wepf, Heidelberg, 1990.

[2] W. Keim, Kunststoffe: Synthese, Herstellungsverfahren, Apparaturen, Wiley-VCH, Weinheim, 2006.

[3] S. Podzimek, Light scattering, size exclusion chromatography and asymmetric flow field flow fractionation: powerful tools for the characterization of polymers, proteins and nanoparticles, John Wiley & Sons, Hoboken, 2011.

[4] H.-G. Elias, Macromolecules: Physical Structures and Properties., Wiley-VCH, Weinheim, 2008.

[5] C. Pryde, M. Hellman, Solid state hydrolysis of bisphenol-A polycarbonate. I. Effect of phenolic end groups, J. Appl. Polym. Sci., 25 (1980) 2573-2587.

[6] H. Pasch, B. Trathnigg, Multidimensional HPLC of polymers, Springer, Heidelberg, 2013.

[7] A. Einhorn, Ueber die Carbonate der Dioxybenzole, Justus Liebigs Ann. Chem., 300 (1898) 135-155.

[8] H. Schnell, Polycarbonate, eine Gruppe neuartiger thermoplastischer Kunststoffe. Herstellung und Eigenschaften aromatischer Polyester der Kohlensäure, Angew. Chem., 68 (1956) 633-640.

[9] H. Schnell, L. Bottenbruch, H. Krimm, Thermoplastic aromatic polycarbonates and their manufacture, US Patent 3028365, (1962)

[10] D.W. Fox, Aromatic carbonate resins and preparation thereof, US Patent 3153008, (1964)

[11] H. Hock, S. Lang, Autoxydation von Kohlenwasserstoffen, IX. Mitteil.: Über Peroxyde von Benzol-Derivaten, Berichte der deutschen chemischen Gesellschaft (A and B Series), 77 (1944) 257-264.

[12] Y. Ito, H. Ogasawara, Y. Ishida, H. Ohtani, S. Tsuge, Characterization of end groups in polycarbonates by reactive pyrolysis-gas chromatography, Polym. J., 28 (1996) 1090-1095.

[13] F. Samperi, S. Montaudo, G. Montaudo, Polycarbonates, in: T. Sabu, P.M. Visakh (Eds.) Handbook of Engineering and Speciality Thermoplastics, Scrivener Publishing, Beverly, MA, 2011, pp. 493.

[14] J.A. King, Synthesis of Polycarbonate, in: J.T. Bendler, D.G. LeGrand (Eds.) Handbook of Polycarbonate Science and Technology, Dekker, New York, 2000, pp. 7.

[15] J.T. Coe, Unlikely victory: How General Electric succeeded in the chemical industry, American Institute of Chemical Engineers, New York, 2000.

[16] J.A. Mahood, P.S. Gautam, Process to prepare high heat polycarbonates, US Patent 2016/0237210, (2014)

[17] J.L. DeRudder, Commercial applications of Polycarbonates, in: D.G. LeGrand, J.T. Bendler (Eds.) Handbook of Polycarbonate Science and Technology, Dekker, New York, 2000, pp. 303.

[18] K. Troev, R. Tsevi, I. Gitsov, A novel depolymerization route to phosphorus-containing oligocarbonates, Polymer, 42 (2001) 39-42.

[19] M.R. Korn, M.R. Gagné, Convenient depolymerization route to telechelic polycarbonate oligomers, Macromolecules, 31 (1998) 4023-4026.

[20] E.E. Bostick, Introduction and Historical Background, in: J.T. Bendler, D.G. LeGrand (Eds.) Handbook of Polycarbonate Science and Technology, Dekker, New York, 2000, pp. 1.

[21] F. Siriani, M. Di Silverio, How Athens' Olympic stadium was finally pulled together, Proceedings of the Institution of Civil Engineers - Civil Engineering, 159 (2006) 114-119.

[22] J. Schmidhauser, P.D. Sybert, Nonbisphenol A Polycarbonates, in: J.T. Bendler, D.G. LeGrand (Eds.) Handbook of Polycarbonate Science and Technology, Dekker, New York, 2000, pp. 61.
[23] L.E. Baccaro, P. Keenan, Current Applications of Polycarbonates, in: J.T. Bendler, D.G. LeGrand (Eds.) Handbook of Polycarbonate Science and Technology, Dekker, New York, 2000, pp. 341.
[24] T.C. Jordan, D. Richards, Polycarbonate melt rheology, in: J.T. Bendler, D.G. LeGrand (Eds.) Handbook of Polycarbonate Science and Technology, Dekker, New York, 2000, pp. 179.
[25] A.R. Shultz, PVT, Specific Heat, and Thermal Transitions, in: J.T. Bendler, D.G. LeGrand (Eds.) Handbook of Polycarbonate Science and Technology, Dekker, New York, 2000, pp. 149.
[26] M.J. Marks, S. Munjal, S. Namhata, D.C. Scott, F. Bosscher, J.A. De Letter, B. Klumperman, Randomly branched bisphenol A polycarbonates. I. Molecular weight distribution modeling, interfacial synthesis, and characterization, J. Polym. Sci., Part A: Polym. Chem., 38 (2000) 560-570.
[27] E. van Ruymbeke, A. Kaivez, A. Hagenaars, D. Daoust, P. Godard, R. Keunings, C. Bailly, Characterization of sparsely long chain branched polycarbonate by a combination of solution, rheology and simulation methods, J. Rheol., 50 (2006) 949-973.
[28] A.M. Striegel, M.R. Krejsa, Complementarity of universal calibration SEC and 13C NMR in determining the branching state of polyethylene, J. Polym. Sci., Part B: Polym. Phys., 38 (2000) 3120-3135.
[29] E. Van Ruymbeke, R. Keunings, C. Bailly, Prediction of linear viscoelastic properties for polydisperse mixtures of entangled star and linear polymers: Modified tube-based model and comparison with experimental results, J. Nonnewton Fluid. Mech., 128 (2005) 7-22.
[30] X. Chen, M.S. Rahman, H. Lee, J. Mays, T. Chang, R. Larson, Combined Synthesis, TGIC Characterization, and Rheological Measurement and Prediction of Symmetric H Polybutadienes and Their Blends with Linear and Star-Shaped Polybutadienes, Macromolecules, 44 (2011) 7799-7809.
[31] J.C. Randall, A review of high resolution liquid 13carbon nuclear magnetic resonance characterizations of ethylene-based polymers, J. Macromol. Sci., Rev. Macromol. Chem. Phys., 29 (1989) 201-317.
[32] F. Malz, H. Jancke, Validation of quantitative NMR, J. Pharm. Biomed. Anal., 38 (2005) 813-823.
[33] W. Liu, D.G. Ray, P.L. Rinaldi, Resolution of signals from long-chain branching in polyethylene by 13C NMR at 188.6 MHz, Macromolecules, 32 (1999) 3817-3819.
[34] B.H. Zimm, W.H. Stockmayer, The Dimensions of Chain Molecules Containing Branches and Rings, J. Chem. Phys., 17 (1949) 1301-1314.
[35] C. Jackson, Y.J. Chen, J.W. Mays, Dilute solution properties of randomly branched poly (methyl methacrylate), J. Appl. Polym. Sci., 59 (1996) 179-188.
[36] S.T. Balke, T.H. Mourey, D.R. Robello, T.A. Davis, A. Kraus, K. Skonieczny, Quantitative analysis of star-branched polymers by multidetector size-exclusion chromatography, J. Appl. Polym. Sci., 85 (2002) 552-570.
[37] P. Castignolles, R. Graf, M. Parkinson, M. Wilhelm, M. Gaborieau, Detection and quantification of branching in polyacrylates by size-exclusion chromatography (SEC) and melt-state 13C NMR spectroscopy, Polymer, 50 (2009) 2373-2383.
[38] A. Gorshkov, T. Prudskova, V. Gur'yanova, V. Evreinov, Functional type separation of oligocarbonates by liquid chromatography under critical conditions, Polym. Bull., 15 (1986) 465-468.

[39] L. Coulier, E. Kaal, T. Hankemeier, Comprehensive two-dimensional liquid chromatography and hyphenated liquid chromatography to study the degradation of poly (bisphenol A) carbonate, J. Chromatogr. A, 1070 (2005) 79-87.
[40] L. Coulier, E. Kaal, T. Hankemeier, Hyphenation of infrared spectroscopy to liquid chromatography for qualitative and quantitative polymer analysis: Degradation of poly (bisphenol A) carbonate, J. Chromatogr. A, 1130 (2006) 34-42.
[41] J.H. Knox, M.T. Gilbert, Preparation of porous carbon US Patent 4 263 268 A (1979)
[42] L. Pereira, Porous graphitic carbon as a stationary phase in HPLC: Theory and applications, J. Liq. Chromatogr. Relat. Technol., 31 (2008) 1687-1731.
[43] J.H. Knox, P. Ross, Carbon-based packing materials for liquid chromatography; Structure, Performance and Retention Mechanisms, Adv. Chromatogr., 37 (1997) 162.
[44] P. Ross, J.H. Knox, Carbon-based packing materials for liquid chromatography: applications, Adv. Chromatogr., 37 (1997) 121-162.
[45] J.H. Knox, B. Kaur, G.R. Millward, Structure and performance of porous graphitic carbon in liquid chromatography, J. Chromatogr. A, 352 (1986) 3-25.
[46] P.T. Jackson, P.W. Carr, Study of polar and nonpolar substituted benzenes and aromatic isomers on carbon-coated zirconia and alkyl bonded phases, J. Chromatogr. A, 958 (2002) 121-129.
[47] D. Mekap, T. Macko, R. Brüll, R. Cong, A. Parrott, P. Cools, W. Yau, Liquid chromatography at critical conditions of polyethylene, Polymer, 54 (2013) 5518-5524.
[48] T. Macko, H. Pasch, Separation of linear polyethylene from isotactic, atactic, and syndiotactic polypropylene by high-temperature adsorption liquid chromatography, Macromolecules, 42 (2009) 6063-6067.
[49] K. Prabhu, R. Brüll, T. Macko, K. Remerie, J. Tacx, P. Garg, A. Ginzburg, Separation of bimodal high density polyethylene using multidimensional high temperature liquid chromatography, J. Chromatogr. A, 1419 (2015) 67-80.
[50] T. Macko, F. Cutillo, V. Busico, R. Brüll, Separation of poly (propylene) samples according to tacticity using a hypercarb column, in: Macromolecular symposia, Wiley Online Library, 2010, pp. 182-190.
[51] T. Macko, R. Brüll, Y. Wang, B. Coto, I. Suarez, Characterization of ethylene-propylene copolymers with high-temperature gradient adsorption liquid chromatography and CRYSTAF, J. Appl. Polym. Sci., 122 (2011) 3211-3217.
[52] T. Macko, A. Ginzburg, K. Remerie, R. Bruell, Separation of High-Impact Polypropylene Using Interactive Liquid Chromatography, Macromol. Chem. Phys., 213 (2012) 937-944.
[53] D. Mekap, T. Macko, R. Brüll, R. Cong, A. deGroot, A. Parrott, W. Yau, One-step method for separation and identification of n-alkanes/oligomers in hdpe using high-temperature high-performance liquid chromatography, Macromolecules, 46 (2013) 6257-6262.
[54] K. Maiko, M. Hehn, W. Hiller, H. Pasch, Comprehensive two-dimensional liquid chromatography of stereoregular poly (methyl methacrylates) for tacticity and molar mass analysis, Anal. Chem., 85 (2013) 9793-9798.
[55] D. Berek, Progress in liquid chromatography of synthetic electroneutral polymers, in: Macromolecular Symposia, Wiley Online Library, 2003, pp. 147-164.
[56] G. Aced, H.J. Möckel, Liquidchromatographie, VCH Verlagsgesellschaft, Weinheim, 1991.
[57] G. Glöckner, Polymercharakterisierung durch Flüssigkeitschromatographie, Deutscher Verlag der Wissenschaften, Berlin, 1982.
[58] I.S. Lipatov, L.M. Sergeeva, R. Kondor, D. Slutzkin, Adsorption of polymers, Wiley, New York, 1976.
[59] B. Trathnigg, Size-Exclusion Chromatography of Polymers, in: Encyclopedia of Analytical Chemistry, John Wiley & Sons, Hoboken, 2006.

[60] A. Striegel, W.W. Yau, J.J. Kirkland, D.D. Bly, Modern size-exclusion liquid chromatography: practice of gel permeation and gel filtration chromatography, John Wiley & Sons, Hoboken, 2009.
[61] B.H. Zimm, The scattering of light and the radial distribution function of high polymer solutions, J. Chem. Phys., 16 (1948) 1093-1099.
[62] B.H. Zimm, R.W. Kilb, Dynamics of branched polymer molecules in dilute solution, J. Polym. Sci. Pol. Chem., 37 (1959) 19-42.
[63] R. Mendichi, A.G. Schieroni, Evaluation of a single-capillary viscometer detector on line to a SEC system used with a new pulse-free pump, J. Appl. Polym. Sci., 68 (1998) 1651-1659.
[64] F. Beer, G. Capaccio, L. Rose, High molecular weight tail and long-chain branching in low-density polyethylenes, J. Appl. Polym. Sci., 80 (2001) 2815-2822.
[65] A.M. Striegel, Mid-chain grafting in PVB-graft-PVB, Polym. Int., 53 (2004) 1806-1812.
[66] S. Ahn, H. Lee, S. Lee, T. Chang, Characterization of branched polymers by comprehensive two-dimensional liquid chromatography with triple detection, Macromolecules, 45 (2012) 3550-3556.
[67] M. Gaborieau, P. Castignolles, Size-exclusion chromatography (SEC) of branched polymers and polysaccharides, Anal. Bioanal. Chem., 399 (2011) 1413-1423.
[68] M. Gaborieau, J. Nicolas, M. Save, B. Charleux, J.-P. Vairon, R.G. Gilbert, P. Castignolles, Separation of complex branched polymers by size-exclusion chromatography probed with multiple detection, J. Chromatogr. A, 1190 (2008) 215-223.
[69] B. Trathnigg, A. Skvortsov, Determination of the accessible volume and the interaction parameter in the adsorption mode of liquid chromatography, J. Chromatogr. A, 1127 (2006) 117-125.
[70] G. Glöckner, Gradient HPLC of copolymers and chromatographic cross-fractionation, Springer Science & Business Media, Berlin, 2012.
[71] Y. Mengerink, R. Peters, S. van der Wal, H. Claessens, C. Cramers, Endgroup-based separation and quantitation of polyamide-6, 6 by means of critical chromatography, J. Chromatogr. A, 949 (2002) 337-349.
[72] T. Macko, D. Hunkeler, Liquid chromatography under critical and limiting conditions: a survey of experimental systems for synthetic polymers, in: Liquid Chromatography/FTIR Microspectroscopy/Microwave Assisted Synthesis, Springer, 2003, pp. 62-136.
[73] J. Falkenhagen, S. Weidner, Determination of critical conditions of adsorption for chromatography of polymers, Anal. Chem., 81 (2008) 282-287.
[74] A. Gorshkov, H. Much, H. Becker, H. Pasch, V. Evreinov, S. Entelis, Chromatographic investigations of macromolecules in the “critical range” of liquid chromatography: I. Functionality type and composition distribution in polyethylene oxide and polypropylene oxide copolymers, J. Chromatogr. A, 523 (1990) 91-102.
[75] D. Berek, M. Janco, K. Hatada, T. Kitayama, N. Fujimoto, Separation of poly (methyl methacrylate) s according to their tacticity II. Chromatographic investigations of poly (methyl methacrylate) s with different tacticity at the critical adsorption point, Polym. J., 29 (1997) 1029-1033.
[76] S.G. Entelis, V.V. Evreinov, A.V. Gorshkov, Functionality and molecular weight distribution of Telechelic polymers, in: K. Dušek (Ed.) Pharmacy/Thermomechanics/Elastomers/Telechelics, Springer, Berlin, Heidelberg, 1986, pp. 129-175.
[77] T. Macko, D. Hunkeler, D. Berek, Liquid Chromatography of Synthetic Polymers under Critical Conditions. The Case of Single Eluents and the Role of ϑ Conditions, Macromolecules, 35 (2002) 1797-1804.

[78] A. Baumgaertel, E. Altuntaş, U.S. Schubert, Recent developments in the detailed characterization of polymers by multidimensional chromatography, J. Chromatogr. A, 1240 (2012) 1-20.
[79] B.G. Belenky, E.S. Gankina, M.B. Tennikov, L.Z. Vilenchik, Fundamental aspects of adsorption chromatography of polymers and their experimental verification by thin-layer chromatography, J. Chromatogr. A, 147 (1978) 99-110.
[80] H. Lee, T. Chang, D. Lee, M.S. Shim, H. Ji, W.K. Nonidez, J.W. Mays, Characterization of Poly (l-lactide)-b lock-Poly-(ethylene oxide)-b lock-Poly (l-lactide) Triblock Copolymer by Liquid Chromatography at the Critical Condition and by MALDI-TOF Mass Spectrometry, Anal. Chem., 73 (2001) 1726-1732.
[81] H. Pasch, K. Mequanint, A. Jörg, Two-dimensional chromatography of complex polymers. 3. Full analysis of polystyrene-poly (methyl methacrylate) diblock copolymers, epoly., 2 (2002) 69-87.
[82] K. Im, Y. Kim, T. Chang, K. Lee, N. Choi, Separation of branched polystyrene by comprehensive two-dimensional liquid chromatography, J. Chromatogr. A, 1103 (2006) 235-242.
[83] K. Im, H.-W. Park, Y. Kim, S. Ahn, T. Chang, K. Lee, H.-J. Lee, J. Ziebarth, Y. Wang, Retention behavior of star-shaped polystyrene near the chromatographic critical condition, Macromolecules, 41 (2008) 3375-3383.
[84] W. Radke, K. Rode, A.V. Gorshkov, T. Biela, Chromatographic behavior of functionalized star-shaped poly(lactide)s under critical conditions of adsorption. Comparison of theory and experiment, Polymer, 46 (2005) 5456-5465.
[85] T. Biela, A. Duda, H. Pasch, K. Rode, Star-shaped poly (L-lactide) s with variable numbers of hydroxyl groups at polyester arms chain-ends and directly attached to the star-shaped core—Controlled synthesis and characterization, J. Polym. Sci., Part A: Polym. Chem., 43 (2005) 6116-6133.
[86] P. Kilz, R.-P. Krüger, H. Much, G. Schulz, Two-dimensional chromatography for the deformulation of complex copolymers, Adv. Chem. Ser., 247 (1995) 223–241.
[87] X. Jiang, A. van der Horst, V. Lima, P.J. Schoenmakers, Comprehensive two-dimensional liquid chromatography for the characterization of functional acrylate polymers, J. Chromatogr. A, 1076 (2005) 51-61.
[88] M. Al Samman, W. Radke, Two-dimensional chromatographic separation of branched polyesters according to degree of branching and molar mass, Polymer, 99 (2016) 734-740.
[89] S. Cheruthazhekatt, G.W. Harding, H. Pasch, Comprehensive high temperature two-dimensional liquid chromatography combined with high temperature gradient chromatography-infrared spectroscopy for the analysis of impact polypropylene copolymers, J. Chromatogr. A, 1286 (2013) 69-82.
[90] J. Adrian, D. Braun, H. Pasch, New analytical methods for epoxy resins, 2. Two-dimensional chromatography, Angew. Makromol. Chem., 267 (1999) 82-88.
[91] F. Bedani, P.J. Schoenmakers, H.G. Janssen, Theories to support method development in comprehensive two-dimensional liquid chromatography–A review, J. Sep. Sci., 35 (2012) 1697-1711.
[92] T. Tsuji, T. Norisuye, H. Fujita, Dilute solution of bisphenol A polycarbonate, Polym. J., 7 (1975) 558-569.
[93] K. Gaudin, P. Chaminade, A. Baillet, Eluotropic strength in non-aqueous liquid chromatography with porous graphitic carbon, J. Chromatogr. A, 973 (2002) 61-68.
[94] S.S. Bhati, T. Macko, R. Brüll, D. Mekap, Liquid Chromatography at Critical Conditions of Poly (propylene), Macromol. Chem. Phys., (2015).
[95] N. Apel, E. Uliyanchenko, S. Moyses, S. Rommens, C. Wold, T. Macko, K. Rode, R. Brüll, Selective chromatographic separation of polycarbonate according to hydroxyl end-groups using a porous graphitic carbon column, J. Chromatogr. A, 1488 (2017) 77-84.

[96] O. Haba, I. Itakura, M. Ueda, S. Kuze, Synthesis of polycarbonate from dimethyl carbonate and bisphenol-a through a non-phosgene process, J. Polym. Sci., Part A: Polym. Chem., 37 (1999) 2087-2093.
[97] H.R. Kricheldorf, S. Böhme, G. Schwarz, Polycondensations of Bisphenol-A with Diphosgene or Triphosgene in Water-Free Organic Solvents, Macromol. Chem. Phys., 206 (2005) 432-438.
[98] G. Montaudo, S. Carroccio, C. Puglisi, Thermal and themoxidative degradation processes in poly (bisphenol a carbonate), J. Anal. Appl. Pyrolysis, 64 (2002) 229-247.
[99] S. Carroccio, C. Puglisi, G. Montaudo, Mechanisms of thermal oxidation of poly (bisphenol A carbonate), Macromolecules, 35 (2002) 4297-4305.
[100] G. Montaudo, S. Carroccio, C. Puglisi, Thermal oxidation of poly (bisphenol A carbonate) investigated by SEC/MALDI, Polym. Degrad. Stab., 77 (2002) 137-146.
[101] H. Pasch, B. Trathnigg, HPLC of Polymers, Springer Science & Business Media, Berlin, 1999.
[102] D. Cho, S. Park, J. Hong, T. Chang, Retention mechanism of poly (ethylene oxide) in reversed-phase and normal-phase liquid chromatography, J. Chromatogr. A, 986 (2003) 191-198.
[103] G. Guiochon, A. Moysan, C. Holley, Influence of various parameters on the response factors of the evaporative light scattering detector for a number of non-volatile compounds, J. Liq. Chromatogr., 11 (1988) 2547-2570.
[104] S. Damodaran, T. Schuster, K. Rode, A. Sanoria, R. Brüll, M. Wenzel, M. Bastian, Monitoring the effect of chlorine on the ageing of polypropylene pipes by infrared microscopy, Polym. Degrad. Stab., 111 (2015) 7-19.
[105] A. Wawkuschewski, H. Cantow, S. Magonov, Scanning tunneling microscopy of alkane adsorbates at the liquid/graphite interface, Langmuir, 9 (1993) 2778-2781.
[106] J. Falkenhagen, J.F. Friedrich, G. Schulz, R.-P. Krüger, H. Much, S. Weidner, Liquid adsorption chromatography near critical conditions of adsorption coupled with matrix-assisted laser desorption/ionization mass spectrometry, Int. J. Polym. Anal. Charact., 5 (2000) 549-562.
[107] K. Watanabe, N. Yamagiwa, Y. Torisawa, Cyclopentyl Methyl Ether as a New and Alternative Process Solvent, Org. Process Res. Dev., 11 (2007) 251-258.
[108] N. Apel, E. Uliyanchenko, S. Moyses, S. Rommens, C. Wold, T. Macko, R. Brüll, Separation of Branched Poly(bisphenol A)carbonate Structures by Solvent Gradient at Near-Critical Conditions and Two-Dimensional Liquid Chromatography, (2018).
[109] N. Apel, V. Ramakrishnan, E. Uliyanchenko, S. Moyses, S. Rommens, C. Wold, T. Macko, R. Brüll, Correlation between Comprehensive 2D Liquid Chromatography and Monte- Carlo Simulations for Branched Polymers, (2018).
[110] H.R. Kricheldorf, M. Rabenstein, M. Maskos, M. Schmidt, Macrocycles. 15. The role of cyclization in kinetically controlled polycondensations. 1. Polyester syntheses, Macromolecules, 34 (2001) 713-722.
[111] A.J.P. Martin, Some theoretical aspects of partition chromatography, in: Biochem. Soc. Symp, 1950, pp. 4-20.
[112] Y. Kim, S. Ahn, T. Chang, Martin's Rule for High-Performance Liquid Chromatography Retention of Polystyrene Oligomers, Anal. Chem., 81 (2009) 5902-5909.
[113] S. Moyses, A. Ginzburg, The chromatography of poly(phenylene ether) on a porous graphitic carbon sorbent, J. Chromatogr. A, 1468 (2016) 136-142.
[114] H. Pasch, Chromatographic investigations of macromolecules in the critical range of liquid chromatography: 3. Analysis of polymer blends, Polymer, 34 (1993) 4095-4099.
[115] Agilent Technologies, Agilent 1260 Infinity Multi-Detector Suite: User Manual, Agilent Technologies, Waldbronn, 2014.
[116] S.P. Trainoff, Method for correcting the effects of interdetector band broadening, US Patent 7386427 B2, (2008)

[117] L.T. Hillegers, M. Kapnistos, A. Nijenhuis, J.J.M. Slot, P.A.M. Steeman, Monte Carlo simulation of randomly branched step-growth polymers: Generation and analysis of representative molecular ensembles, Macromol. Theory Simul., 20 (2011) 219-229.
[118] L.T. Hillegers, A. Blokhuis, J.J.M. Slot, A fast method to compute the msd and mwd of polymer populations formed by step-growth polymerization of polyfunctional monomers bearing A and B coreactive groups, Macromol. Theory Simul., 21 (2012) 553-564.
[119] L.T. Hillegers, J.J.M. Slot, Step-growth polymerized systems of general type "afiBgi": Generating functions and recurrences to compute the MSD, Macromol. Theory Simul., 24 (2015) 248-259.
[120] L.T. Hillegers, J.J.M. Slot, Step-Growth Polymerizing Systems of General Type “AfiBgi”: Calculating the Bivariate (Molecular Size) × (Number of Branch Points) Weight Distribution Using Generating Functions and Recurrences, Macromol. Theory Simul., 25 (2016) 348-359.
[121] N. Metropolis, S. Ulam, The Monte Carlo Method, Journal of the American Statistical Association, 44 (1949) 335-341.
[122] Z. Grubisic, P. Rempp, H. Benoit, A universal calibration for gel permeation chromatography, J. Polym. Sci. B, 5 (1967) 753-759.
[123] R. Endō, M. Takeda, Note on the relationship between the intrinsic viscosity and the molecular weight of crystalline and amorphous polystyrene, J. Polym. Sci. Pol. Chem., 56 (1962).
[124] J. Kim, H.S. Gracz, G.W. Roberts, D.J. Kiserow, Spectroscopic analysis of poly (bisphenol A carbonate) using high resolution 13 C and 1 H NMR, Polymer, 49 (2008) 394-404.
[125] T. Adamek, Statistik für Anwender: Statistik aus der Münze, Springer, Berlin, 2015.

Datum:

Erklärung

Ich erkläre hiermit, dass ich meine Dissertation selbstständig und nur mit den angegebenen Hilfsmitteln angefertigt habe.

Nico Apel

Datum:

Erklärung

Ich erkläre hiermit, noch keinen Promotionsversuch unternommen zu haben.

Nico Apel

Werdegang

Wurde aus Datenschutzgründen entfernt.

Nico Apel